DEVELOPMENT OF STABILITY INDICATING METHOD OF EFONIDIPIE HCl ETHANOLATE

7.1. SELECTION OF DRUG

Efonidipine Hydrochloride Ethanolate (EFO) is an antihypertensive and antianginal agents with dihydropyridine moiety. It was developed by Nissan Chemical Industries, Saitama and marketed in Japan. It blocks both L and T-type Calcium channels. It differs from other dihydropyridine in having a phosphonate nucleus at 5^{th} position of the dihydropyridine ring [1, 2].

T-type calcium channels are different from L type channels which are involved in cardiac pace making and regulation of blood flow. EFO is a calcium channel blocker which blocks both T- and L- type calcium channels. EFO has negative chronotropic and vasodilator effect. It has weak inotropic effect. It causes increase in glomerular filtration rate without increasing intra glomerular pressure. It causes relaxation of afferent and efferent arterioles and reduces proteinuria. It has organo-protective effects on heart and kidney [3].

Components of rennin–angiotensin aldosterone system are believed to contribute to the development and progression of cardiovascular tissue and organ injuries. Effects of two calcium channel blockers EFO and amlodipine are compared on the rennin angiotensin aldosterone in patients with end stage renal diseases on maintenance with hemodialysis. EFO causes decrease in plasma aldosterone level in patients subjected to hemodialysis .In patients with renal impairment, it provides additional benefit in cardiovascular protection [4, 5,6].

Compared to amlodipine, EFO decreases heart rate and plasma aldosterone level in hypertensive patients. EFO blocks T-type calcium channels and cause reduction of aldosterone secretion by suppressing 11-beta hydroxylase and aldosterone synthase expression [7, 8].

Compared to nifedipine, EFO improves endothelial lining in patients with essential hypertension, reduces urinary secretion of 8-hydroxy-2’de-oxyguanosine and serum malondialdehyde-modified LDL. It improves blood pressure, endothelial function and metabolic parameters without variation in insulin sensitivity in non-diabetic patients with hypertension [9].

It was launched by Shionogi and Co. (Japan) in 1995 as brand name Landel. It is approved for marketing in India by Drug Controller General India to Zuventus Pharma as Efnocar in 2016. It is not official in any pharmacopoeia.

7.2. DRUG PROFILE

General Properties

IUPAC name: 2-(N-benzylanilino) ethyl 5-(5, 5-dimethyl-2-oxo-1, 3, 2^5}-dioxaphosphinan-2-yl)-2, 6-dimethyl-4-(3-nitrophenyl)-1, 4-dihydropyridine-3-carboxylate; ethanol; hydrochloride [10]

Molecular Formula: $C_{36}H_{45}ClN_3O_8P$

Molecular Weight: 714.19 g/mole

Log P: 5.35

pKa: Strongest acidic (19.49), strongest basic (2.33)

Solubility: alcohol

Drug category: Antihypertensive [11]

Marketed Formulation: It is marketed as EFNOCAR film coated tablets by Zuventus Healthcare containing 20 mg EFO/tablet

7.3. LITERATURE REVIEW

- *Development and validation of Liquid Chromatography (RP-HPLC) Methodology for estimation of Efonidipine HCl Ethanolate by Kumar A et. al [12].*

RP-HPLC method was developed for determination of EFO using symmetry C 18, 5.0 mm column. Mobile phase was acetonitrile and water in the ratio of 85: 15 with flow rate of 0.8 mL/min. Detection was performed at 254 nm. Method was validated as per ICH guidelines.

- *Determination of Efonidipine in human plasma by LC-MS/MS for pharmacokinetic applications by Liu H et. al [13].*

LC-MS/MS method was developed for determination of EFO in human plasma over the range of 0.1-20 ng/mL. EFO was extracted from plasma by LLE procedure, separated by LC and detected by MS/MS in positive mode ESI. Intra-day and inter-day precisions were less than 12.5% in terms of %RSD and accuracies were between -5 and 5% in terms of relative error. The method was applied to pharmacokinetics of EFO in human subject.

- *A Chiral LC-MS/MS method for stereospecific determination of efonidipine in human plasma by Liu M et. al [14].*

Enantio-selective LC-MS/MS method was developed for determination of EFO enantiomers in human plasma and validated to characterize stereo selective pharmacokinetics. Plasma samples were separated by liquid-liquid extraction. Chiral separation was achieved on Chiralpak ID column with mobile of acetonitrile: water in the ratio of 60:40 in an isocratic mode. Detection was performed by MS in multiple reaction mode with clinidipine as an internal standard. The calibration curves were in the range of 0.100-20 ng/mL for each enantiomer. The lower limit of quantification (LLOQ) for each isomer was at 0.100 ng/mL. Intra-day and inter-day precisions were less than 12.1% for each isomer in terms of relative standard deviation (RSD) and accuracies were between -5.0% and 5.0% in terms of relative error (RE) for each enantiomer.

7.4. SECTION - A

METHOD DEVELOPMENT OF EFONIDIPINE HCL ETHANOLATE BY QbD

7.4.1. EXPERIMENTAL

7.4.1.1. Chemicals and Reagents

- EFO bulk was purchased from Shouguang Qihang International Trade Co. China.
- HPLC grade Acetonitrile (ACN), was purchased from Rankem Pvt. Ltd. Mumbai.
- 0.22 µm Nylon 6, 6 membrane filter, Ultipore® N, 66® for filtration of mobile phase was procured from Pall Life Sciences, USA.

7.4.1.2. Equipments and Instruments

Equipments and Instruments utilized in the present study are same as those mentioned in section

3.4.1.2. Statease Design Expert v.11.0 and Microsoft Excel 2010 were employed.

7.4.1.3. Design of experiments

Based on the control, noise and experimental (CNX) approach, initial trials and various parameters were selected, which could have a possible impact on Critical Quality Attributes and were further screened using 2 level fractional factorial design. 2 level Fractional Factorial Design and Box-Behnken design were used for method development and optimization. Fractional factorial design was chosen for screening of parameters since it is suitable for assessment of a large number of factors or factor levels and also evaluates all possible combinations of interactions.

7.4.1.3.1. 2-Level Fractional Factorial: Quality by Design for screening stage

A design layout using fractional factorial design was generated by Design Expert 11.0.0, 5 factors which may influence the method parameters were screened for their significance on the analytical method. Variables studied were pH , buffer concentration, % organic, detection wavelength and flow rate . Fractional factorial screening design was applied to investigate the significance of these 5 factors. 3 response parameters were retention time, asymmetry factor and theoretical plates of EFO. Factors screened for fractional factorial design are shown in Table 7.1. Experimental runs for fractional factorial design are shown in Table 7.2.

Table 7. 1- Factors screened for Fractional Factorial Design

Name	Type	Low	High
%Organic (A)	Numeric	65	75
pH of buffer (B)	Numeric	3	5
Buffer concentration (C)	Numeric	5mM	15mM
Flow rate (D)	Numeric	0.8	1.2
Wavelength (E)	Numeric	250	254

Table 7. 2- Experimental Runs for the Fractional Factorial Design

Std	Run	Organic A	B pH	C:Buffer Concentration	D: F.R.	E: Wavelength	Retention Time	Asymmetry	T.P.
4	1	75	5	5	0.8	254	6.358	1.124	8409
15	2	65	5	15	1.2	250	7.157	1.015	8658
7	3	65	5	15	0.8	254	10.312	1.02	8765
8	4	75	5	15	0.8	250	6.432	1.187	8891
2	5	75	3	5	0.8	250	6.532	1.108	8661
12	6	75	5	5	1.2	250	4.272	1.157	6882
16	7	75	5	15	1.2	254	4.164	1.175	7984
10	8	75	3	5	1.2	254	4.284	1.147	7017
14	9	75	3	15	1.2	250	4.19	1.16	7432
9	10	65	3	5	1.2	250	8.023	1.012	8505
13	11	65	3	15	1.2	254	7018	1.012	8726
5	12	65	3	15	0.8	250	10.357	1.019	8914
3	13	65	5	5	0.8	250	10.672	1.012	8855
11	14	65	5	5	1.2	254	7.013	1.039	8372
1	15	65	3	5	0.8	254	10.672	1.012	8855
6	16	75	3	15	0.8	254	6.201	1.13	8810

7.4.2. RESULTS

7.4.2.1. Screening of factors

Analytical method development depends on number of factors which directly or indirectly affect the performance of the method. In QbD first step is to identify the variable which affects critical responses and to study the effects of each of them.

Cause and Effect diagram (Ishikawa) is given in Fig. 7.1. Five factors like pH of buffer, % organic, buffer concentration, flow rate and wavelength were screened by fractional factorial design.

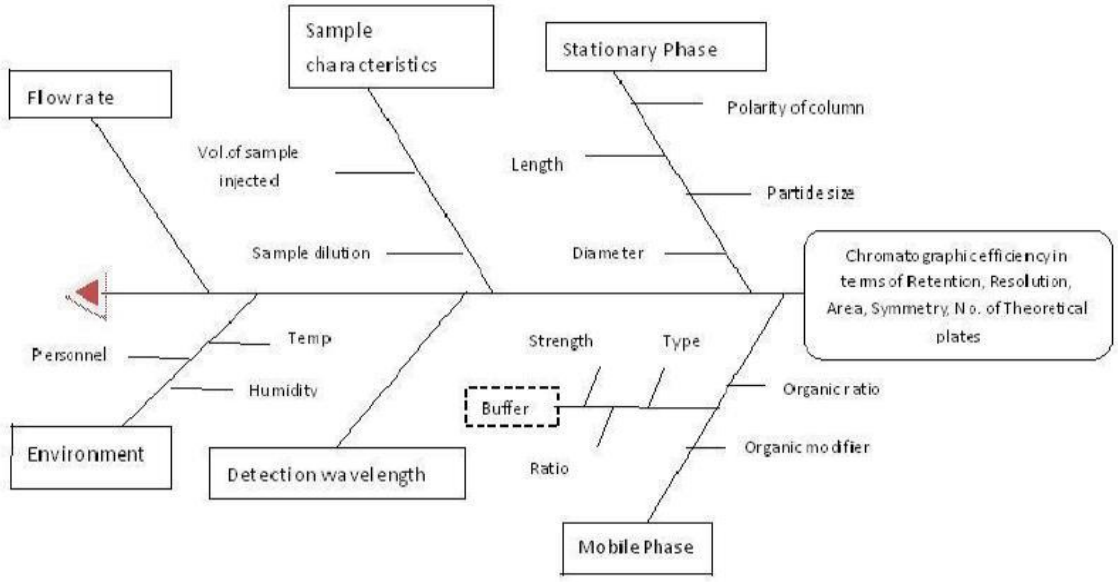

Fig.7. 1 - Cause and effect Ishikawa Fish bone diagram

7.4.2.2. Diagrammatic outputs of Fractional Factorial Design

7.4.2.2.1. Pareto charts

Pareto charts explain the degree of effect of each factor on the selected responses in the form of bars. This begins with the most significant response followed by other responses in decreasing order of their contribution to the corresponding factor. From the Pareto charts, it may be

concluded that % organic is the most critical factor affecting retention time, asymmetry and theoretical plates. pH is showing effect on retention time. Flow rate and buffer concentration show effect on theoretical plates. Detection wavelength does not show any significant effect on any studied response (Fig. 7.2-7.4).

7.4.2.2.2. Half-normal plots

Half normal plots directly mark out the factors which cause significant variation in selected critical process parameters. % Organic is the most critical factor in retention time, asymmetry and theoretical plates. pH shows effect on asymmetry while flow rate and buffer concentrations shows effect on theoretical plates (Fig.7.2-7.4).

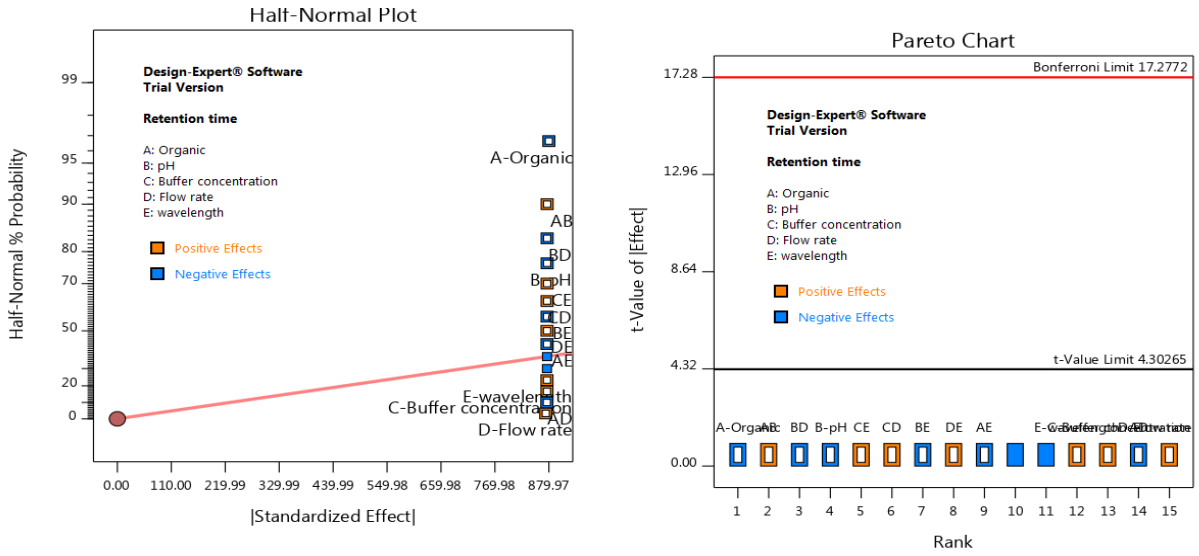

Fig.7. 2 - Half-normal plot and Pareto chart for retention time

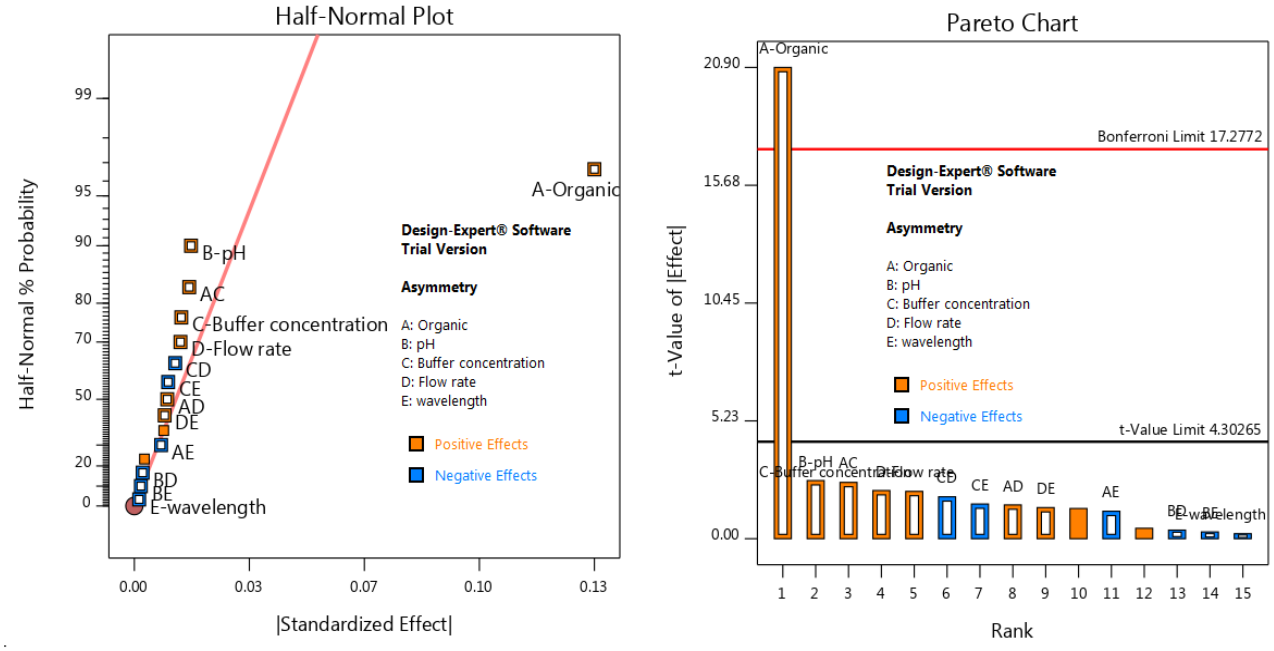

Fig.7. 3 - Half normal plot and Pareto chart for asymmetry

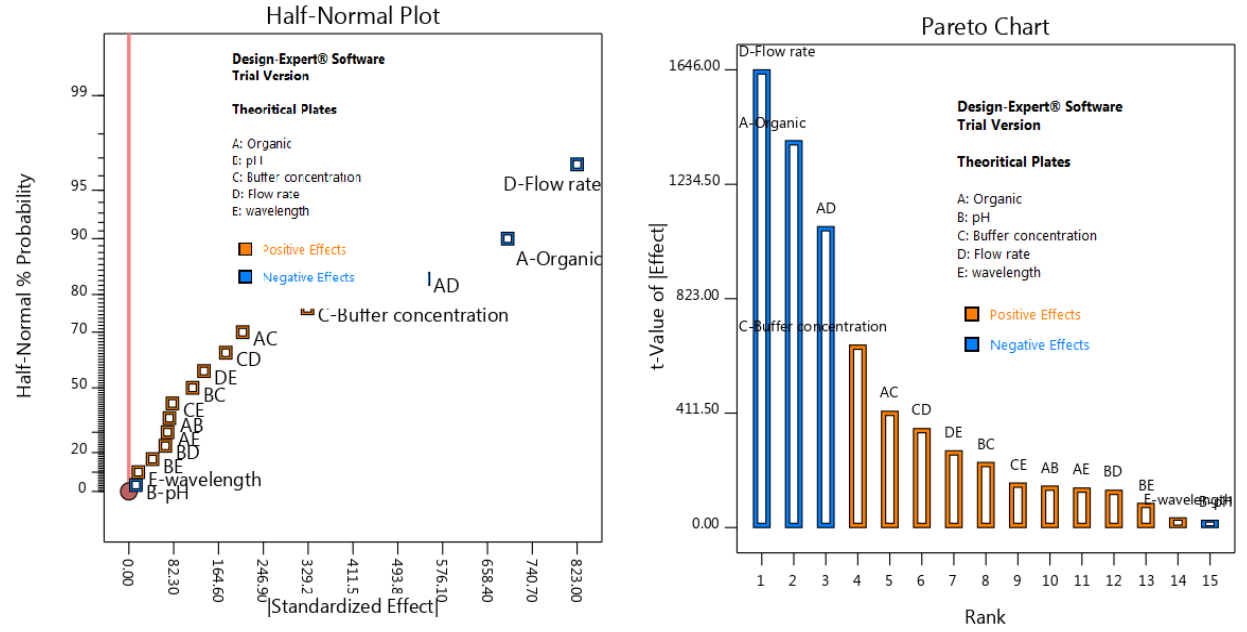

Fig.7. 4 – Half normal plot and Pareto chart for theoretical plates

7.4.2.3. 3-DResponse Surface Plots

3-D Response surface plots tell about the interaction between the five factors and which factors plays the significant role in the response. Plot for retention time shows that with decrease in pH RT increase, with increase in % organic RT decreases (Fig. 7.5)

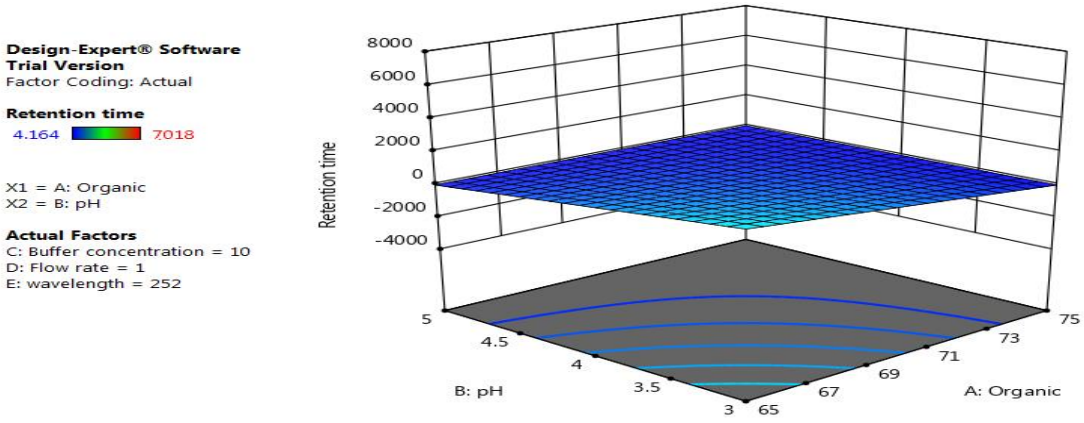

Fig.7. 5 –3- D Response surface plot for retention time

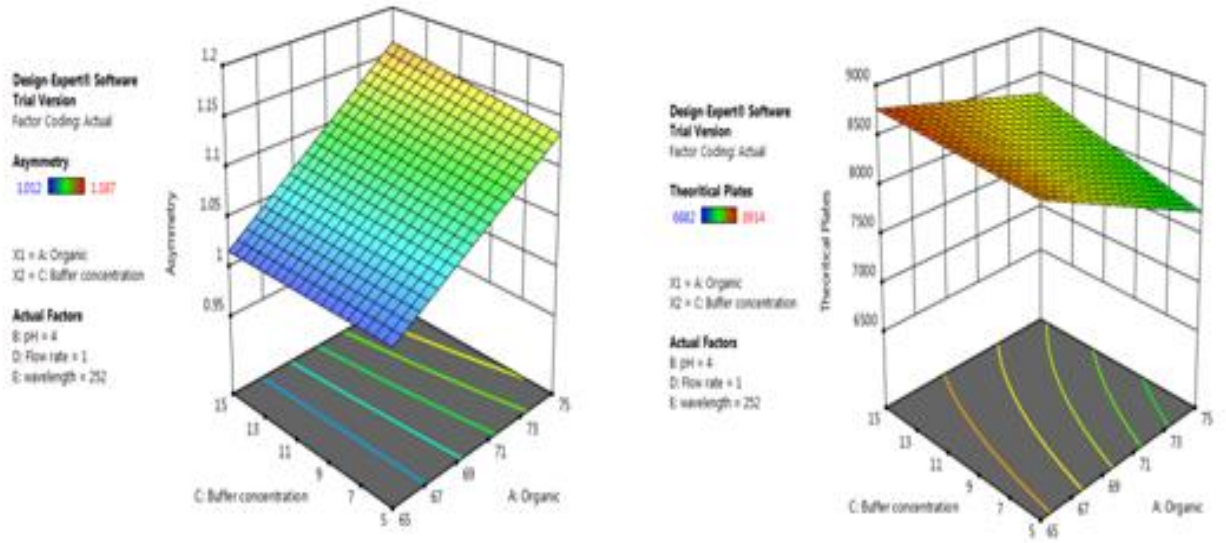

Fig.7. 6 – 3-D Response surface plots for asymmetry and theoretical plates

Plot for asymmetry shows that with increase in % organic, asymmetry also increases, while with increase in buffer concentration from 5 mM to 10mM, asymmetry is constant (Fig. 7.6). Plot for

theoretical plates shows that with increase in buffer concentration, theoretical plates increases and with increase in % organic, theoretical plates decreases (Fig. 7.6).

Four factors pH, % organic, buffer concentration and flow rate were found to be most significant overall affecting all the responses involved. These 4 factors were selected for the next stage of optimization in QbD by applying Box-Behnken design.

7.4.1.3.2. Box-Behnken design for RP-HPLC method optimization and validation of developed hplc method

7.4.1.3.2.1. Experimental

7.4.1.3.2.1.1. Box-Behnken design

On the basis of four selected factors obtained from fractional factorial design that is pH, percent organic concentration, buffer concentration, flow rate, these are used to get an optimized method which led to the design space in which the method was found to be robust. For optimization of method Box-Behnken design of experiments was utilized. The factors and their levels are shown in Table 7.3.

Table 7. 3 - Factors and their levels for BBD

Factors	Factor ID	Low	Middle	High
% Organic	A	60	65	70
pH	B	3	4	5
Buffer concentration	C	5	10	15
Flow rate	D	0.8	1.0	1.2

7.4.1.3.2.1.2. Preparation of standard solution

EFO standard solution (1mg/mL) - 25 mg of EFO was weighed accurately and transferred to 25 mL volumetric flask, dissolved in acetonitrile and volume was made up to the mark with acetonitrile.

Working standard solutions were prepared in mobile phase to produce concentration in the range of 20-120 µg/mL with respect to EFO.

7.4.1.3.2.1.3. Preparation of sample solution

Tablets equivalents to 25 mg were accurately weighed and transferred to 25 mL of volumetric flask and 20 mL of acetonitrile was added and sonicated for 15 min. The volume was made up to the mark with acetonitrile. From this 1mL was transferred to 10 mL and made up to volume with mobile phase . The solution was filtered with 0.45µ syringe filter and analysed by RP-HPLC.

7.4.1.3.2.1.4. HPLC method validation

The developed method was validated as per ICH Q2B guideline.

For linearity, standard dilutions of EFO were prepared in the concentration ranging from 20 to 120µg/mL from EFO stock solution and were injected in triplicate. Linearity was determined by plotting peak area and concentration of solution. From the graph regression equation and regression coefficient was determined.

For precision, intra-day and inter-day precision were evaluated at concentration levels ranging from 20-120µg/mL (in triplicates). Peak areas corresponding to the concentration was calculated and % RSD was determined for intra-day and inter -day precision.

% Recovery was evaluated by standard addition method. Accuracy of method was evaluated at concentration of 40 µg/mL. Accuracy of method was confirmed by recovery study from formulation at 3 level of standard addition (50%, 100% and 150%). The final concentrations for accuracy were 40, 60, 80, 100 µg/mL. The concentrations were analysed in triplicates. % recovery and % RSD were calculated.

Limit of detection and limit of quantitation were calculated on the basis of standard deviation of the intercept and slope of the calibration curve. LOD and LOQ were calculated using equation 3.3*(σ/S) and 10*(σ/S), where σ is the standard deviation of intercept and S is the slope of the calibration curve.

For robustness, pH of buffer (4.8, 5.0 and 5.2), % organic (63, 65, 67) and flow rate (0.9, 1.0, 1.1mL/min) were changed. Robustness of the method was evaluated at 40 µg/mL of concentration in triplicates.

As per Recommendation by ICH, the method is specific when the results are unaffected by the presence of the dosage form excipients. The specificity of the method was determined by analyzing the marketed formulation to check any interference of excipients.

System suitability parameters such as theoretical plates, asymmetry factor were calculated for n=6 replicates.

7.4.2. RESULTS

Table 7. 4- Experimental runs for BBD

		Factor 1	**Factor 2**	**Factor 3**	**Factor 4**	**Response 1**	**Response 2**	**Response 3**
Std	Run	A:Organic	B:pH	C:Buffer concentration	D:Flow rate	Retention time	Asymmetry	Theoretical Plates
22	1	70	5	10	0.8	8.06	1.07	8075
2	2	75	3	10	1	5	1.14	8968
5	3	70	4	5	0.8	8.154	1.071	9595
8	4	70	4	15	1.2	5.293	1.086	8599
4	5	75	5	10	1	5.143	1.132	7745
21	6	70	3	10	0.8	7.866	1.079	8630
26	7	70	4	10	1	6.275	1.093	8368
10	8	75	4	10	0.8	6.28	1.131	8621

23	9	70	3	10	1.2	5.233	1.09	7596
7	10	70	4	5	1.2	5.366	1.14	8337
14	11	70	5	5	1	6.378	1.112	8122
11	12	65	4	10	1.2	6.923	1.04	8342
13	13	70	3	5	1	6.38	1.106	8306
24	14	70	5	10	1.2	5.424	1.09	7739
25	15	70	4	10	1	6.275	1.093	8398
9	16	65	4	10	0.8	10.634	1.018	8861
19	17	65	4	15	1	8.493	1.08	8798
18	18	75	4	5	1	5.369	1.14	8337
6	19	70	4	15	0.8	10.536	1.017	9640
1	20	65	3	10	1	8.416	1.048	8968
3	21	65	5	10	1	8.578	1.031	8816
20	22	75	4	15	1	5.058	1.144	9261
15	23	70	3	15	1	6.299	1.109	8429
17	24	65	4	5	1	8.695	1.014	9969
27	25	70	4	10	1	6.274	1.093	8368
16	26	70	5	15	1	6.457	1.087	8403

28	27	70	4	10	1	6.275	1.093	8368
12	28	75	4	10	1.2	4.266	1.141	8368

Table 7. 5- Summary of optimized Box-Behnken Design

Design Summary								
Study time : Response Surface			**Sub type** : Randomized					
Design : Box-Behnken			**Runs** : 28					
Design Type : Quadratic Blocks : No Blocks								
Factors								
Factor	**Name**	**Type**	**Minimum**	**Maximum**	**Coded Low**	**Coded High**	**Mean**	**Std. Dev.**
A	% Organic	Numeric	65.00	75.00	-1↔ 65.00	+1↔ 75.00	70.00	3.33
B	pH	Numeric	3.00	5.00	-1↔ 3.00	+1↔ 5.00	4.00	0.66
C	Buffer concentration	Numeric	5.00	15.00	-1↔ 5.00	+1↔ 15.00	10.00	3.33
D	Flow Rate	Numeric	0.80	1.20	-1↔ 0.80	+1↔ 1.20	1.00	0.13

Responses										
Responses	**Name**	**Observations**	**Analysis**	**Maximum**	**Minimum**	**Mean**	**Std Dev.**	**Ratio**	**Transform**	**Model**
R1	Retention Time	28	Polynomial	4.266	10.634	6.76	1.65	2.49	None	Linear
R2	Asymmetry	28	Polynomial	1.014	1.144	1.09	0.0397	1.13	None	Linear
R3	Theoretical Plates	28	Polynomial	7596	9969	8572.39	557.39	1.31	None	Quadratic

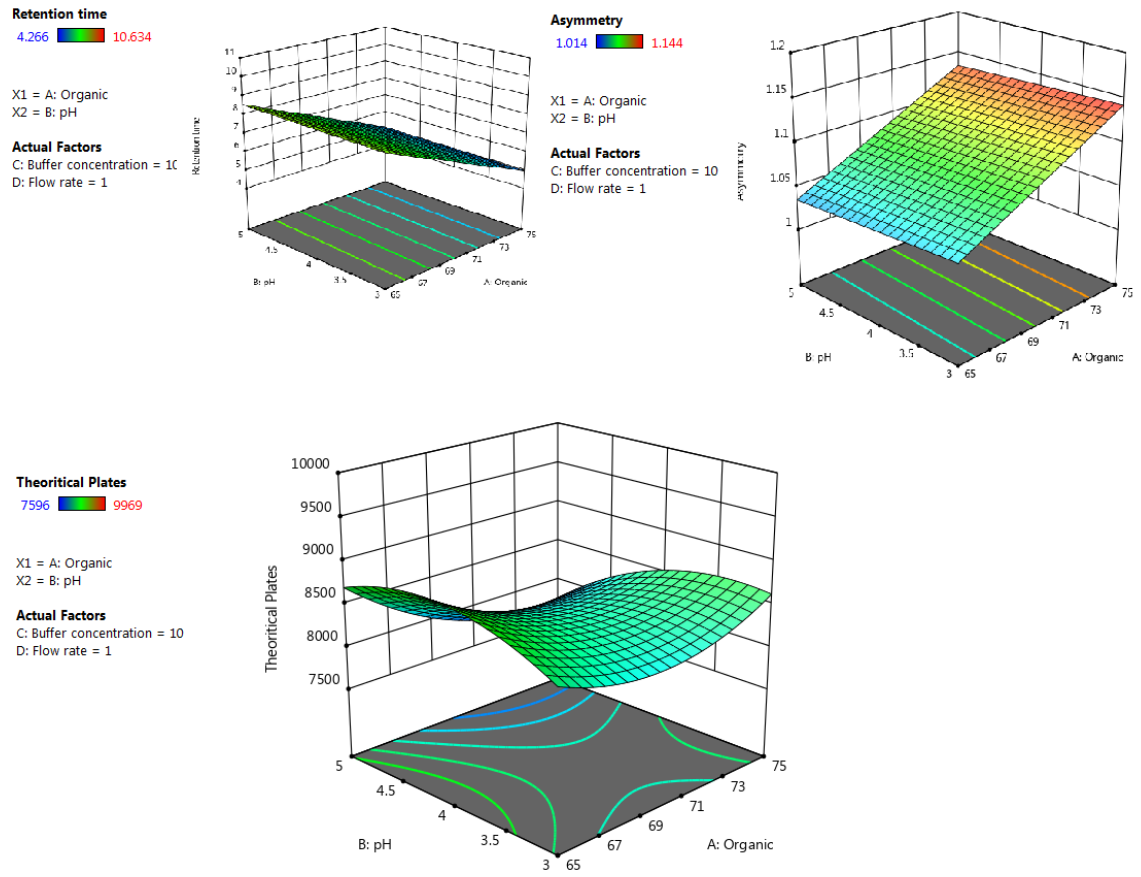

Fig.7. 7- 3-D response surface plots retention time, Asymmetry and theoretical plates

The BBD including 28 runs was worked out for four factors and the results of runs are shown in Table 7.4. Summary of optimized Box-Behnken Design is shown in Table 7.5. Out of the 30 solutions generated by software, 6 solutions were selected for checkpoint analysis (Table 7.6) to verify whether the predicted and experimental results are closely correlated. All these six predictions are tested by experimental trials and responses observed must lie within 95% confidence interval of their predicted values. One of these solutions was selected as final optimized working point for the proposed stability indicating method development. Ammonium acetate buffer pH 5: acetonitrile in the ratio of 35: 65 was selected as working point. 3-D response surface plots for retention time, asymmetry and theoretical plates are shown in Fig. 7.7. The multi dimensional combination of input variables and process parameters that have been demonstrated to provide assurance of quality is called as design space. Fig. 7.8 shows the

desirability plot for the optimized solution. The red indicates the desirability of 1 (maximum desirability). The overlay plot (Fig. 7.9) displays the design space. Yellow region shows that varying the experimental variables in this region, the method remains robust. Grey area indicate non-robust region. Final optimised RP-HPLC parameters are shown in Table 7.7. Chromatogram of EFO is shown in Fig. 7.10.

Table 7. 6 - Method obtained after optimization of design

Number	Organic	pH	Buffer concentration	Flow rate	Retention time	Asymmetry	Theoretical Plates	Desirability	
1	**65.00**	**5.00**	**10.00**	**1.00**	**8.55**	**1.03**	**8701.79**	**1.00**	**Selected**
2	65.00	3.00	10.00	1.00	8.41	1.04	8499.12	1.00	
3	70.00	4.00	10.00	1.00	6.76	1.08	8375.50	1.00	
4	66.42	3.68	10.00	1.00	7.97	1.05	8655.63	1.00	
5	65.73	3.29	10.00	1.00	8.18	1.04	8596.56	1.00	

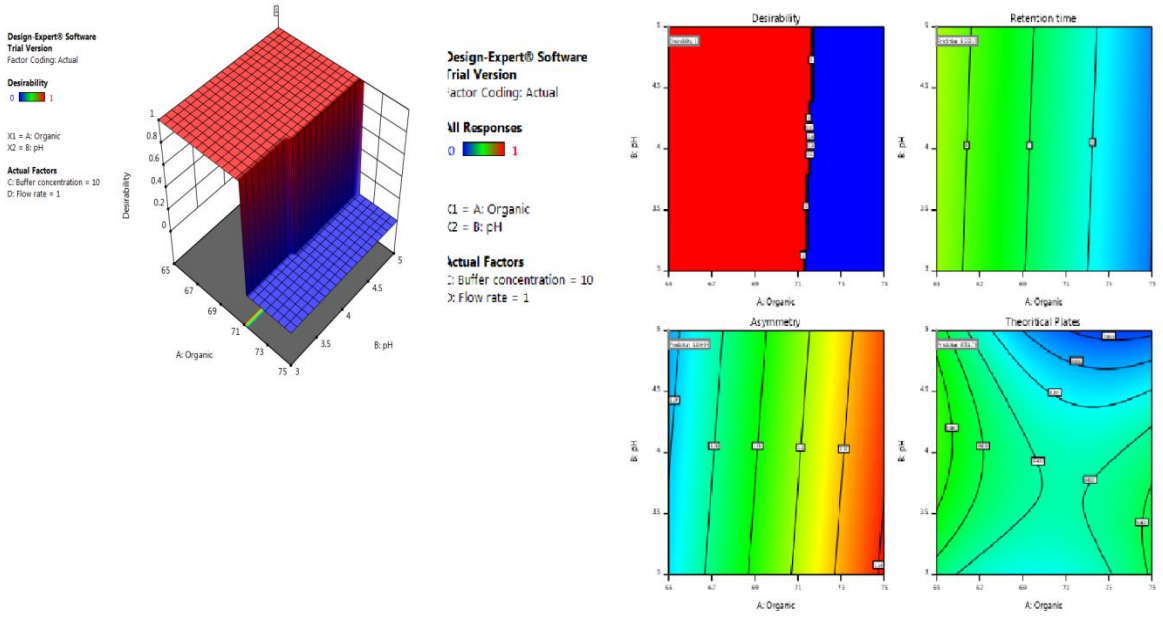

Fig.7. 8- 3-D Desirability contour plots

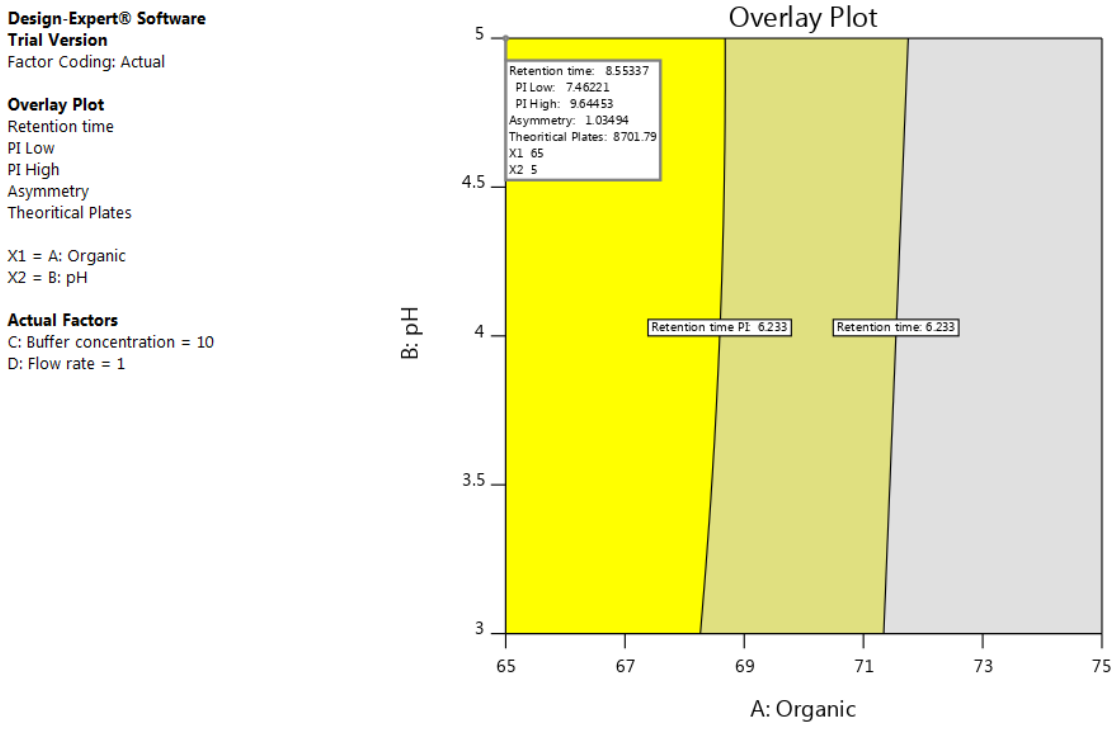

Fig.7. 9- Overlay Plot

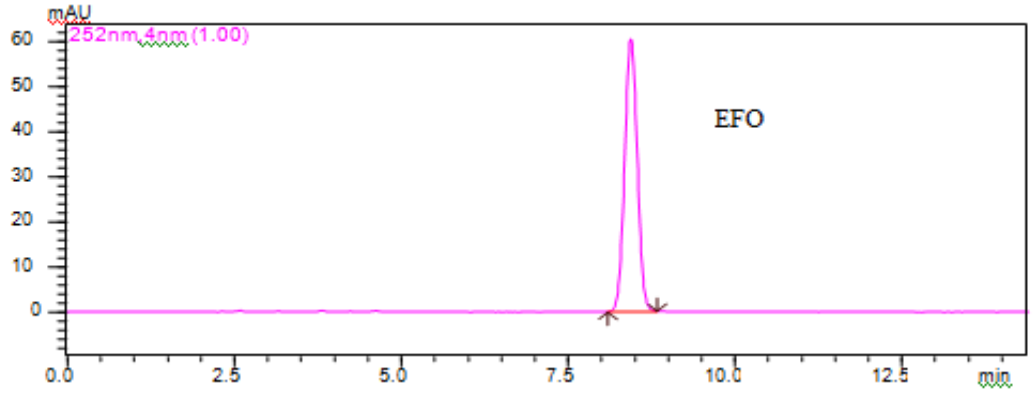

Fig.7. 10 - Chromatogram of EFO (40µg/mL)

Table 7. 7 - Optimised RP-HPLC parameters

Parameters	Optimised Value
Column	Thermo Hypersil BDS C 18 (250 x 4.6mm i.d. , 5µ particle size)
Flow rate	1.0 mL/min
Retention time	8.45± 0.013 min
Mobile phase	Ammonium acetate buffer pH 5 : acetonitrile (35 : 65)
Detection wavelength	254 nm
Needle wash	Mobile phase
Column temperature	Ambient

7.4.2.1. Validation of RP-HPLC method

The calibration plotted for EFO was found to be linear in the range of 20-120 µg/mL. The regression equation was found to be y=33223x+15744 with regression coefficient (r^2) of 0.9994. Intra-day precision was performed by repeating the experiment three times in a day and inter-day precision was performed by repeating the experiments on three consecutive days. The average %RSD of intra-day and inter-day were found to be 1.11 and 1.23. The developed method was found to be precise. Accuracy of the method was confirmed by recovery studies. To the sample concentration of 40µg/mL, standard solution of EFO was added as 50%, 100% and 150% to give

final concentrations as 60, 80, 100 µg/mL. Recovery greater than 99% indicates the developed method was accurate. LOD and LOQ were found to be 0.23 and 0.75 µg/mL respectively. For robustness study, slight changes were pH of buffer, % organic and flow rate. The results were expressed as % RSD. % RSD less than 2 indicated that the developed method was robust. Results of validation parameters are shown in Table 7.8.

Table 7. 8 - Summary of validation parameters

Parameters		**Values**
Calibration range		20-120 µg/mL
LOD(µg/mL)		0.23
LOQ(µg/mL)		0.75
Regression Equation		y=33233x+15744
Correlation coefficient		0.999
Accuracy		%Recovery±SD
50%		99.88±0.14
100%		100.16±0.13
150%		99.88±0.05
Precision		%RSD
Intraday		1.11
Interday		1.23
Robustness		
Parameter	Levels	Mean ±%RSD
pH	4.8	8.44±0.22
	5.0	8.44±0.27
	5.2	8.42±0.14
% Organic	63	8.92±0.17

	65	8.44±0.27
	67	8.02±0.39
Flow rate	0.9	8.91±0.13
	1.0	8.44±0.27
	1.1	8.00±0.29

7.4.2.2. Stability in sample solutions

Stock solution of EFO was stored at room temperature for 24 hrs. No additional peaks were observed which indicated stability of EFO sample solution.

7.4.2.3. System Suitability Parameters

System suitability tests were performed on freshly prepared solution with n=6 containing EFO. The results of system suitability parameters are shown in Table 7.9. Peak purity data of EFO is shown in Table 7.10 and peak purity curve is shown in Fig.7.11.

Table 7. 9- System suitability parameters of EFO

Parameters	Data Obtained
Retention Time (min ±SD)	8.45 ±0.01 min
Tailing Factor ± SD	1.05 ± 0.001
Theoretical Plates ± SD	8993 ±136.03

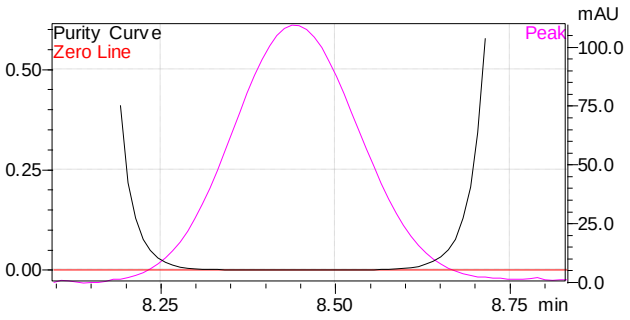

Fig.7. 11 - Peak purity curve of EFO

Table 7. 10 – Peak Purity Data of EFO

Drug Name	Peak Purity Index	Threshold
EFO	0.999990	0.999989

7.4.2.4. Analysis of formulation

The developed method was applied to the determination of EFO in formulation without the interference of excipients. The results of the assay are shown in Table.7.11.

Table 7. 11 - Results of Assay of formulation

	EFO formulation
Label Claim	20 mg
% Assay ± SD	99.33± 0.28

7.4.3. DISCUSSIONS

Method development of EFO was optimized using QbD approach. Fractional factorial design was performed for screening of factors. Factors selected for screening were pH of buffer (3-5), concentration of buffer (5mM-15 mM), % Organic (60-70), flow rate (0.8-1.2) and wavelength (252-254nm). Diagrammatic outputs of Fractional Factorial Design were interpreted in terms of pareto charts, half normal plots and response surface plots. From pareto charts, % organic is the most critical factor in retention time, asymmetry and theoretical plates. pH is showing effect on

retention time. Flow rate, buffer concentration show effect on theoretical plates while wavelength does not show any significant effect on any response. From half-normal plots, % organic is the most critical factor in retention time, asymmetry and theoretical plates. pH shows effect on asymmetry while flow rate and buffer concentrations shows effect on theoretical plates.

Four factors pH, % organic, buffer concentration and flow rate were found to be most significant overall affecting all the responses involved. These 4 factors were selected for the optimization in QbD by applying Box-Behnken design. The BBD including 28 runs was worked out for four factors. Out of the 30 solutions generated by software, 6 solutions were selected for checkpoint analysis to verify whether the predicted and experimental results are closely correlated. Ammonium acetate buffer (10 mM) pH 5: acetonitrile in the ratio of 35: 65 was selected as working point for optimisation of HPLC method. The method was validated as per ICH guidelines. The developed optimised method was selected for development of stability indicating assay method.

7.5 SECTION - B

DEVELOPMENT AND VALIDATION OF STABILITY INDICATING HPLC METHOD

7.5.1. EXPERIMENTAL

7.5.1.1. Chemicals and Reagents

- Hydrochloric acid (HCl), sodium hydroxide (NaOH), hydrogen peroxide H_2O_2) were purchased from S.D. Fine Chemical Ltd. Mumbai.
- 0.22 µm Nylon 6,6 membrane filter , Ultipore® N,66® for filtration of mobile phase was procured from Pall Life Sciences ,USA.
- 0.45 µm Nylon 6,6 syringe filter for sample filtration was procured from Pall life Sciences , USA.

7.5.1.2. Equipments and Instruments

Equipments and Instruments utilized in the present study are same as those mentioned in 7.4.1.2.

7.5.1.3. Chromatographic conditions

Initially method was optimized using QbD approach with ammonium acetate buffer pH 5 and acetonitrile in the ratio of 35 : 65 as mentioned in section 7.4.1.3.1**.** and 7.4.1.3.2. For separation of degradation products from EFO in forced degradation, the method was modified to gradient as shown in Table 7.12.

Before use, mobile phase was filtered with 0.2µ membrane filter and sonicated for 5 min. Analysis was performed with detection wavelength of 254 nm and flow rate of 1mL/min. The injection volume was 20µL. Analysis was performed on Hypersil BDS C 18 column (250 x 4.6 mm i.d. x 5µm particle size).

Table 7. 12 - Gradient programme for EFO

Time (min)	Mobile Phase A (Ammonium acetate buffer pH 5.8)	Mobile Phase B (Acetonitrile)
0.01	75	25
6	75	25
35	50	50
45	50	50
50	47	53
60	47	53
65	Stop	

7.5.1.4. Preparation of Standard solution

EFO standard solution (1mg/mL) - 25 mg of EFO was weighed accurately and transferred to 25 mL volumetric flask, dissolved in acetonitrile and volume was made up 25 mL with acetonitrile.

Working standard solutions were prepared in mobile phase to produce concentration in the range of 20-120 µg/mL with respect to EFO.

7.5.1.5. Preparation of forced degradation sample

For forced degradation study, stock solution of EFO (1mg/mL) was prepared in methanol.

7.5.1.5.1. Acid degradation

5 mL of EFO stock solution was transferred to 10 mL of volumetric flask, to this was added 5 mL of 1 M HCl. The solution was heated at 80ºC for 5 hrs. 2 mL of solution was taken and the solution was neutralized with 1 M NaOH and volume was made up to 10 mL with mobile phase to make the concentration of 100µg/mL. The solution was filtered through 0.45 µ Nylon 6, 6 syringe filter before injecting into HPLC system.

7.5.1.5.2. Alkaline degradation

5 mL of EFO stock solution was transferred to 10 mL of volumetric flask, to this was added 5 mL of 0.5 M NaOH. The solution was kept at room temperature (40ºC) for 6 hrs. 2 mL of solution was taken and the solution was neutralized with 0.5 M HCl and volume was made up to 10 mL with mobile phase to make the concentration of 100µg/mL. The solution was filtered through 0.45 µ Nylon 6, 6 syringe filter before injecting into HPLC system.

7.5.1.5.3. Oxidative degradation

5mL of EFO stock solution was transferred to 10 mL of volumetric flask, to this was added 5 mL of 10 % hydrogen peroxide. The solution was kept at room temperature (40ºC) for 24 hrs. 2mL of solution was taken and volume was made up to 10 mL with mobile phase to make the concentration of 100µg/mL. The solution was filtered through 0.45 µ Nylon 6, 6 syringe filter before injecting into HPLC system.

7.5.1.5.5. Dry heat degradation

For dry heat degradation, 50 mg of EFO was spread in petridish and kept in oven at 80ºC for 11 days. From this, 10 mg of EFO was transferred to 10 mL of volumetric flask, dissolved in mobile phase to make concentration of 1mg/mL. From this, concentration of 100 µg/mL of solution was prepared and injected into HPLC system.

7.5.1.5.6. Photolytic degradation (Dry)

For photolytic degradation, 50 mg of EFO was spread in 1 mm thickness and was exposed in photolytic chamber for 11 days. From this, 10 mg of EFO was transferred to 10 mL of volumetric flask, dissolved in mobile phase to make concentration of 1mg/mL. From this, concentration of 100 µg/mL of solution was prepared and injected into HPLC system

7.5.1.5.6. Photolytic degradation (Solution)

For photolytic degradation in solution form, 1mg/mL of solution of EFO was kept in photolytic chamber for 11 days. From this, concentration of 100 µg/mL of solution was prepared and injected into HPLC system.

7.5.1.6. HPLC method validation

The developed method was validated as per ICH Q2B guideline.

For linearity, standard dilutions of EFO were prepared in the concentration ranging from 20 to 120µg/mL from EFO stock solution and were injected in triplicate. Linearity was determined by plotting peak area and concentration of solution. From the graph regression equation and regression coefficient was determined.

For precision, intra-day and inter-day precision were evaluated at concentration levels ranging from 20-120µg/mL (in triplicates). Peak areas corresponding to the concentration was calculated and % RSD was determined for intra-day and inter -day precision.

% Recovery was evaluated by standard addition method. Accuracy of method was evaluated at concentration of 40µg/mL. Accuracy of method was confirmed by recovery study from formulation at 3 level of standard addition (50%, 100% and 150%). The total concentrations for accuracy were 40, 60, 80, 100 µg/mL. The concentrations were analysed in triplicates. % recovery and % RSD were calculated.

Limit of detection and limit of quantitation were calculated on the basis of standard deviation of the intercept and slope of the calibration curve. LOD and LOQ were calculated using equation 3.3*(σ/S) and 10*(σ/S), where σ is the standard deviation of intercept and S is the slope of the calibration curve.

For robustness, pH of buffer (5.6, 5.8, 6.0), factors like initial gradient ratio (5, 7, 9) and flow rate (0.9, 1.0, 1.1mL/min) were changed. Robustness of the method was evaluated at 40 µg/mL of concentration in triplicates.

7.5.2. RESULTS

7.5.2.1. Method optimization and development

Initially method was optimized using QbD approach with ammonium acetate buffer pH 5 and acetonitrile in the ratio of 35: 65 as mentioned in section 7.4.1.3.1**.** and 7.4.1.3.2. During forced degradation study of EFO, degradation products (DP6-DP2) in alkaline conditions were co-eluting in the mobile phase with ammonium acetate buffer pH 5 and acetonitrile in the ratio of

35: 65. For separation of degradation products modification the ratio of mobile phase was made from 35% buffer to 55% buffer, acetate buffer in the pH range 3-6 were tried, various gradient trials were performed.

One of the degradation products DP8 in photolytic condition was co-eluting with the peak of EFO. To separate DP8 from EFO, various gradient conditions were tried, trial was performed on column C-8 and using column oven temperature, modification was done with methanol. Various trials for separation of DP8 from EFO are shown in Table 7.13. Finally separation of degradation products in alkaline conditions and separation of degradation product DP8 from EFO was achieved by acetate buffer pH 5.8 and acetonitrile in gradient mode as shown in Table 7.12. EFO eluted at retention time of 57.66 min. Chromatogram of EFO is shown in Fig. 7.12.

Table 7. 13 - Trials for separation of DP8 from EFO

		EFO and DP8
S.No.	**Mobile Phase**	EFO Rt- 34.8 min, EFO and DP8 were co-eluting
2.	Gradient [Time (min)- % ACN] – 0.01-25, 6-25, 11-40, 25-65,30-35. 40-35, 41-25, 45-STOP	EFO Rt- 35 min , EFO and DP8 were co-eluting
3.	Gradient [Time (min)- % ACN]- 0.01-25, 6-25, 11-40, 22-40, 30-55, 45-55, 46-25, 50-STOP	EFO Rt- 44.1 min, EFO and DP8 were co-eluting
4.	Gradient [Time (min)- % ACN]- 0.01-25, 6-25, 11-40, 30-65,50-65,51-25,55-STOP	EFO Rt- 34.6 min EFO and DP8 were co-eluting

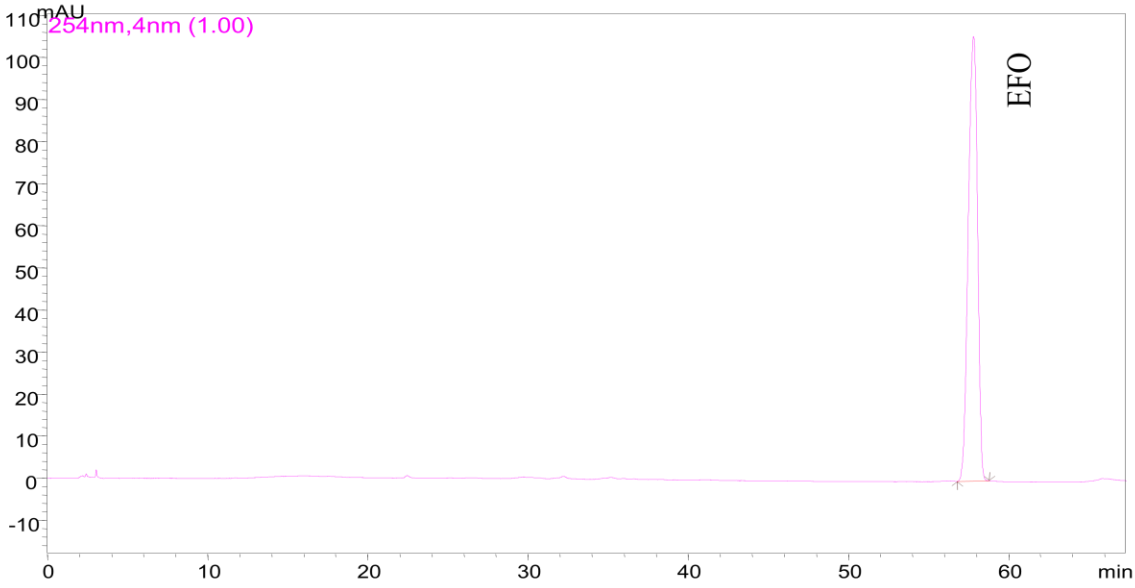

Fig.7. 12 - Chromatogram of EFO (100µg/mL)

Table 7. 14 - Optimised HPLC parameters

Parameters	Optimised Value
Column	Thermo Hypersil BDS C 18 (250 x 4.6mm i.d. , 5µ particle size)
Flow rate	1.0 mL/min
Retention time	57.66 min ± 0.05
Mobile phase	Gradient programme (Table 7.12)
Detection wavelength	254 nm
Needle wash	Acetate buffer and acetonitrile (50 : 50)
Column temperature	Ambient

7.5.2.2. Method validation using ICH Q2 (R1) guideline

7.5.2.2.1. Linearity and range

The calibration plotted for EFO was found to be linear in the range of 20-120 µg/mL. The regression equation was found to be y=33223x+15744 with regression coefficient (r^2) of 0.9994.The linearity data is shown in Table 7.15 and calibration curve is shown in Fig. 7.13.

Table 7. 15 - Linearity data of EFO

Conc. (µg/mL)	Peak Area (Mean*± %RSD)
20	870013.7± 0.79
40	1466091±1.28
60	2181799±1.15
80	2850937±1.05
100	3749303±0.43
120	4092543±1.08

*Average of three determinants

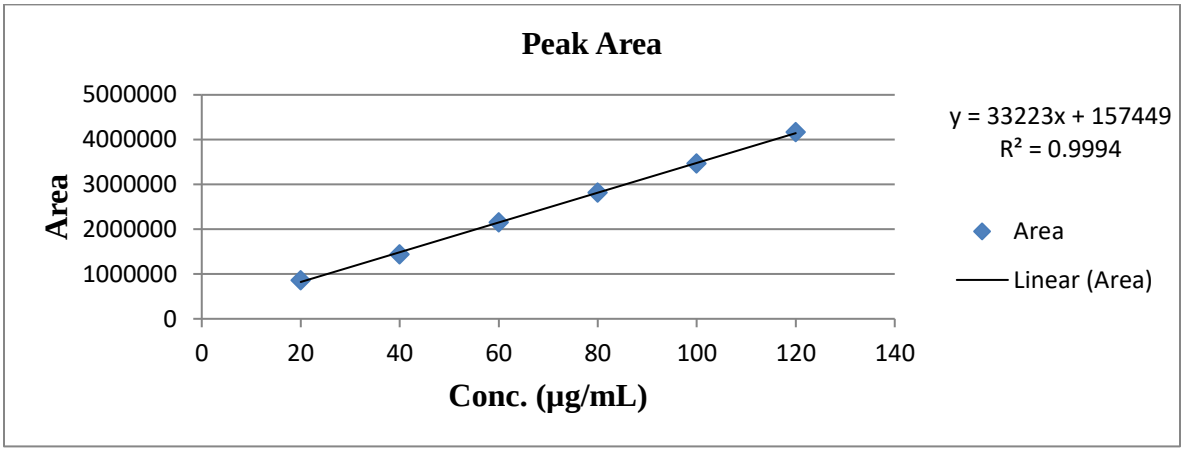

Fig.7. 13- Calibration curve of EFO

7.5.2.2.2. Precision

Intra-day precision was performed by repeating the experiment three times in a day and inter-day precision was performed by repeating the experiments on three consecutive days. The average %RSD of intra-day and inter-day were found to be 1.20 and 1.48. The developed method was found to be precise (Table 7.16 and 7.17).

Table 7. 16- Intraday Precision of EFO

Conc. (µg/mL)	Set 1	Set 2	Set 3	Mean	%RSD
20	862043	863954	873924	866640.3	0.73
40	1466624	1487252	1503546	1485807	1.24
60	2104917	2037642	2083465	2075341	1.65
80	2816761	2902364	2854156	2857760	1.50
100	3463001	3492466	3482465	3479311	0.43
120	4165098	4031643	4122854	4106532	1.66
				%RSD	1.20

Table 7. 17- Interday Precision of EFO

Conc. (µg/mL)	Set 1	Set2	Set 3	Mean	%RSD
20	862043	872456	888565	874354.7	1.52
40	1466624	1481547	1438456	1462209	1.49
60	2104917	2072567	2046267	2074584	1.41
80	2826761	2907421	2879456	2871213	1.42
100	3463001	3356284	3382583	3400623	1.63
120	4165098	4085356	4053789	4101414	1.39
				%RSD	1.48

7.5.2.2.3. Accuracy

Accuracy of method was determined by calculating % percent recovery of the analyte recovered. To the sample concentration of 40µg/mL, standard solution of EFO was added as 50%, 100% and 150% to give concentrations as 60, 80, 100 µg/mL. Recovery greater than 99% indicates the developed method was accurate (Table 7.18).

Table 7. 18- Accuracy data of EFO

Excess drug added to analyte (%)	Theoretical content (µg/mL)	*Amount found (µg/mL)	% Recovery±SD
0	40	39.96	99.91±0.38
50%	60	60.03	100.16±0.28
100%	80	80.1	100.25±0.25
150%	100	99.86	99.77±0.09

*Average of three determinations

7.5.2.2.4. Limit of detection and limit of quantification

LOD and LOQ were found to be 0.41 and 1.24 µg/mL respectively.

7.5.2.2.5. Robustness

For robustness study, slight changes were made in pH of buffer, initial gradient ratio (buffer: ACN 75: 25) and flow rate. The results were expressed as % RSD. % RSD less than 2 indicated that the developed method was robust (Table 7.19).

Table 7. 19- Robustness data of EFO

Parameter	Levels	Area		Retention time		Tailing Factor		Theoretical Plates	
		Mean	% RSD	Mean	%RSD	Mean	%RSD	Mean	%RSD
pH	5.6	57.55	0.15	1467677	0.87	0.95	0.32	69404.67	0.08
	5.8	57.27	0.07	1464314	0.72	0.94	0.16	69333	0.12
	6.0	57.56	0.18	1471063	0.75	0.94	0.47	69517.67	0.32
Initial gradient ratio	23	58.24	0.14	1476253	0.37	0.94	0.68	68667.33	0.20
	25	57.52	0.20	1479049	0.38	0.94	0.60	69383.33	0.15
	27	57.18	0.10	1454634	0.48	0.95	0.86	68313	0.10
Flow rate	0.9	58.08	0.12	1466259	0.51	0.95	0.61	68292.33	0.16
	1	57.66	0.04	1452935	0.37	0.95	0.39	69284.33	0.25
	1.1	57.25	0.03	1460510	0.39	0.95	0.41	69616.33	0.18

None of the factors affecting robustness of the method .

7.5.2.2.5. Specificity

The specificity was determined from the forced degradation studies as described in section 7.5.1.5. and 7.5.2.4. where Fig.7.15,7.20 and 7.22 shows EFO peak is well separated from all degradation products peaks formed during different stress conditions with sufficient resolution. In the forced degradation studies, for all degradation products peak purity index was greater than single point threshold, ensures degradation peaks are pure and peaks are not co-eluting. The specificity study ensures selectivity o the developed method which is able to separate and

quantify EFO in presence of degradation products. Peak purity data of EFO and degradation products are shown in Table 7.20.

Table 7. 20 - Peak purity data of EFO and degradation products

S.No.	Peaks	Rt	Peak Purity Index	Single Point threshold
1	EFO	57.33 min	1.0000	0.9999
2	DP6	14.33 min	0.9939	0.7090
3	DP5	18.83 min	0.9999	0.9987
4	DP4	20.29 min	0.9998	0.9960
5	DP3	24.09 min	0.9999	0.9993
6	DP2	26.66 min	0.9999	0.9985
7	DP1	52.91 min	0.9999	0.9987
8	DP7	31.9 min	0.9987	0.9717
9	DP8	55.92 min	0.9999	0.9988
10	DP9	30.01 min	0.9993	0.9831
11	DP10	11.67 min	0.9996	0.9910

7.5.2.3.6. Stability in sample solutions

Stock solution of EFO and stressed samples were prepared from standard stock solution and then stored at room temperature for 24 hrs. No additional peaks were observed which indicated stability of EFO sample solution.

7.5.2.3.7. System Suitability Parameters

System suitability tests were performed on freshly prepared solution with n=6 containing EFO. The results of system suitability parameters are shown in Table 7.21.

Table 7. 21- System suitability parameters of EFO

Parameters	Data Obtained
Retention Time (min ±SD)	57.66 ± 0.05
Tailing Factor ± SD	0.94 ±0.007
Theoretical plates ± SD	69040±424.6

7.5.2.3. Stress Degradation studies

7.5.2.3.1. Acid degradation – No degradation was observed when EFO was subjected to 1 M HCl at 80ºC for 6 hrs (Fig. 7.14).

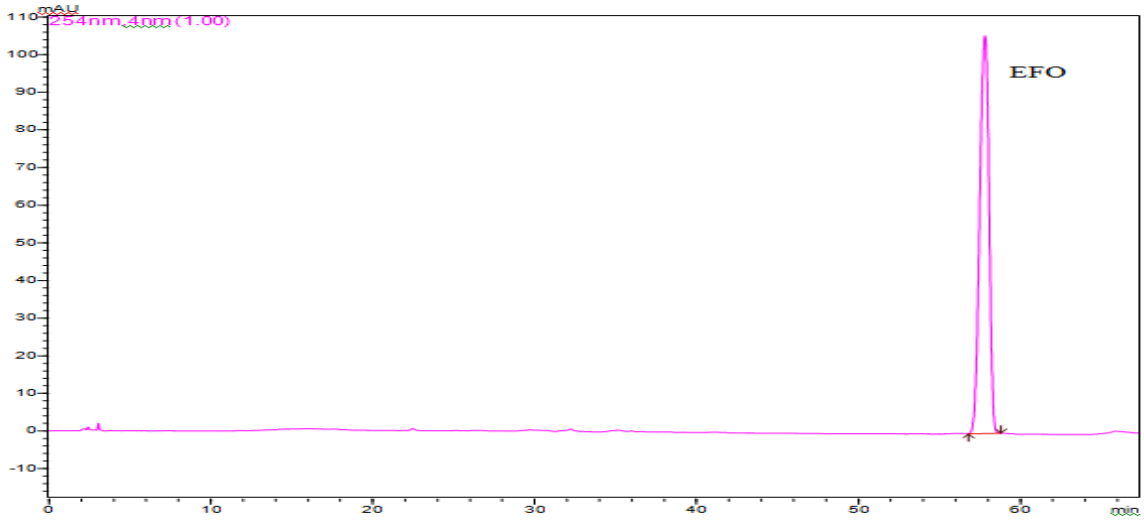

Fig.7. 14- Chromatogram of acid degradation (API)

7.5.2.3.2. Alkaline induced degradation – significant degradation (44.18%) was observed when EFO was treated with 0.5 M NaOH at RT (40ºC) for 6 hrs with the formation of six degradation products DP1 (28.14%), DP2 (4.01%) , DP3 (8.8%), DP4 (2.17%), DP5 (0.66%), DP6 (0.63%) at retention time of 52.91min, 26.66 min, 24.09 min, 20.29 min, 18.83 min, 14.33 min respectively (Fig. 7.15).

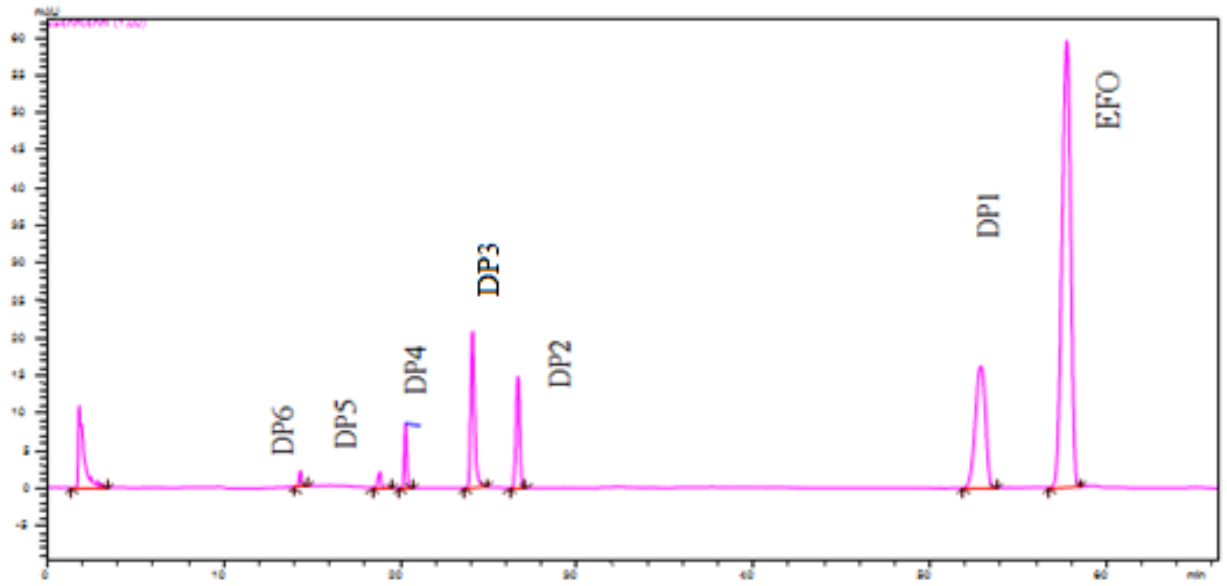

Fig.7. 15- Chromatogram of alkaline degradation (API)

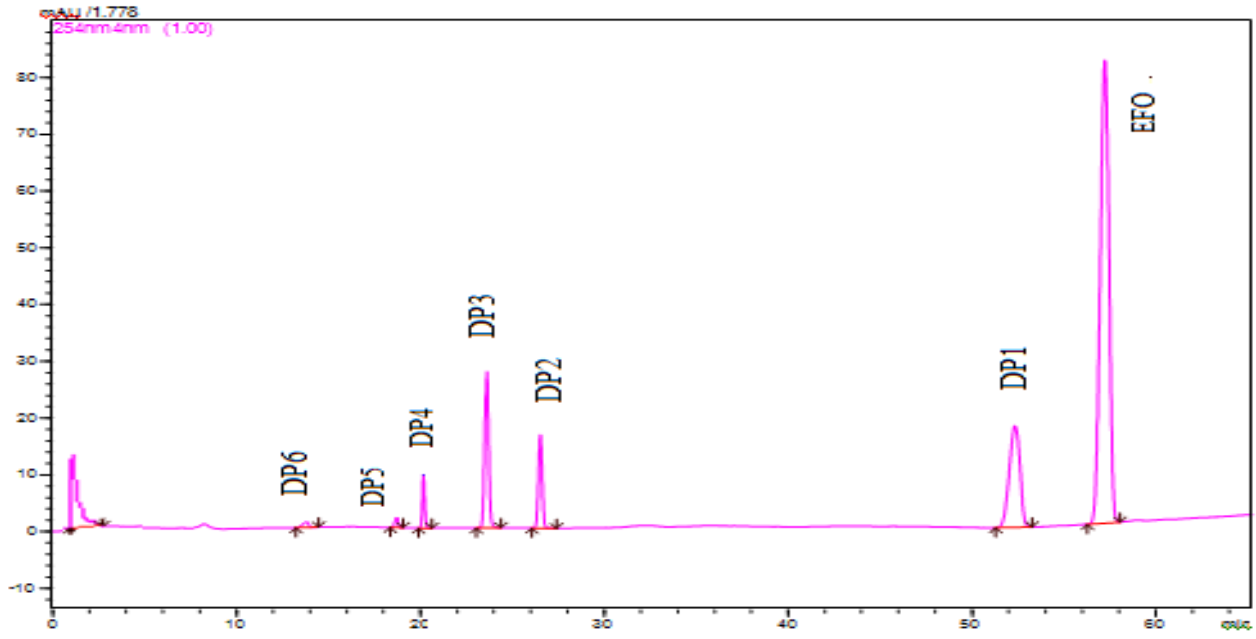

Fig.7. 16- Chromatogram of alkaline degradation (formulation)

7.5.2.3.3. Oxidative degradation- No degradation was observed when EFO was subjected to 10 % hydrogen peroxide at room temperature (40ºC) for 24 hrs (Fig. 7.17).

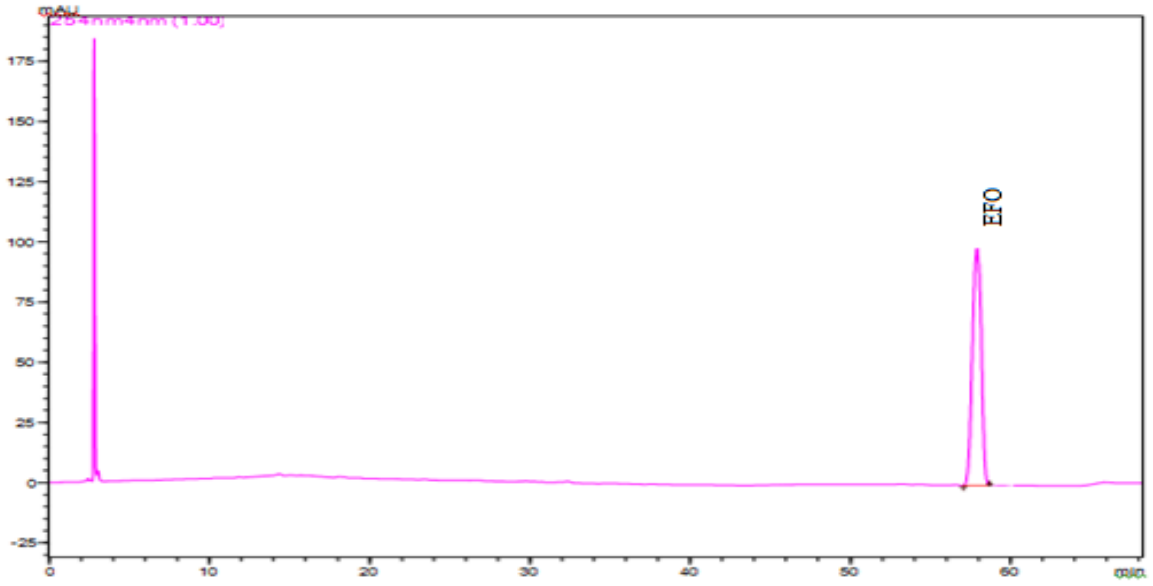

Fig.7. 17- Chromatogram of oxidative degradation (API)

7.5.2.3.4. Dry heat degradation- No degradation was observed when EFO was subjected thermal degradation at 80ºC for 11 days (Fig. 7.18).

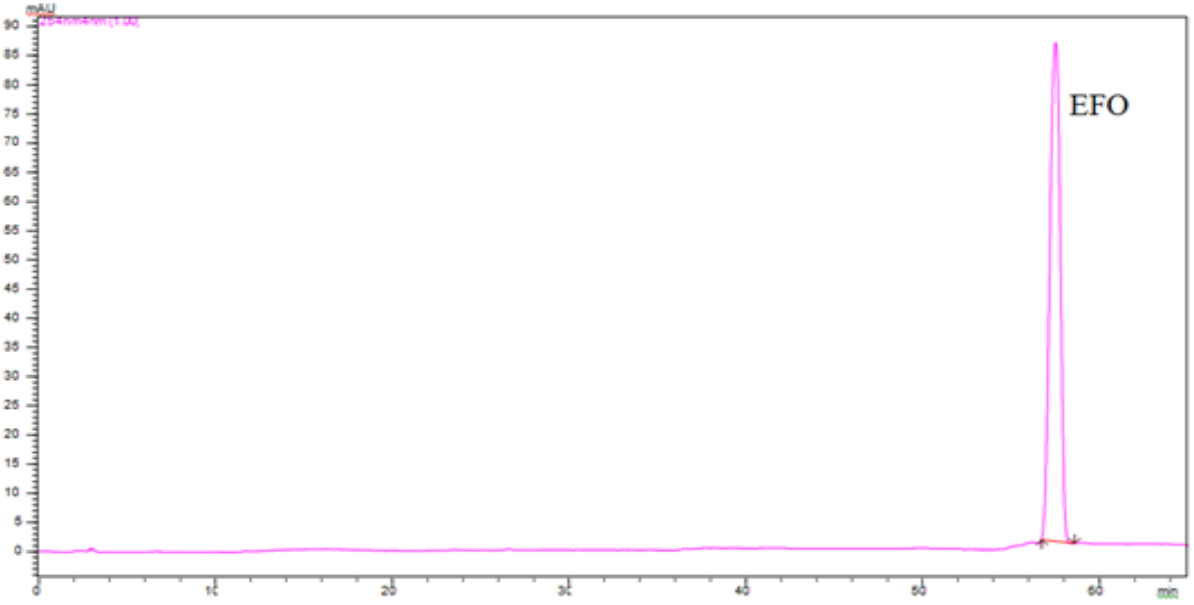

Fig.7. 18 - Chromatogram of dry thermal degradation (API)

7.4.2.3.5. Photolytic degradation - No degradation was observed when EFO was subjected to photolytic condition (dry) for 11days (Fig.7.19) . Slight degradation (11.6 %) was observed in EFO was subjected to solution form in photolytic condition with the formation of degradation products DP 10, DP 9, DP8 and DP7 min at retention time of 11.67 min(1.7%), 30.01 min (0.48%), 55.92 (8.1%) and 31.9 (0.98%)min respectively (Fig. 7.20).

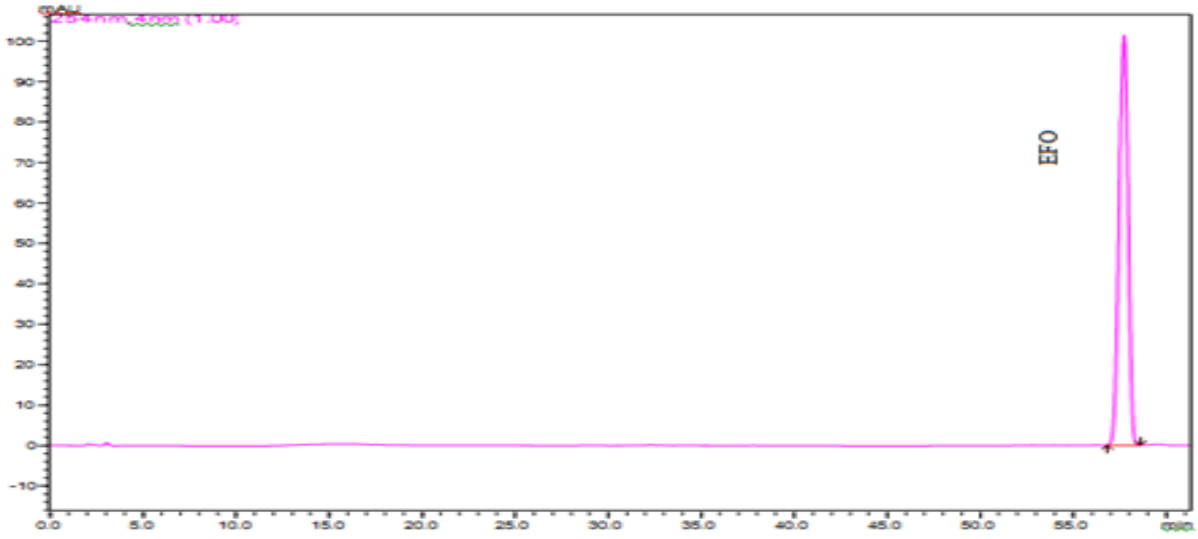

Fig.7. 19- Chromatogram of photolytic degradation (dry) (API)

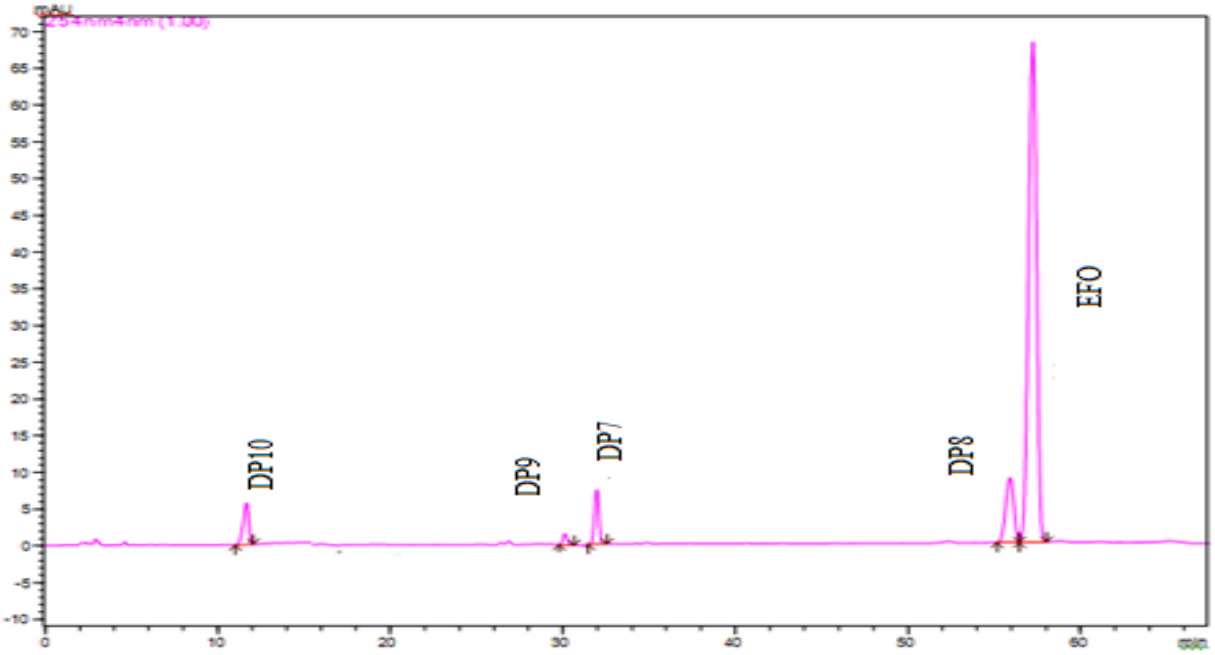

Fig.7. 20- Chromatogram of photolytic degradation (Solution)(API)

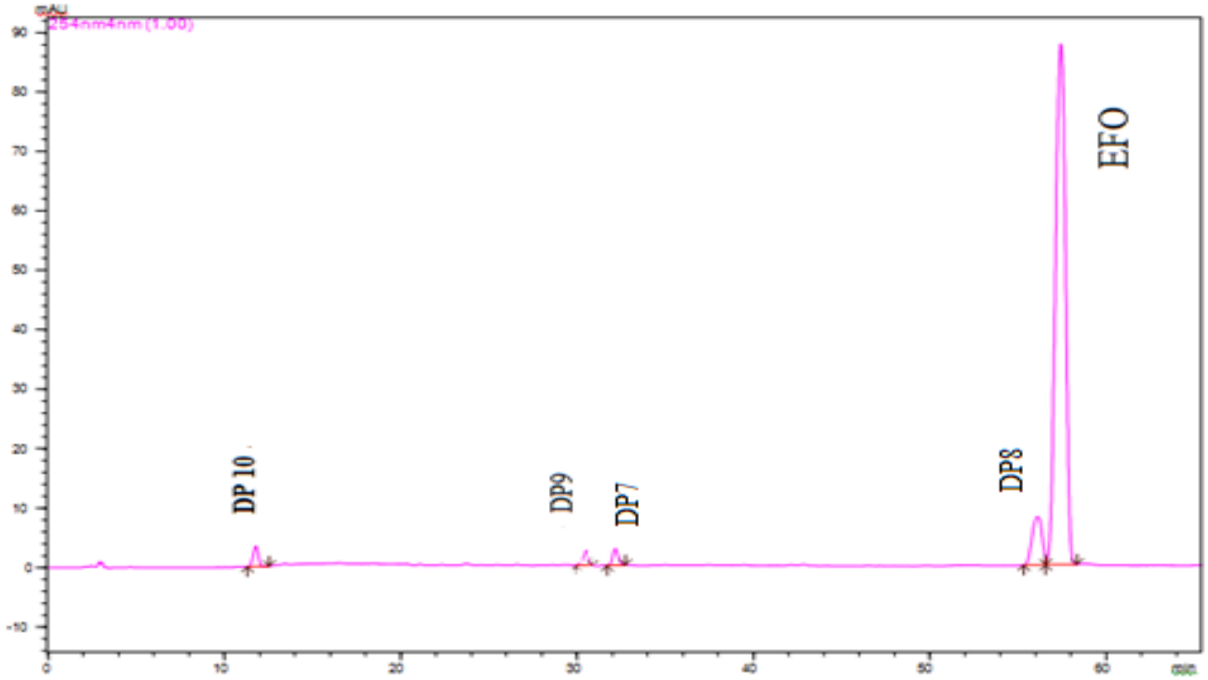

Fig.7. 21- Chromatogram of photolytic degradation (Solution) (formulation)

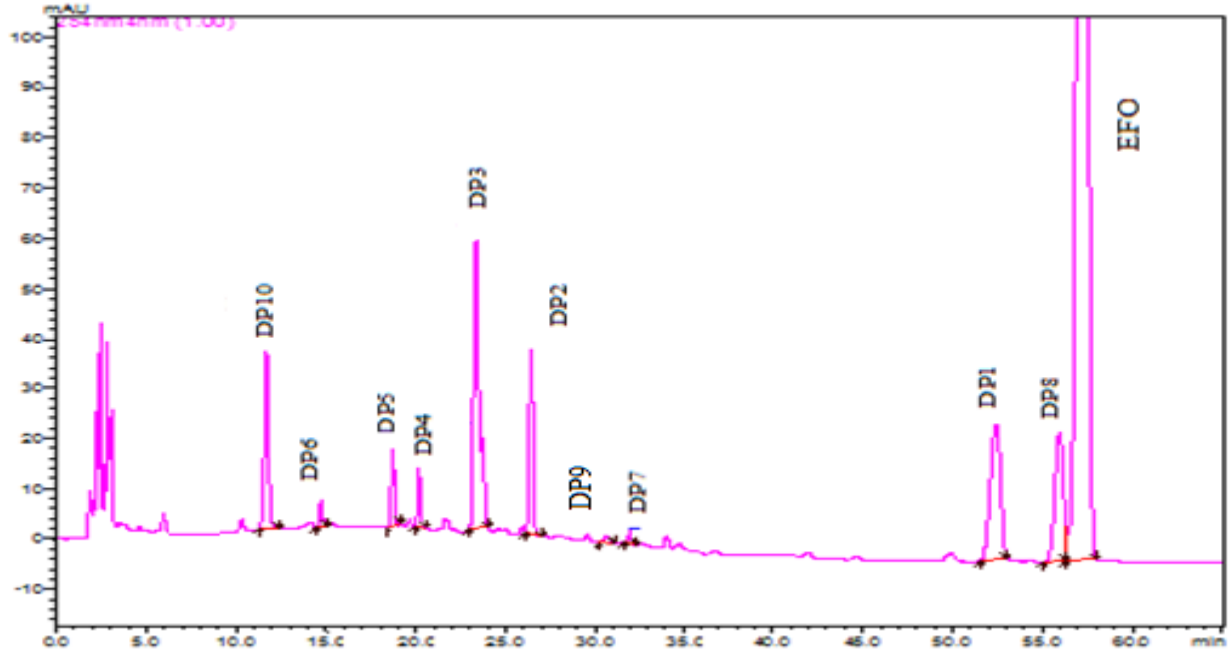

Fig.7. 22- Chromatogram of combined degradation products of all stressors

Table 7. 22- Summary of forced degradation of EFO

Stressor	Conditions	RT of Degradation Products	% of Degradation Products in API	% of Degradation products in Formulation
Acid	1 M HCl at 80ºC for 6 hrs	--	---	---
Alkaline	0.5 M NaOH at RT(40ºC) for 6 hrs	14.33(DP6) 18.83(DP5) 20.29(DP4) 24.09(DP3) 26.66(DP2) 52.91(DP1)	0.63% 0.66% 2.17% 8.8% 4.01% 28.14% (44.18%)	0.60% 0.60% 2.1% 9.1% 4.1% 27.8% (46.4%)
Oxidation	10% hydrogen peroxide at RT(40˚C) for 24 hrs	---	--	---
Thermal	Dry at 80℃ for 11 days	--	--	--
Photolytic	Dry for 11 days	--	--	--

	Solution for 11 days	11.67 min(DP10) 30.01min (DP9) 31.9 min(DP7) 55.92 min(DP8)	1.7% 0.48% 0.98% 8.1% (11.6%)	1.0% 0.42% 0.60% 7.8% 9.8%

7.5.2.4. Applicability of the developed method for the analysis of formulation

Forced degradation study was performed on formulation. The conditions were same as mentioned for API and were analyzed in the same way as that of API. The degradation products were separated. Minor variation was observed in the degradation of API and formulation as shown in Table 7.22.

7.5.3. DISCUSSIONS

Stability indicating method was developed for determination of EFO in presence of its degradation products. For separation of degradation products in alkaline conditions, various isocratic trials were performed by modifying ammonium acetate buffer from 35% to 55%, in pH range from 3 to 6, various gradient trials were performed. For separation of DP8 from EFO various gradient trials were performed. Finally separation of degradation products in alkaline conditions and separation of DP8 from EFO was achieved with mobile phase with ammonium acetate pH 5.8 and acetonitrile in gradient mode as shown in Table 8.12. In forced degradation study, significant degradation (44.18%) was observed in alkaline condition with the formation of formation of degradation products DP1, DP2, DP3, DP4, DP5 and DP6. Slight degradation (11.6%) was observed in photolytic conditions with the formation of degradation products DP7, DP8, DP9 and DP10. No degradation was observed in acidic, oxidative, thermal and photolytic condition (dry state) as there was not any additional peak in the chromatogram and peak height of EFO was not reduced.

7.6. SECTION - C

DEGRADATION KINETIC STUDY OF EFONIDIPINE HCL ETHANOLATE BY HPLC METHOD

The degradation kinetics was studied for alkaline degradation since EFO was susceptible to alkaline condition.

7.6.1. EXPERIMENTAL

7.6.1.1. Chemicals and Reagents

The chemicals and reagents used in the present section were same as those mentioned in section 7.4.1.1.

7.6.1.2. Equipments and Chromatographic Conditions

Equipments and chromatographic conditions were same as those mentioned in section 8.4.1.2.

7.6.1.3. Preparation of stock, sample and buffer solutions

Stock solution was same as those mentioned in section 8.5.1.5.2. To the 5 mL of stock solution of EFO in 10 mL of volumetric flask. , 5 mL of 0.1M/0.5M/1 M NaOH was added. The solutions were kept at RT (40ºC) / 50˚C/60ºC from 2 hrs to 10 hrs. From this 2 mL of solution was taken and neutralized with 0.1M/0.5 M/ 1M HCl and solution was made up to volume with mobile phase to make the concentration 100µg/mL and injected into the HPLC system.

7.6.2. RESULTS

A regular decrease in concentration of EFO was observed with increasing time intervals and with increase in temperature. Regression equation and regression coefficient was obtained for zero order and first order kinetics for different concentration of NaOH and at different temperatures. On the basis of regression, degradation follows first-order kinetics since r^2 values are highest (close to 1) (Table 7.23).

On the basis of first-order kinetics, further study was performed to study the effect of temperature on the rate constant the Arrhenius plots were plotted (log of rate constant versus

reciprocal of temperature). Arrhenius plot was obtained by plotting lnK versus 1/T. Graph was linear in the temperature range. The first order kinetic plot and Arrhenius plot for alkaline degradation are shown in Fig 7.23-7.28. The values of degradation rate constant, half-life and activation energy are shown in Table 7.24.

Table 7. 23- r^2 value and Regression Equation for zero order, first order reaction for alkaline degradation

S.No.	Conc. of NaOH	Temp. (°C)	r^2		Regression Equation	
			Zero order	First order	Zero order	First order
1	0.1 M	40	0.946	0.970	y=-4.735x+104.7	y=-0.026x+2.035
		50	0.977	0.998	y=-6.21x+87.02	y=-0.055x+2.004
		60	0.969	0.988	y=-6.17x+66.04	y=-0.106x+2.005
2	0.5 M	40	0.898	0.959	y=-6.49x+98.18	y=-0.046x+2.030
		50	0.965	0.966	y=-5.135x+58.59	y=-0.089x+1.912
		60	0.941	0.997	y=-4.22x+43.52	y=-0.115x+1.838
3	1.0 M	40	0.986	0.952	y=-6.71x|+77.89	y=-0.090x+2.047
		50	0.895	0.993	y=-5.76x+53.6	y=-0.167x+2.056
		60	0.834	0.941	y=-2.94x+26.9	y=-0.197x+1.869

Table 7. 24- Degradation rate constant, half-life and Activation Energy Ea for first order kinetics of alkaline degradation

S.No.	Conc. of NaOH	Temp(˚C)	K	$t_{(1/2)}$ hrs	Ea(KJ/mole)
1	0.1M	40	0.059	11.57	9.65KJ/mole
		50	0.126	5.47	
		60	0.244	2.83	
2	0.5M	40	0.105	6.54	
		50	0.204	3.38	
		60	0.264	2.61	
3	1.0 M	40	0.221	3.13	
		50	0.384	1.8	
		60	0.453	1.52	

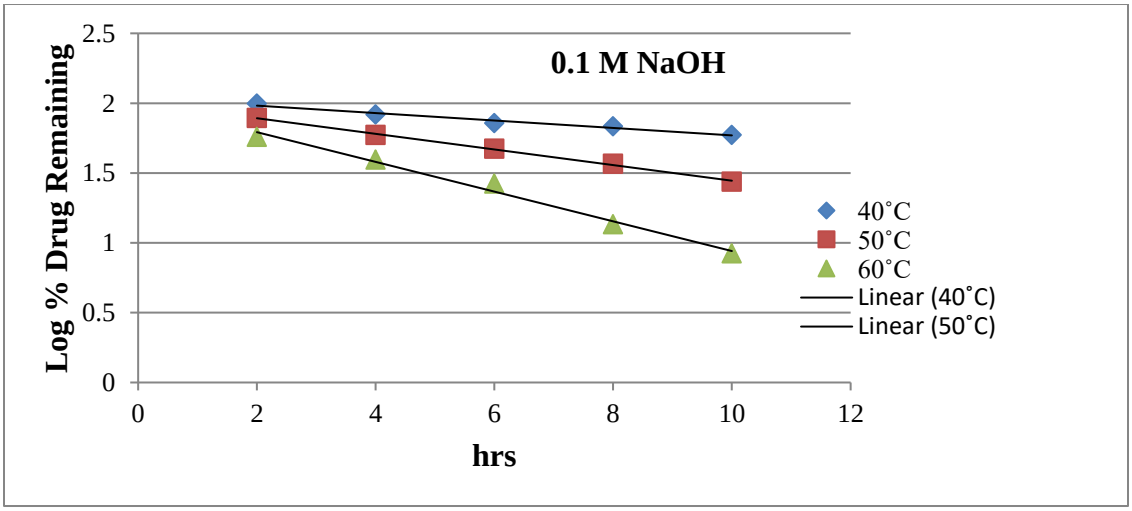

Fig.7. 23 - First order kinetics of 0.1 M NaOH

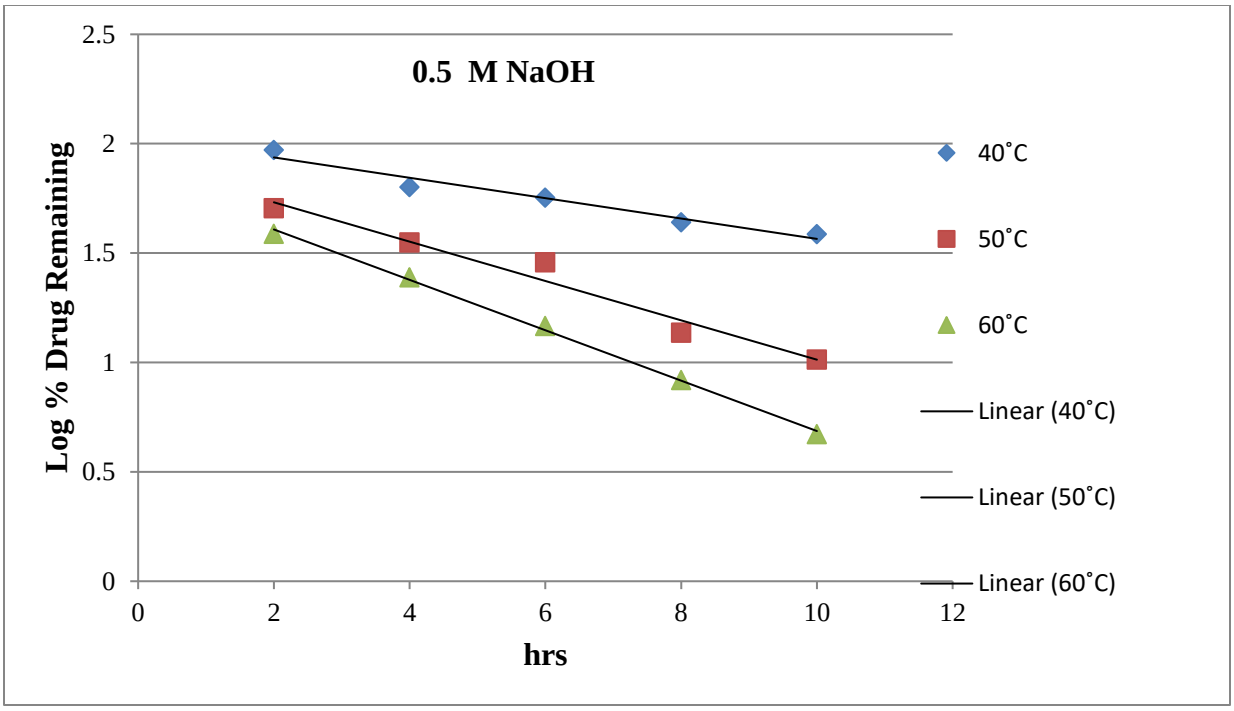

Fig.7. 24- First order kinetics of 0.5 M NaOH

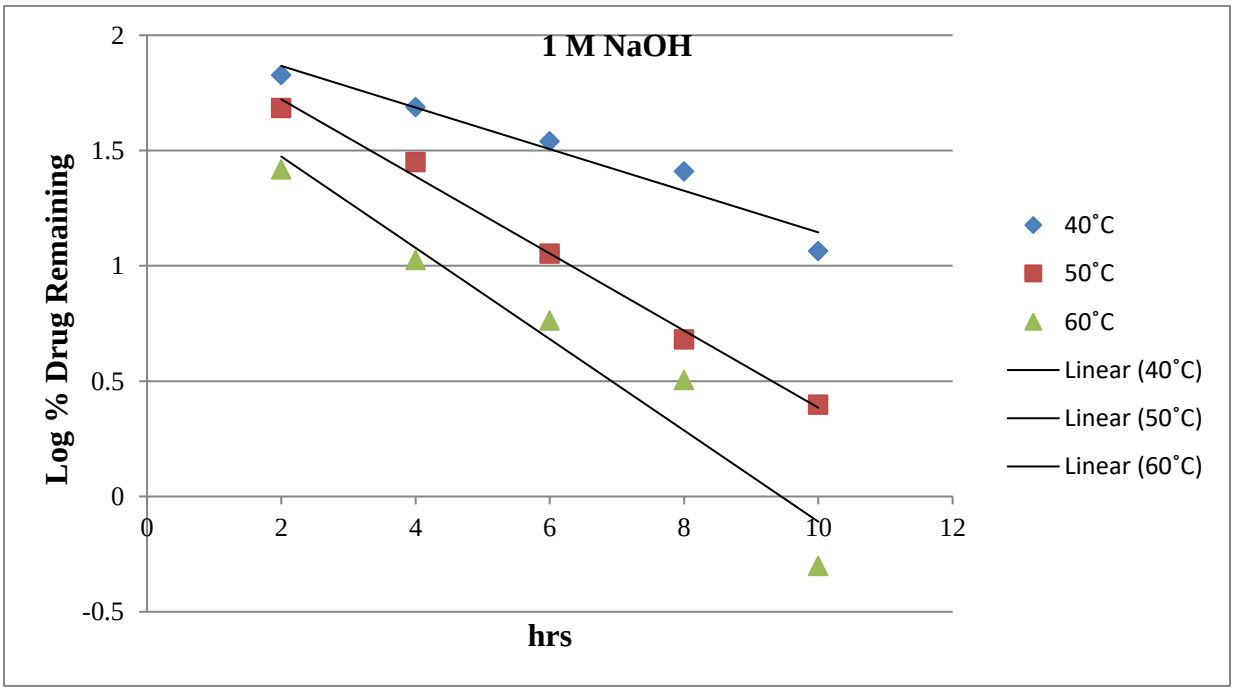

Fig.7. 25- First order kinetics of 1 M NaOH

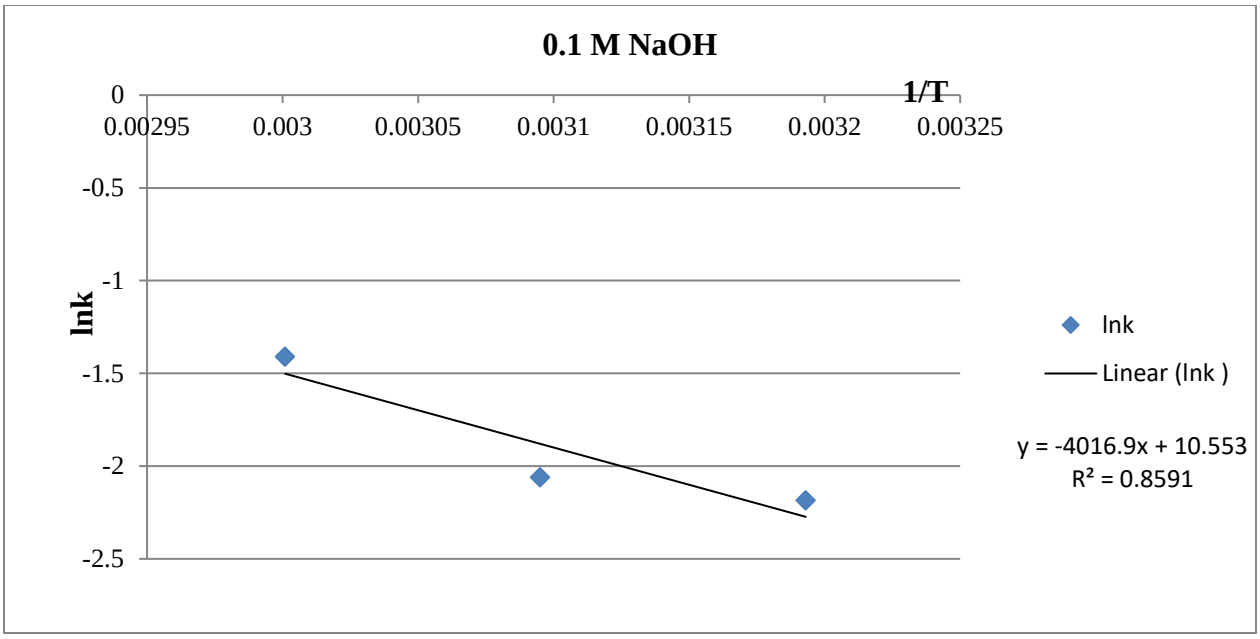

Fig.7. 26- Activation energy plot for 0.1 M NaOH

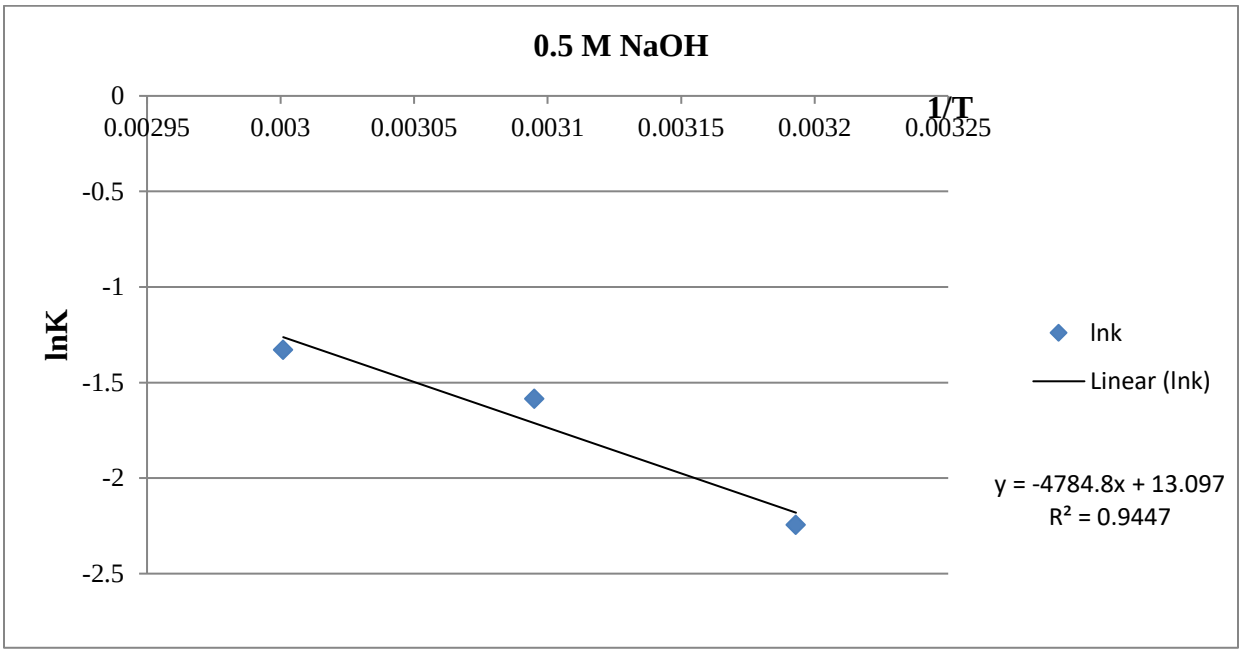

Fig.7. 27- Activation energy plot for 0.5 M NaOH

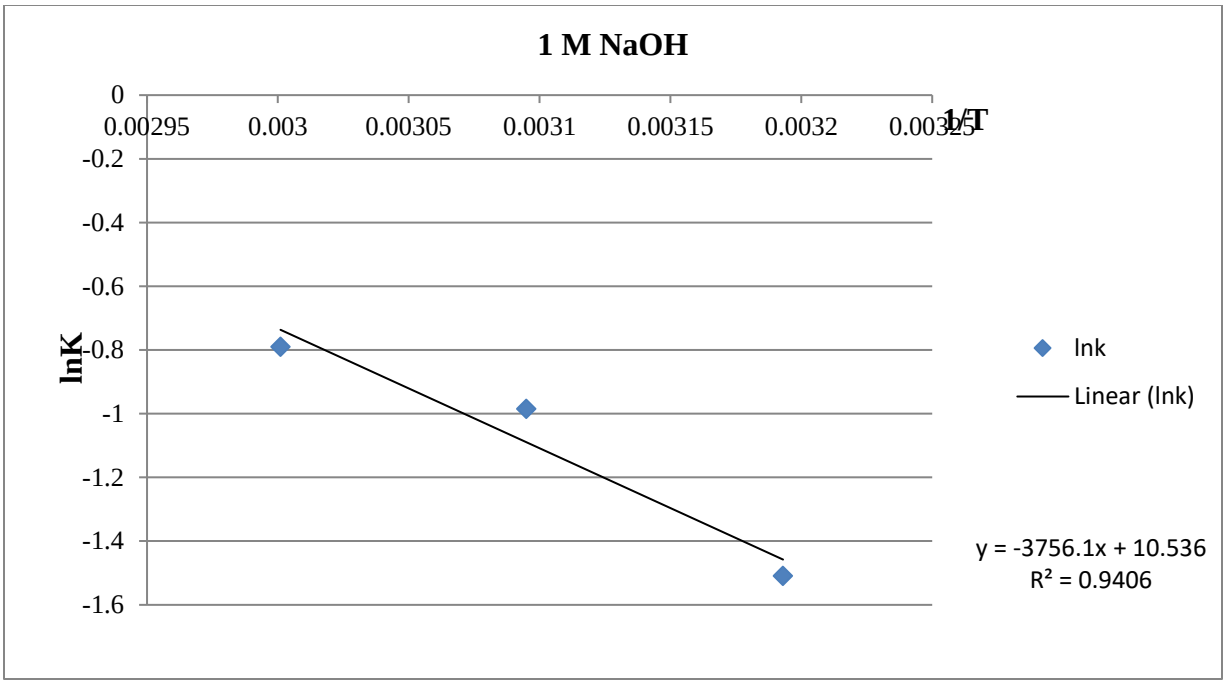

Fig.7. 28- Activation energy plot for 1 M NaOH

7.6.3. DISCUSSIONS

Degradation kinetics was performed for alkaline conditions. Factors taken for kinetics study were: concentration of sodium hydroxide (0.1 M, 0.5M and 1M), temperature (40º, 50ºand 60º C), and time (2 to 10 hrs). Zero order kinetics study was performed by plotting graph between % drug remaining versus time and first order by plotting graph between log % Drug remaining versus time. Regression equation and regression coefficient were obtained for both zero and first order kinetics. Degradation follows first-order kinetics since regression coefficient r^2 *was* highest in first –order kinetics. Based on this degradation rate constant and half-life was calculated. On the basis of degradation rate constant by plotting lnk (rate constant) versus 1/T, activation energy was calculated which was found to be 9.65 KJ/mole.

7.7. SECTION - D

ISOLATION AND CHARACTERIZATION OF MAJOR DEGRADATION PRODUCTS OFEFONIDIPINE HCL ETHANOLATE

7.7.1. EXPERIMENTAL

7.7.1.1. Chemicals and Reagents

Chemicals and reagents used in the present section are same as those mentioned in 7.4.1.1.

7.7.1.2. Equipments and chromatographic conditions

Preparative HPLC **c**hromatographic separation was performed on Shimadzu (Shimadzu Corporation, Kyoto, Japan) chromatographic system equipped with Shimadzu LC-20AP pump (binary) and Shimadzu SPD-20A uv-visible detector. Samples were injected through Rheodyne 7725 injector valve. Data acquisition and integration was performed using Class VP software. Phenomenex Luna column C 18 (250X 50 mm, 10µ) was used for isolation of degradation products. The flow rate was kept at 50 mL/min. Detection was performed at 254 nm. The gradient programme was (time/% Acetonitrile): 0/5, 90/40,120 /80.

Attached proton test in ^{13} CNMR was performed , indicated presence of quaternary carbon and methylene as negative peaks, methyl and methine groups as positive peaks.

LC-Q-TOF-MS system (Agilent Technologies, Inc, United States) comprising of 1290 Infinity UHPLC system, 1260 infinity Nano HPLC with Chipcube, 6550 ifunnel Q-TOF. Chemstation-LC control software was used for mass spectroscopic studies.

Major degradation products formed were DP1, DP3 and DP4 in alkaline hydrolysis.

7.7.1.3. Enrichment and analysis of alkaline degradation samples

1 g of EFO was weighed accurately and transferred to 50 mL of volumetric flask. To this was added 30 mL of methanol and 20 mL of 0.5 M NaOH. The solution was kept at room temperature (40ºC) for 48 hrs. The solution was neutralized with 0.5 M HCl and analysed by analytical HPLC as mentioned in section 7.5.1.5.2. The degradation samples in alkaline conditions were diluted to respective concentration and were analysed as mentioned in section

7.5.1.5.2. In alkaline condition total six degradation products, DP1-DP6 (Fig. 7.29) are formed, DP1, DP3 and DP4 formed with 50%, 25% and 10% area by normalization were considered major degradation products and studied further.

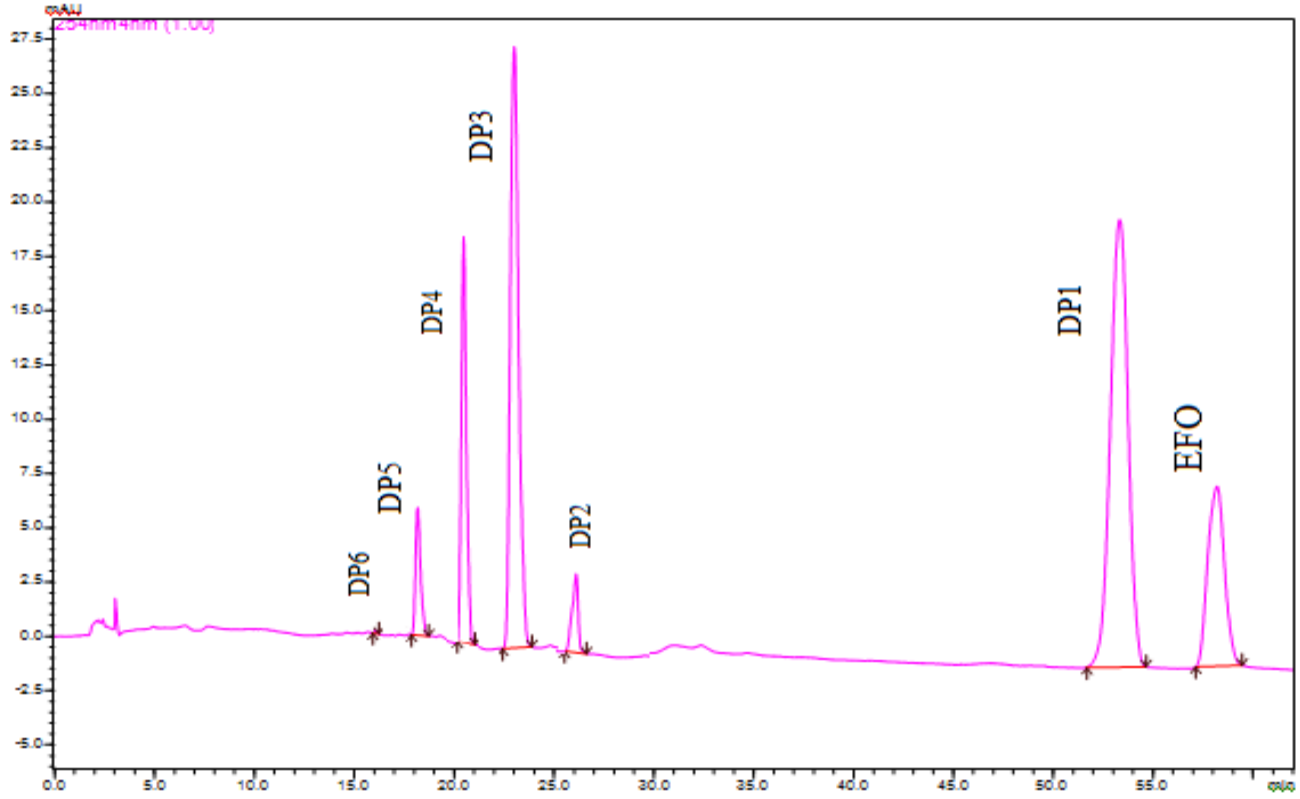

Fig.7. 29- Chromatogram of alkaline condition for isolation

7.7.1.4. Isolation of degradation products by preparative HPLC

Fraction of greater than 97% purity collected from preparative HPLC were pooled together. To remove acetonitrile, solutions were concentrated on rotavapour. For confirmation of retention time of isolated impurity, isolated fractions were analyzed by HPLC. The solutions were dried in lyophilizer. DP1, DP3 and DP4 were obtained as white solids with % purity of 99.1, 99.4 and 99.2% respectively. Chromatogram of isolated DP1, DP3 and DP4 are shown in Fig. 7.30.

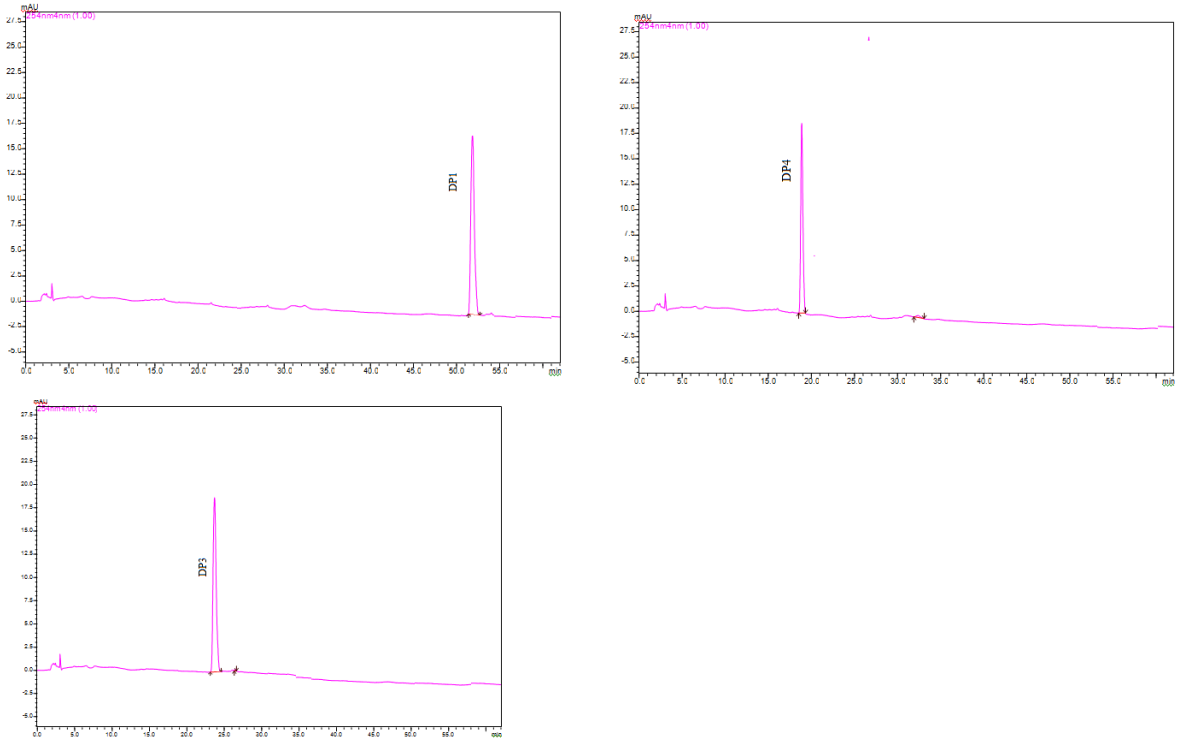

Fig.7. 30- Chromatogram of isolated DP1, DP3 and DP4

7.7.2. RESULTS AND DISCUSSIONS

7.7.2. 1. Structural characterization of EFO and degradation products

Spectral data of EFO was obtained so as to understand the spectral changes in degradation products to elucidate the structures.

7.7.2.1.1. Characterisation of EFO

Mass spectra

ESI-MS/MS spectrum of EFO is provided in Fig. 7.31(a). Molecular mass of Efonidipine HCl ethanolate is $C_{36}H_{45}ClN_3O_8P$. EFO shows protonated mass 632.2500 (Calculated 632.2524) which corresponds to the molecular formula $C_{34}H_{38}N_3O_7P$. EFO shows corresponding mass of Efonidipine base. HCl and Ethanolate masses are absent in mass spectra since their masses are less than 50 m/z and ethanol is volatile so its mass is absent in mass spectra. Mass spectra of EFO shows protonated molecular ion at *m/z* of 632.

EFO undergoes fragmentation at *m/z* of 562 (loss of C_4H_5O from *m/z* 632), 449 (loss of N-benzyl amino group from *m/z* 632), 405(loss of ethoxy group from *m/z* 449), 337(loss of C_5H_8 from *m/z* 405), 210 (loss of $C_{19}H_{22}N_2O_7P^+$ from *m/z* 632). Fragmentation pathway of EFO is shown in Fig. 7.31 (b).

NMR spectra

In ^{1}H NMR spectra of EFO, protons of methyl group are present at position 0.86-0.87, 0.93, 2.20 and 2.26-2.27 ppm. Protons of methylene group are present at 3.59-3.70, 3.99-4.00, 4.22-4.30 and 4.58 ppm. Proton of -CH- in dihydropyridine ring is present at 4.75-4.78 ppm. Protons corresponding to aromatic nitro group are present at 7.4, 7.5, 7.9 and 8.0 ppm respectively.

A ^{13}CNMR spectrum of EFO indicates presence of ester group at 166.41 ppm. APT spectra of EFO shows four methyl groups and methine group as positive peaks and five methylene groups as negative peaks (Table 7.25).

IR SPECTRA

In IR spectra of EFO, secondary amino group is present at 3435cm^{-1}, aromatic groups are present at 3185 and 3083cm^{-1}. Methyl groups are present at 2967 cm^{-1}, methylene groups are present at 3083cm^{-1}. Ester group is present at 1705cm^{-1} and cyclic ether group is present at 1645cm^{-1} (Table 7.29 and Fig. 7.35).

7.7.2.1.2. Characterisation of DP1

Mass spectra

ESI-MS/MS spectrum of DP1 is shown in Fig 7.36 (a). ESI-MS/MS spectra of DP1 shows protonated molecular ion peak at m/z of 664 with elemental composition $C_{35}H_{42}N_3O_8P^+$. DP1 has 32 m/z more than EFO.

On fragmentation of DP1 , product ions are formed at *m/z* of 608(loss of C_3H_3O from 664), m/z 481 (loss of $C_{13}H_{12}N$ from *m/z* 664), *m/z* 437(loss of $C_6H_{13}NO_6P$ from 664), m/z 351(loss of $C_{17}H_{23}O$ from *m/z* 608), *m/z* 269 (loss of $C_{16}H_{23}N_2O_4P^+$ from 608), m/z 210 (loss of $C_{14}H_{13}NO_2^+$ from m/z 437), *m/z* 181(loss of C_2H_5 from *m/z* 210). Fragmentation pathway of DP1 is shown in Fig. 7.36 (b).

NMR spectra

In DP1, there is ring opening of phosphinane ring which is indicated by shifting of methylene protons from 3.99 ppm-4.05 ppm to 3.31-3.34 ppm and 3.51-3.55 ppm. Addition of 3 protons from methyl group is indicated by chemical shift at 3.35-3.42 ppm and presence of one –OH group is indicated at 3.42-3.43 ppm. In ^{13}C NMR spectra of DP1, methylene groups in phosphinane ring are shifted from 74 ppm to 69.89 ppm and 66.41 ppm. Formation of additional methyl groups is indicated at 51.35 ppm. This indicates opening of phosphinane ring and esterification by methanol (Table 7.26).

IR spectra

IR spectra of DP1 (Fig. 7.40, Table 7.29) indicates formation of broad peak covering hydroxyl group and –NH group. Broad peak is observed in the bending region covering 1705, 1598, 1775 cm^{-1}. Peak at 1645 cm-1 in EFO has been disappeared in DP1, formation of peak at 1598 and 1574 cm^{-1} indicated ring opening of phosphinane ring with the formation of P-OH group and esterification with methanol.

Mechanism of formation of DP1

In alkaline hydrolysis, there is ring opening of phosphinane ring and nucleophilic attack of methoxide ion on carbocation, proton is abstracted by negatively charged oxygen and there is formation of DP1 [15] (Fig. 7.36 c).

DP1 is characterized as 3-2-(N-benzylanilino) ethyl 3-oxo-2, 2-dimethylpropyl hydrogen 1,4-dihydro-2,6-dimethyl-4-(3-nitrophenyl)pyridin-3-yl-3-phosphonate.

7.7.2.1.3. Characterisation of DP3

Mass spectra

An ESI-MS/MS spectrum of DP3 is provided in Fig. 7.41 a. DP3 is formed with protonated molecular m/z of 228 which is 404 m/z less the parent EFO.

The mass fragmentation from 228 also confirm this (Fig.7.41b) .From DP3, $C_{15}H_{18}NO^{+}$, fragments are formed with *m/z* 209 (loss of hydronium ion from m/z 228), m/z 180 (loss of ethyl

group from m/z 209), m/z 160 (loss of C_4H from m/z 209), m/z 122 (loss of C_7H_6O from m/z 228), *m/z* 102 (loss of C_6H_6 from *m/z* 180), m/z 86 (loss of $C_{11}H_{10}$ from *m/z* 228) respectively.

NMR spectra

NMR is not showing the methyl and methylene proton peaks at 0.87-2.27 and 4.43-3.99 ppm and aromatic nitro ring at 8.00-7.4 ppm. A broad peak at 4.69 ppm appears which may be due to hydroxyl group. Absence of methyl and methylene protons are further confirmed by ^{13}C NMR as peaks at 17.48, 17.58 and 18.59 ppm are absent and ester group at 166.41 ppm are also absent (Table 7.27).

IR spectra

Absence of ester group is further confirmed by IR where carbonyl peak of EFO at 1705 cm^{-1} is absent.

Mechanism of formation of DP3

EFO contains ester functional group. There is a nucleophilic attack of hydroxide ion on ester, carbonyl bond is broken and there is formation of tetrahedral intermediate. Tetrahedral intermediate collapses reforming the carbonyl group leaves 2-(N-benzyl-N-phenylamino) ethoxide ion. 2-(N-benzyl-N-phenylamino) ethoxide ion abstracts proton to form the corresponding acid and forms DP3 that is 2-(N-benzyl-N-phenylamino) ethanol (Fig. 7.41c).

Based on the above DP3 is characterized as 2-(N-benzyl-N-phenyl amino) ethanol.

7.7.2.1.4. Characterisation of DP4

Mass spectra

An ESI-MS/MS spectrum of DP4 is provided in Fig. 7.46 (a). ESI-MS/MS spectra shows protonated molecular ion peak at m/z 469 with elemental composition $C_{21}H_{29}N_2O_8P^+$. DP4 shows fragment ions of m/z of 422 (loss of CH_2O_2) and m/z 271 (loss of $C_6H_{14}O_5P^+$).Fragment ion of m/z 422 undergoes further fragmentation to produce ions at *m/z* 351(loss of C_5H_{11} from *m/z* 422), *m/z* 243 (loss of $C_2H_5O_3P$ from 351) and *m/z* 181 (loss of $C_{14}H_{13}N_2O_2$ from *m/z* 422).Fragmentation pathway of DP4 is provided in Fig. 7.46 (b).

NMR spectra

In ^{1}H NMR spectra of DP4, there are absence of two rings which are indicated by absence of peaks in the region from 6.3 to 7.14 ppm, absence of two methylene protons are indicated by absence of peak at 3.59 ppm and 3.62 ppm. Formation of two methyl groups are indicated at 4.58, 4.30-4.22 ppm and there is formation of one hydroxyl group at 3.29-3.28 ppm. One of the methylene groups is shifted to 3.63-3.51 ppm. ^{13}C NMR spectra of DP4 indicate absence of aromatic rings, absence of two methylene groups at 53 ppm and 60 ppm. Esterification with methanol and formation of additional methyl group is indicated at 51.20 and 51.15 ppm. DP4 might have been formed from DP1 by hydrolysis at ester linkage with the loss of two aromatic rings and esterification with co-solvent methanol (Table 7.28).

IR spectra

An IR spectrum of DP4 indicates broad peak covering –OH group and –NH group. Presence of aromatic ring is indicated in the region of 3192 and 3166 cm^{-1}.Methyl groups are indicated in the region of 2951, 2873 and 2848 cm^{-1} . Opening of phosphinane ring and further etherification by methanol is shown by ether linkage at 1645cm^{-1} (Fig.7.50 and Table 7.29).

Mechanism of formation of DP4

DP4 is formed from DP1 by alkaline hydrolysis. In DP1, there nucleophilic attack of methoxide ion to carbonyl carbon and there is formation of tetrahedral intermediate. With further loss of benzyl phenyl ethyl amino group there is formation of DP4 (Fig.7.46 c).

Based on the above, DP4 is characterized as 3-methoxy-2,2-dimethylpropyl hydrogen 1,4-dihydro-2,6-dimethyl-5-methyloxycarbonyl-4-(3-nitro)phenylpyridin-3-yl-3-phosphonate.

Table 7. 25 - NMR assignments of EFO

EFO

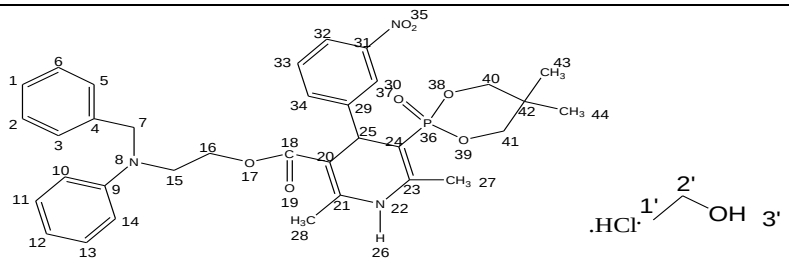

Position	^{1}H (Fig. 7.32)	Chemical Shift(δ ppm)	Position	^{13} C(Fig. 7.33)	APT* (Fig. 7.34)
22	1H	9.4,s, -NH absent in D_2O exchange	18	166.41	Ester
30, 32, 33, 34	4H	8.00-7.98,d, 8.00-7.98,d, 7.52-7.48,t, 7.6-7.58,d, 7.6	1, 2, 3, 5, 6	127.16, 129.09, 129.09, 128.28, 128.28	Aromatic –CH-
1, 2, 3, 5, 6	5H	6.9,m,7.1,m,6.9,m, 6.9,m, 7.1,m	9	148.29	Quaternary carbon
10, 11,12, 13, 14	5H	6.3,s,7.1-6.99,m, 6.2,s,7.1-6.99,m, 6.1, s,	4	147.5	Quaternary carbon
25	1H	4.75-4.78,d	10	98.97	Aromatic –CH-
7	2H	4.58,s	11, 12, 13, 14	129.63, 121.4, 129.63, 98.89	Aromatic –CH-
16	2H	4.30-4.22,m	20, 21, 23, 24	98.97, 148.99, 147.67, 92.47	Quaternary carbon

15	2H	4.05-3.99,m	29, 31,	147.50, 148.06	Quaternary carbon
40	2H	4.0 -3.99,m	30, 32, 33,34	121.46, 121.24, 133.88, 133.86	Aromatic –CH-
41	2H	3.70 -3.59,m	40	74.16	$-CH_2$
27	3H	2.27-2.26,d	41	74.10	$-CH_2$
28	3H	2.20,d	16	74.16	$-CH_2$
43	3H	0.93,d	15	60.12	$-CH_2$
44	3H	0.87-0.86,d	7	56.0	$-CH_2$
1’	3H	1.07-1.05,t	42	38.62	Quaternary carbon
2’	2H	3.47-3.42,m	43	21.02	$-CH_3$
3’	-OH	6.72 broad peak	44	21.02	$-CH_3$
			25	18.53	-CH-
			27, 28	17.48, 17.51	$-CH_3$

*(CH_3 and CH signals positive, $CH_2$and quaternary carbon negative)

Table 7. 26 - NMR assignments of DP1

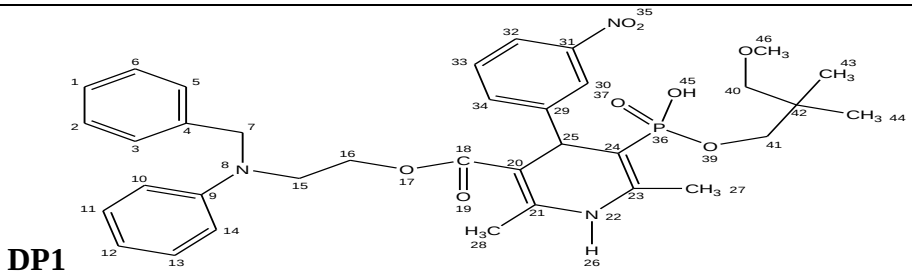

DP1

Position	**^{1}H (Fig. 7.37)**	**Chemical Shift(δ ppm)**	**Position**	**^{13} C(Fig. 7.38)**	**APT* (Fig. 7.39)**
22	1H	9.16,s	18	166.64	Ester group
1, 2, 3, 5, 6	5H	7.16-7.13,t, 7.29-7.25,t, 6.60-6.56,t, 7.16-7.14,t, 7.29-7.25,t	1, 2, 3, 5, 6	129.56, 129.56, 126.59, 126.59, 129.56	Aromatic -CH
10, 11, 12, 13, 14	5H	7.10-7.07,t, 7.22-7.18,t, 6.66-6.63,m, 7.10-7.07, t, 6.66-6.63, m	4	138.86	Quaternary carbon
30, 32, 33, 34	1H	8.04-8.00,t, 8.04-8.00,t, 7.53-7.49,t, 7.62-7.64,d	9	149.47	Quaternary carbon
25	1H	4.81,t	10, 11, 12, 13, 14	115.99, 129.68, 121.20, 129.68, 115.99	Aromatic -CH
7	2H	4.52-4.49,d	20, 21, 23, 24	98.98, 149.63, 147.59, 93.69	Quaternary carbon
16	2H	4.205-4.17, m	29, 31	146.81, 147.67	Quaternary carbon
15	2H	3.66-3.50,m	30, 32, 33, 34	121.68, 121.68, 129.68,134.15	Aromatic -CH-
40	2H	3.55-3.51,m, 3.34-	40	69.89	$-CH_2$

		3.31,m			
45	1H	3.43-3.42,m	41	66.41	$-CH_2$
46	3H	3.42-3.35,m	16	60.52	$-CH_2$
41	2H	3.07-2.97,m	15	53.79	$-CH_2$
27	3H	2.17,m	46	51.35	$-CH_3$
28	3H	2.21,m	7	49.40	$-CH_2$
43	3H	0.70,d	42	36.17	Quaternary carbon
44	3H	0.69,d	25	18.54	-CH-
			43	17.47	$-CH_3$
			44	18.49	$-CH_3$

*(CH_3 and CH signals positive, $CH_2$and quaternary carbon negative)

Table 7. 27- NMR assignments of DP3

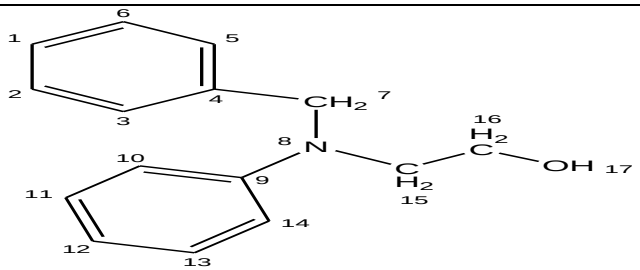

DP3

Position	**^{1}H(Fig. 7.42)**	**Chemical Shift(δ ppm)**	**Position**	**^{13} C (Fig. 7.43)**	**APT (Fig. 7.44)**
1, 2, 3, 5,	5H	7.13-7.11,d, 7.23-7.19,t,	9	149.6	Quaternary

6		7.02-6.99,t, 7.02-6.99,t, 7.23-7.19,t			carbon
10,11, 12, 13, 14	5H	6.59-6.56,d, 7.13-7.11,t, 6.49-6.45,t, 7.13-7.11,t, 6.59-6.56,d	10, 11, 12, 13, 14	111.70, 128.91,115.40, 128.91, 111.70	Aromatic –CH-
17	---	4.69, broad peak	1, 2, 3, 5,6	126.34,128.37, 126.48,126.48, 128.37	Aromatic –CH-
7	2H	4.51,s	4	139.26	Quaternary carbon
15	2H	3.44-3.40,t	16	58.28	$-CH_2$
16	2H	3.54-3.51,t	15	53.96	$-CH_2$
			7	53.17	$-CH_2$

Table 7. 28- NMR assignments of DP4

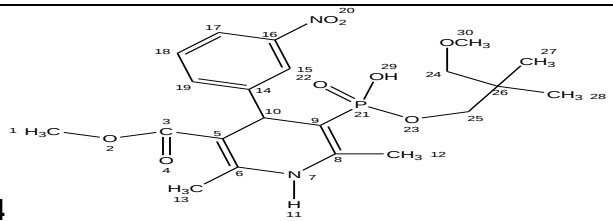

DP4

Position	**^{1}H(Fig. 7.47)**	**Chemical Shift(δ ppm)**	**Position**	**^{13} C(Fig. 7.48)**	**APT (Fig. 7.49)**
7	1H	9.2	3	167.03	Ester

			5, 6, 8, 9	99.12, 149.58, 147.25, 95.63	Quaternary carbon
15, 17, 18, 19	4H	8.0-7.99,t, 8.0-7.99,t, 7.57-7.53,t, 7.63-7.61,t	14, 16	146.71, 149.54	Quaternary carbon
10	1H	4.77-4.72,t	15, 17, 18, 19	121.71, 121.19, 129.6, 135.08	Aromatic –CH-
1	3H	3.63-3.51,t	24	69.86	$-CH_2$
24	2H	3.50-3.44,m	25	66.38	$-CH_2$
30	3H	3.45-3.35,m	1	51.15	$-CH_3$
29	-OH, absent in D_2O exchange	3.33-3.28,m	30	51.39	$-CH_3$
25	2H	3.0-2.9,m	26	36.16	Quaternary carbon
12	3H	2.28-2.14,d	27	20.75	$-CH_3$
13	3H	2.20-2.15,d	28	20.82	$-CH_3$
27	3H	0.69-0.68,d	10	18.45	-CH-
28	3H	0.61-0.56,d	12	18.38	$-CH_3$
			13	17.44	$-CH_3$

Table 7. 29- IR spectra interpretation of EFO, DP1, DP3 and DP4

EFO		**DP1**	
Wave number (cm^{-1})	Assignments	Wave number (cm^{-1})	Assignments
3435	-NH Stretch	3500	-OH stretch
3185, 3083	Aromatic C-H Stretch	3278	-NH Stretch
2967, 2860	Alkyl C-H stretch	3199, 3088, 3064	Aromatic C-H Stretch
1705	Ester C=O stretch	2872	Alkyl C-H stretch
1526, 1494	Aromatic nitro stretch	2444	Broad peak O=P-OH Stretch
1348, 1248	C-N stretch	1705	Ester
1102	P=O stretch	1598, 1574	O=P-OH Stretch
		1528, 1494	Aromatic nitro stretch
		1348, 1179	C-N stretch
DP4		**DP3**	
Wave number (cm^{-1})	Assignments	Wave number (cm^{-1})	Assignments
3500and	Broad peak covering –OH	3304	Broad peak –OH

3400	and –NH group		
3192, 3166	Aromatic C-H stretch	3000	Aromatic C-H stretch
2951, 2873, 2848	Alkyl C-H stretch	2970	Alkyl stretch
2444	O=P-OH Stretch	1591, 1432	Aromatic C=C Stretch
1740	Ester C=O stretch		
1644, 1628	O=P-OH Stretch	850	Out of plane bending
1530, 1497	Aromatic nitro stretch	640	Out of plane bending
1348, 1280	C-N Stretch		
1053	P=O stretch		

(a)

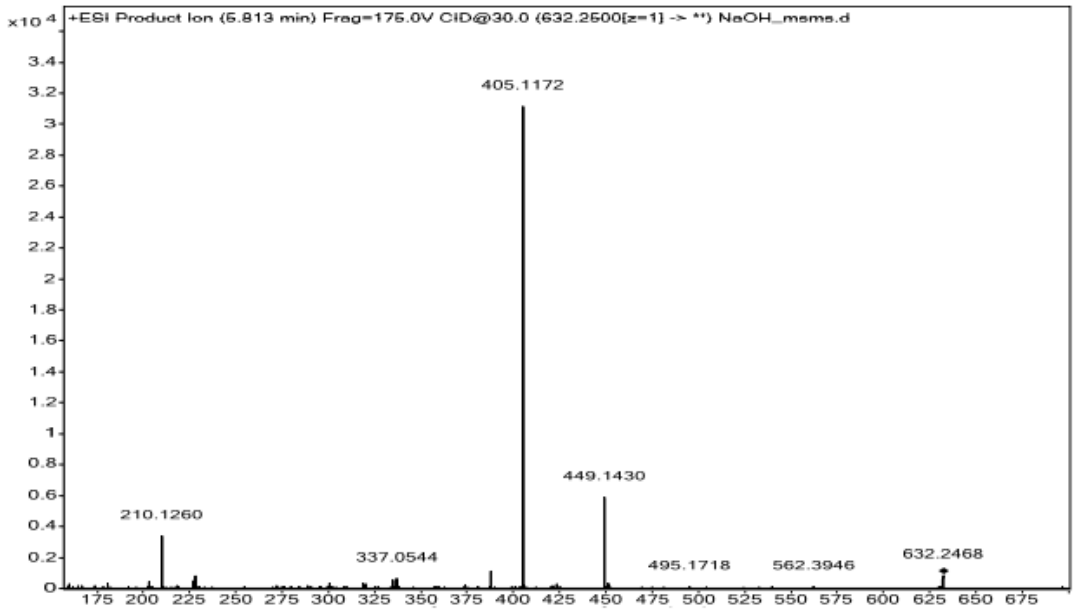

(b)

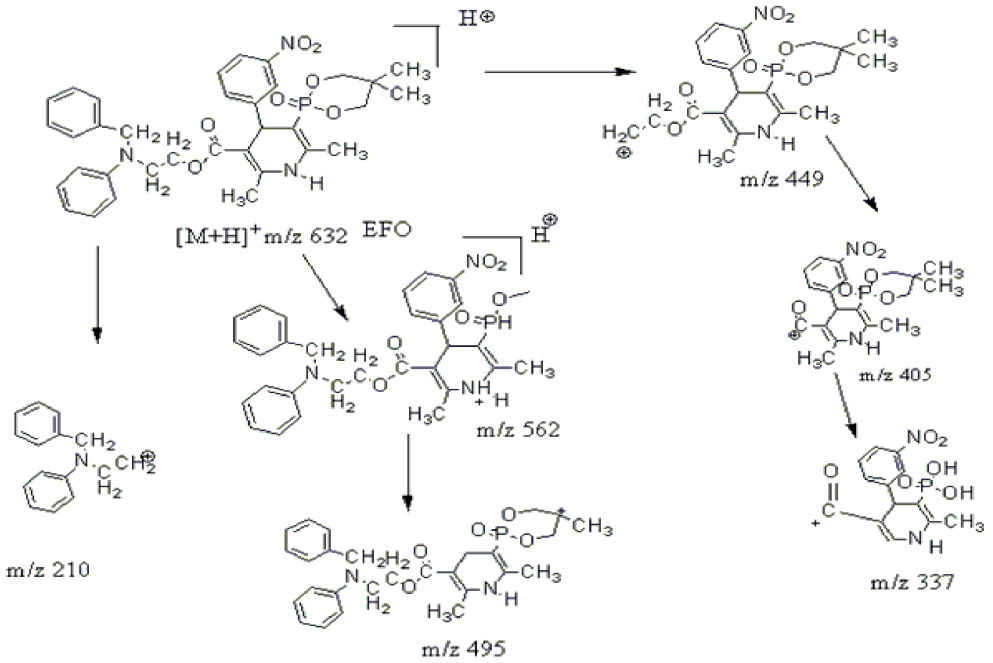

Fig.7. 31 - (a) ESI-MS/MS spectra (b) Fragmentation pathway of EFO

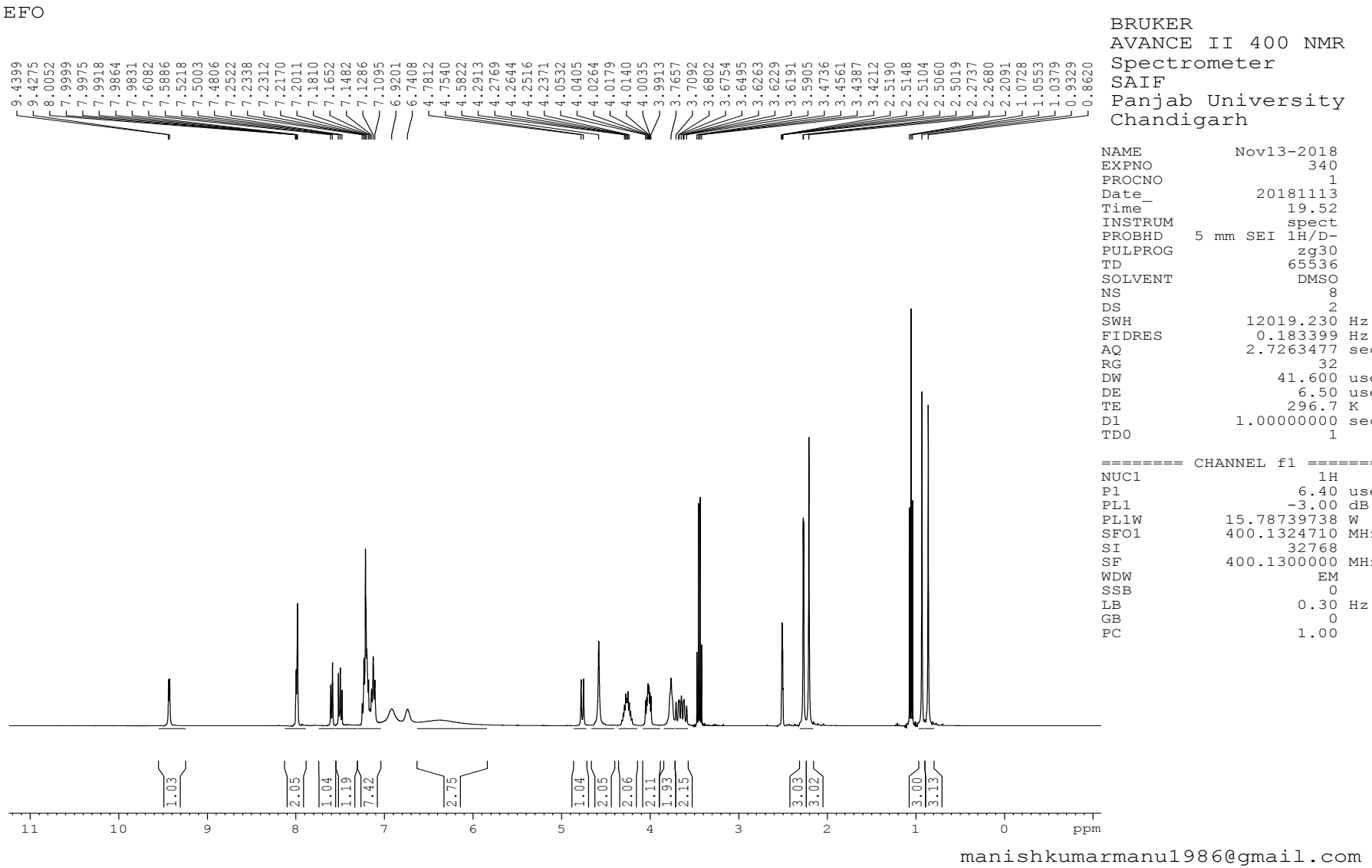

Fig.7. 32- ^{1}H NMR spectra of EFO

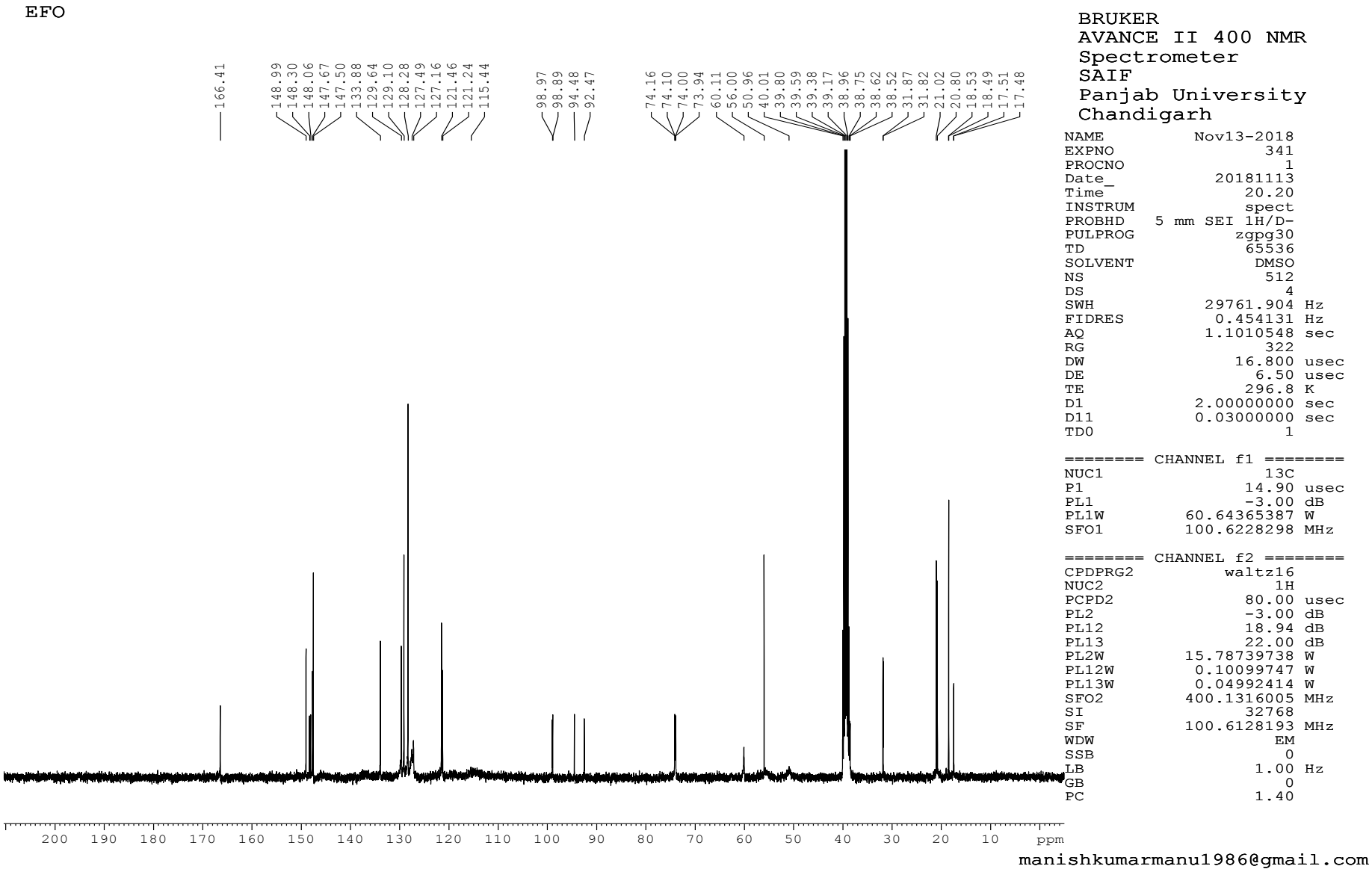

Fig.7. 33 - ^{13}C NMR spectra of EFO

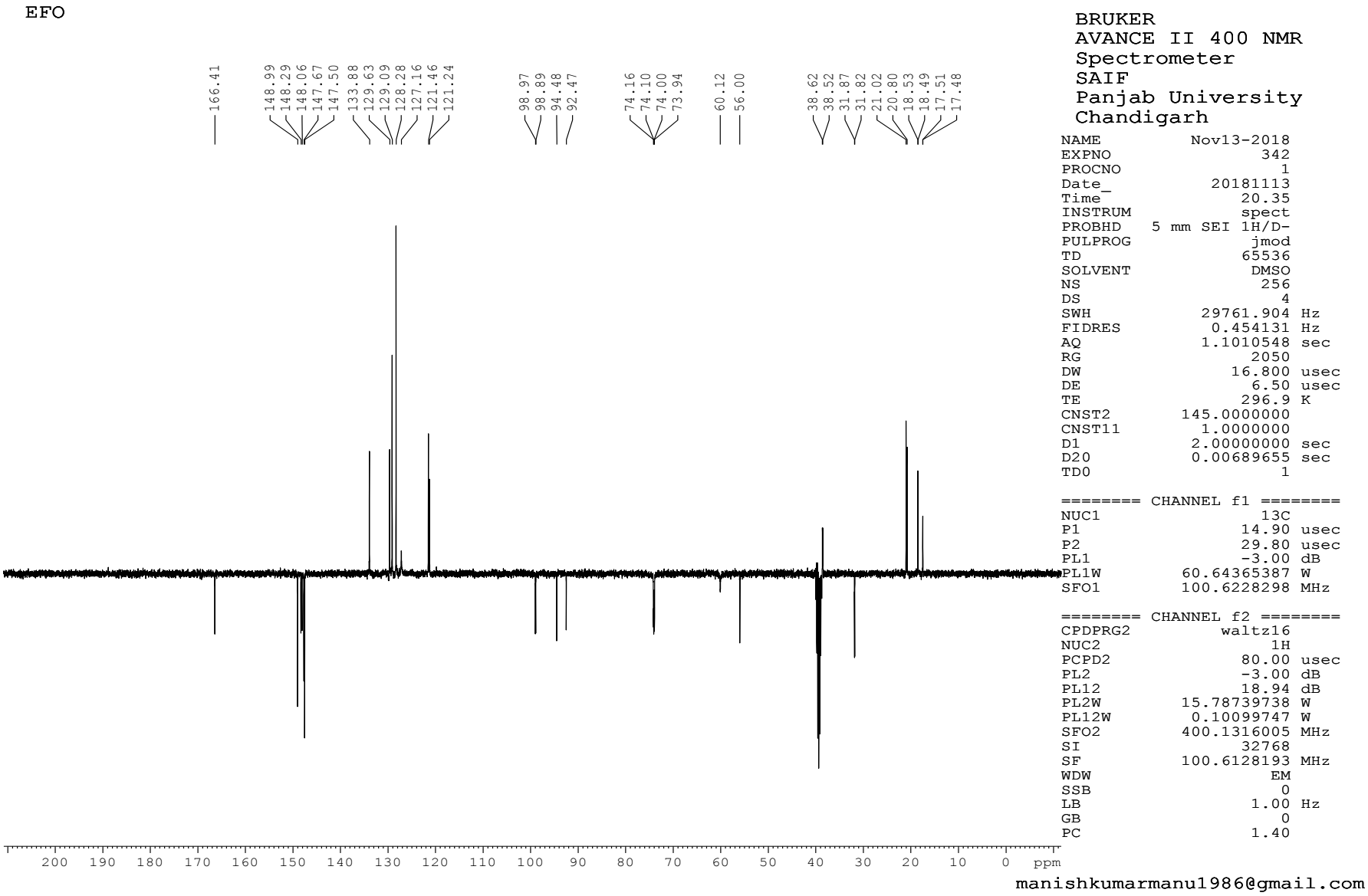

Fig.7. 34 - APT spectra of EFO

EFO

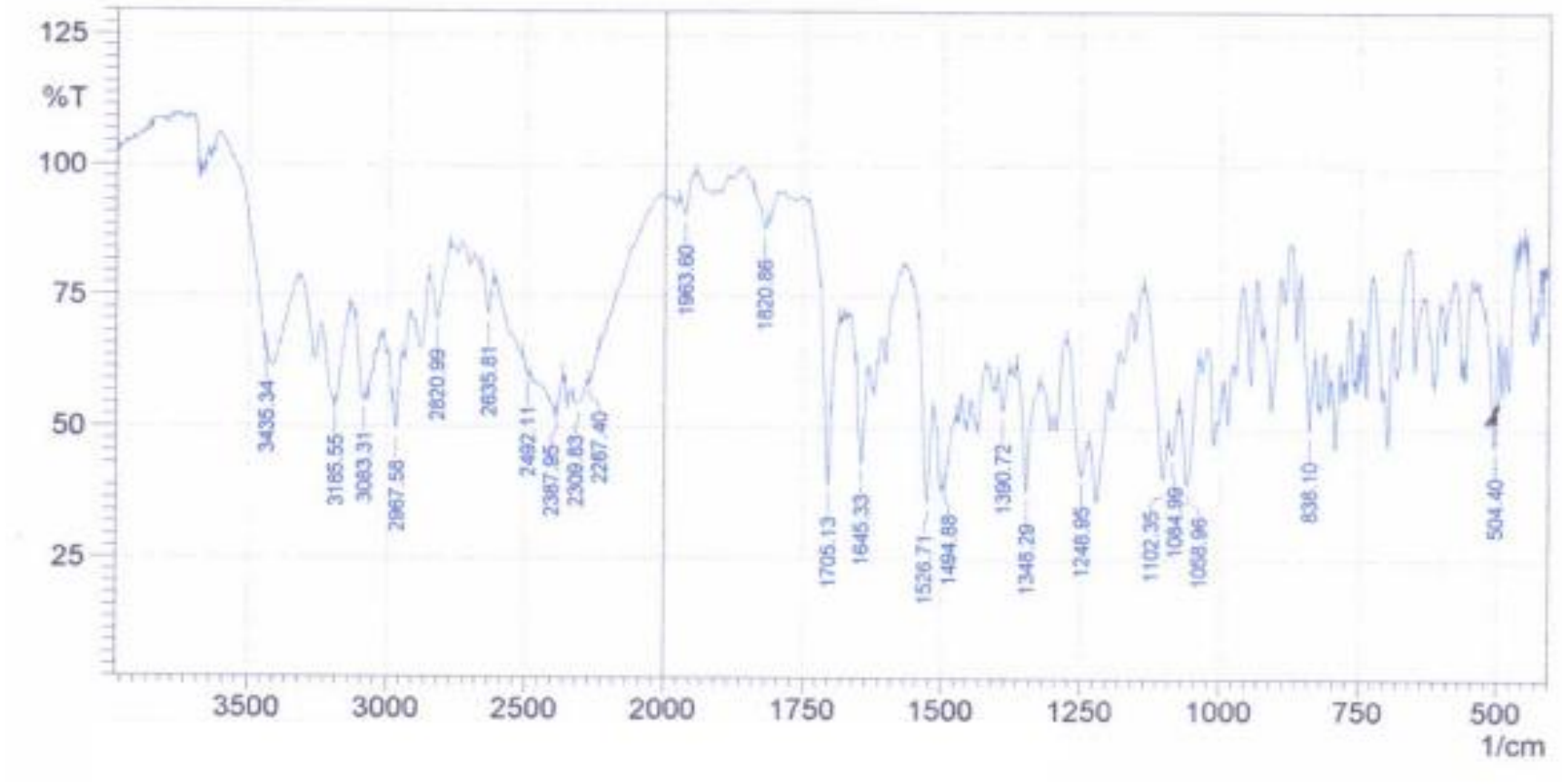

Fig.7. 35 - IR spectra of EFO

(a)

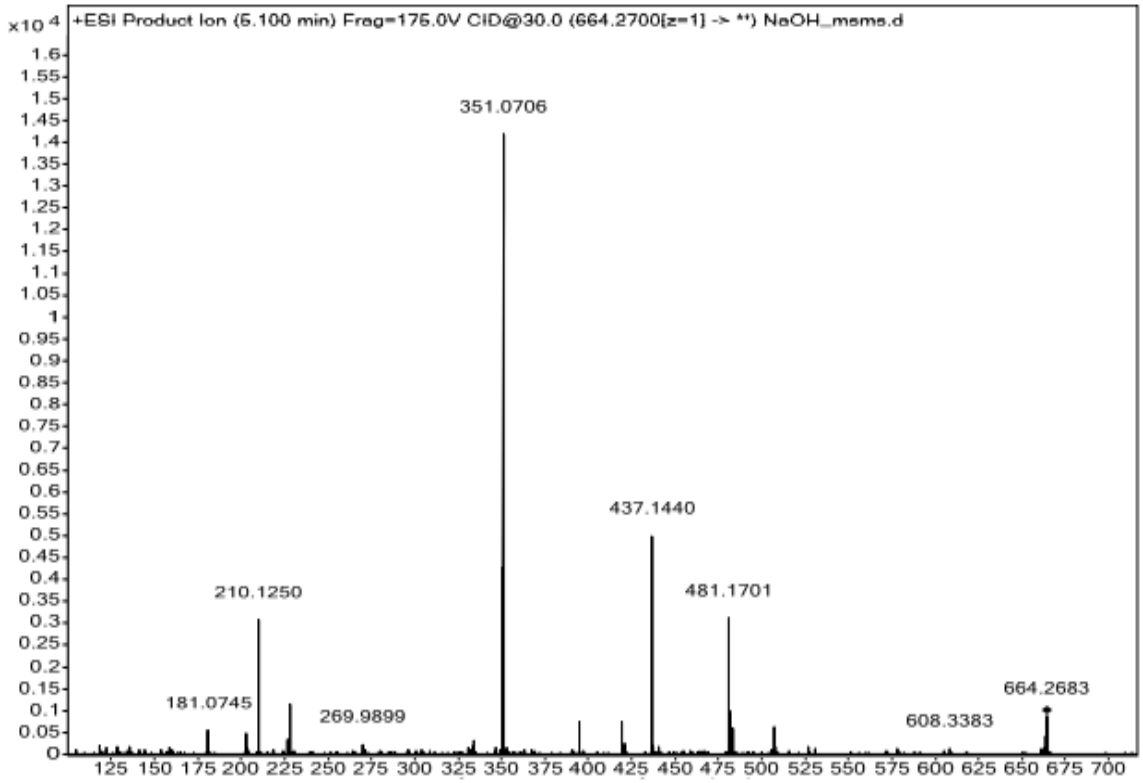
+ESI Product Ion (5.100 min) Frag=175.0V CID@30.0 (664.2700[z=1] -> **) NaOH_msms.d
x10 4
351.0706
437.1440
210.1250
481.1701
181.0745
269.9899
608.3383
664.2683

(b)

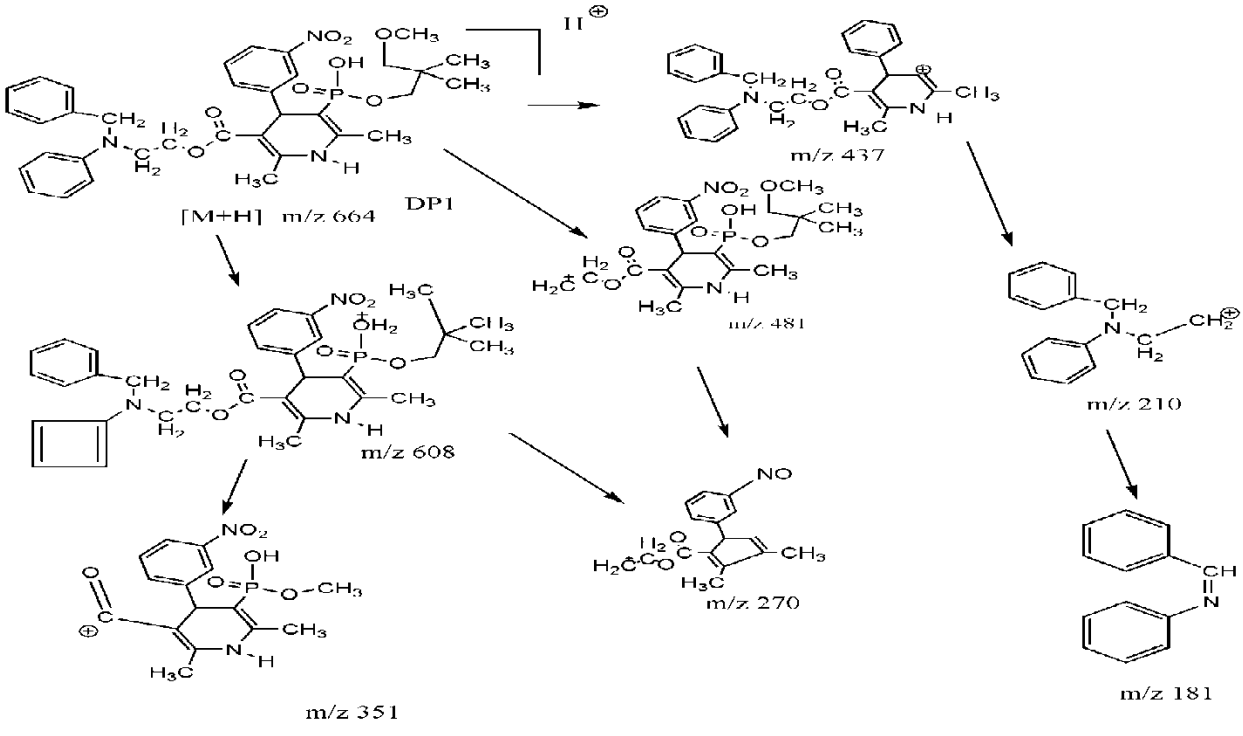
[M+H] m/z 664
DP1
m/z 437
m/z 481
m/z 608
m/z 210
m/z 270
m/z 351
m/z 181

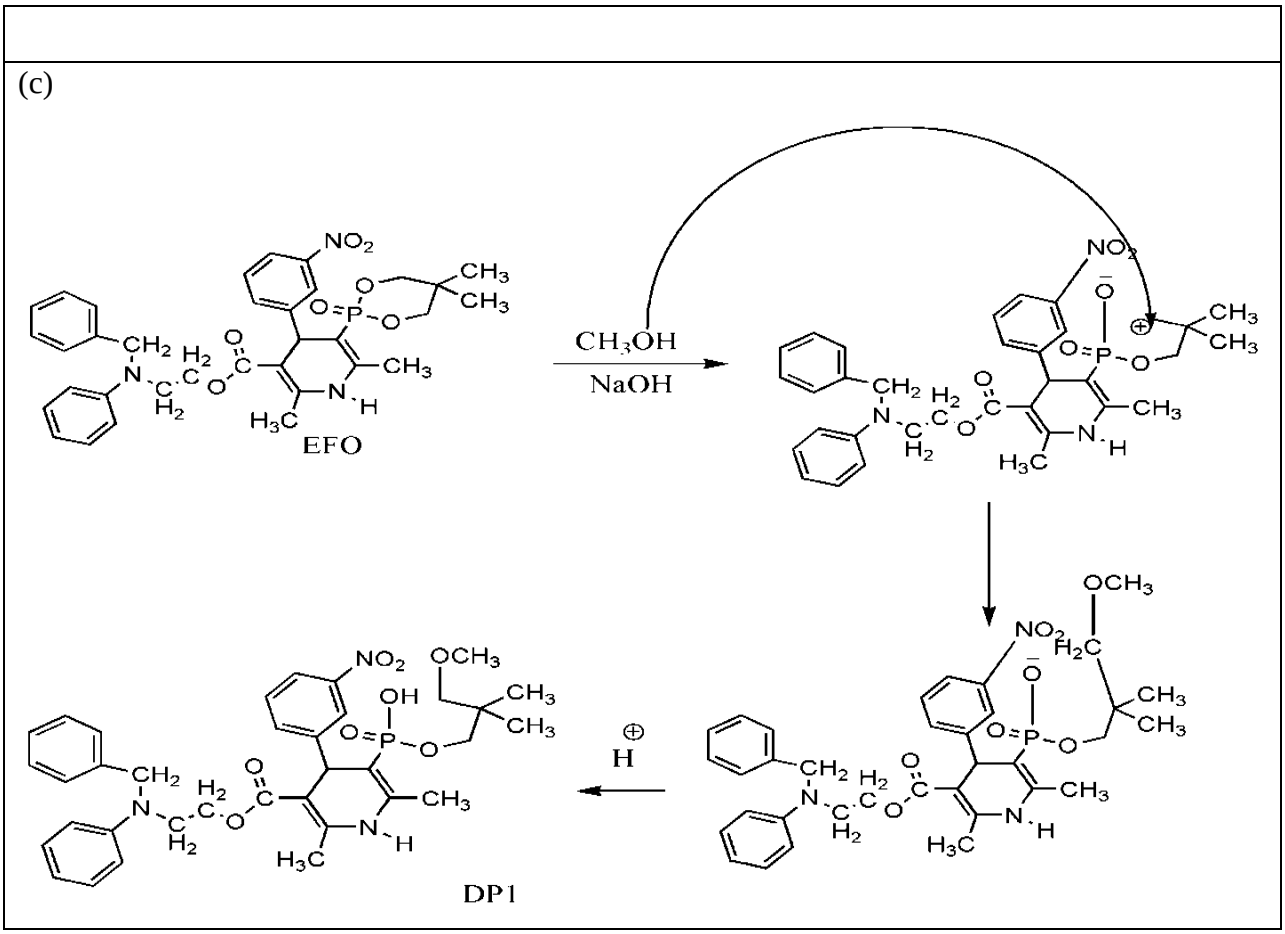

Fig.7. 36- (a) ESI-MS/MS spectra (b) Fragmentation pathway of DP1(c) Mechanism of formation of DP1

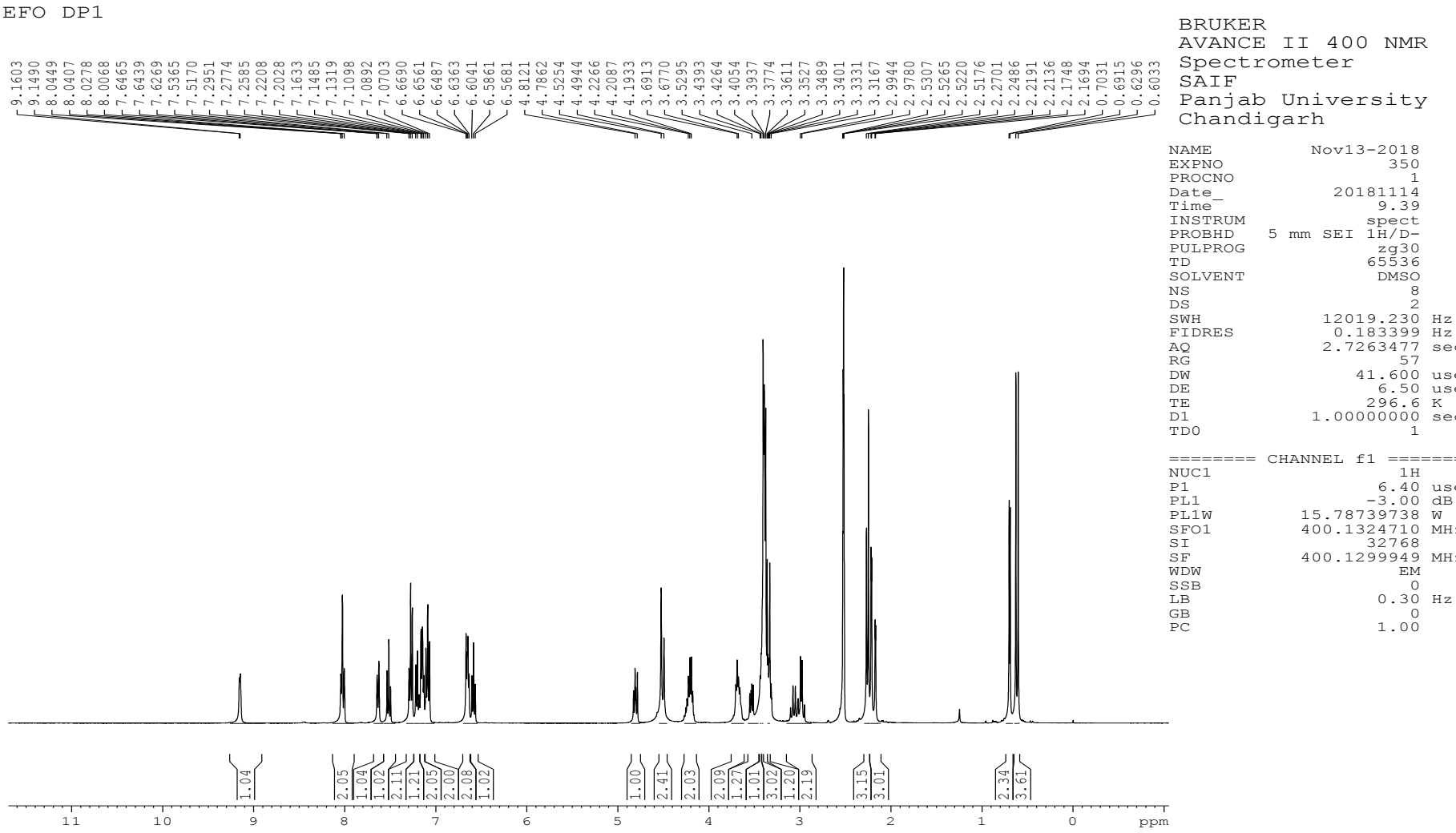

Fig.7. 37 - ^{1}H NMR spectra of DP1

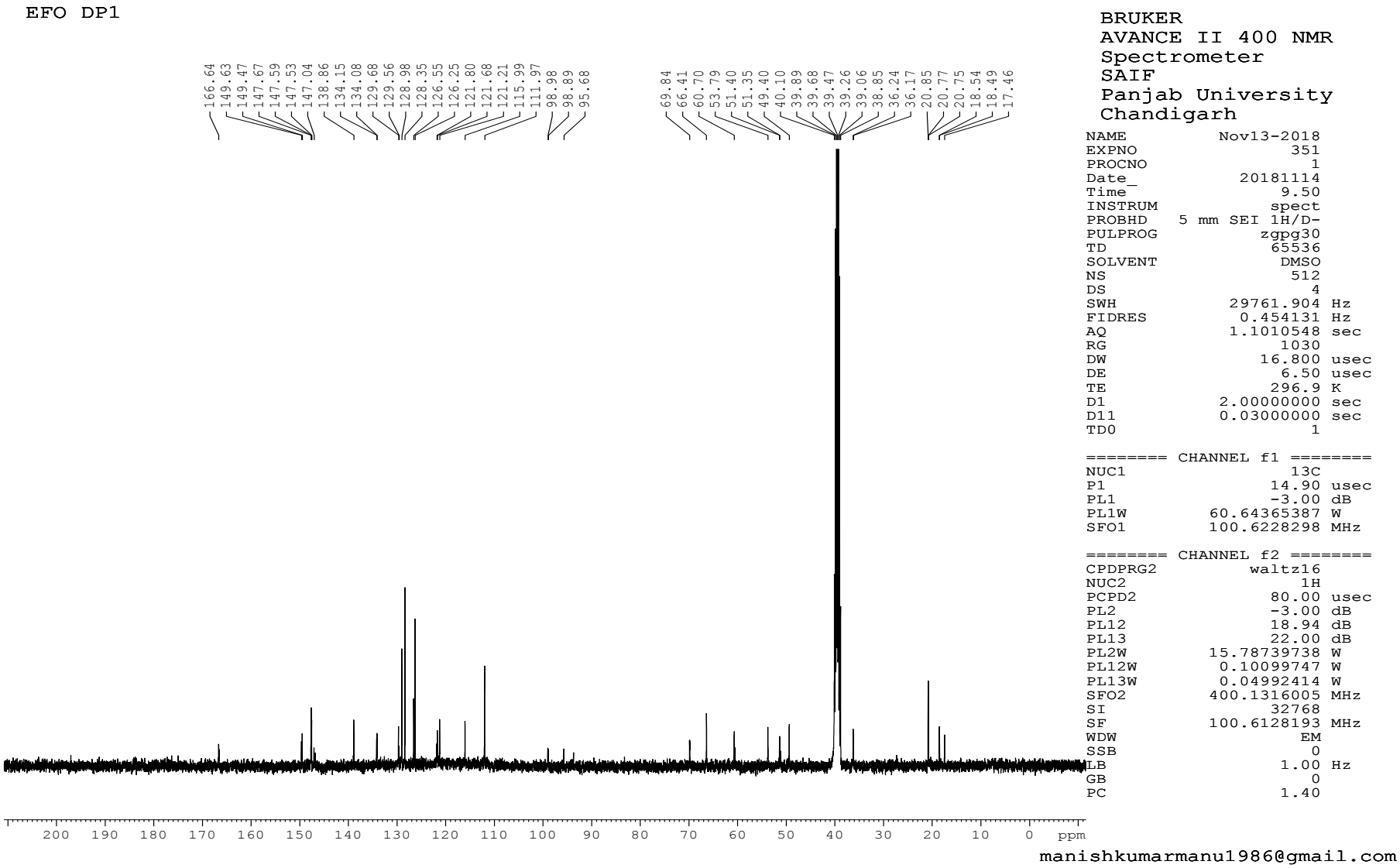

Fig.7. 38- ^{13}C NMR spectra of DP1

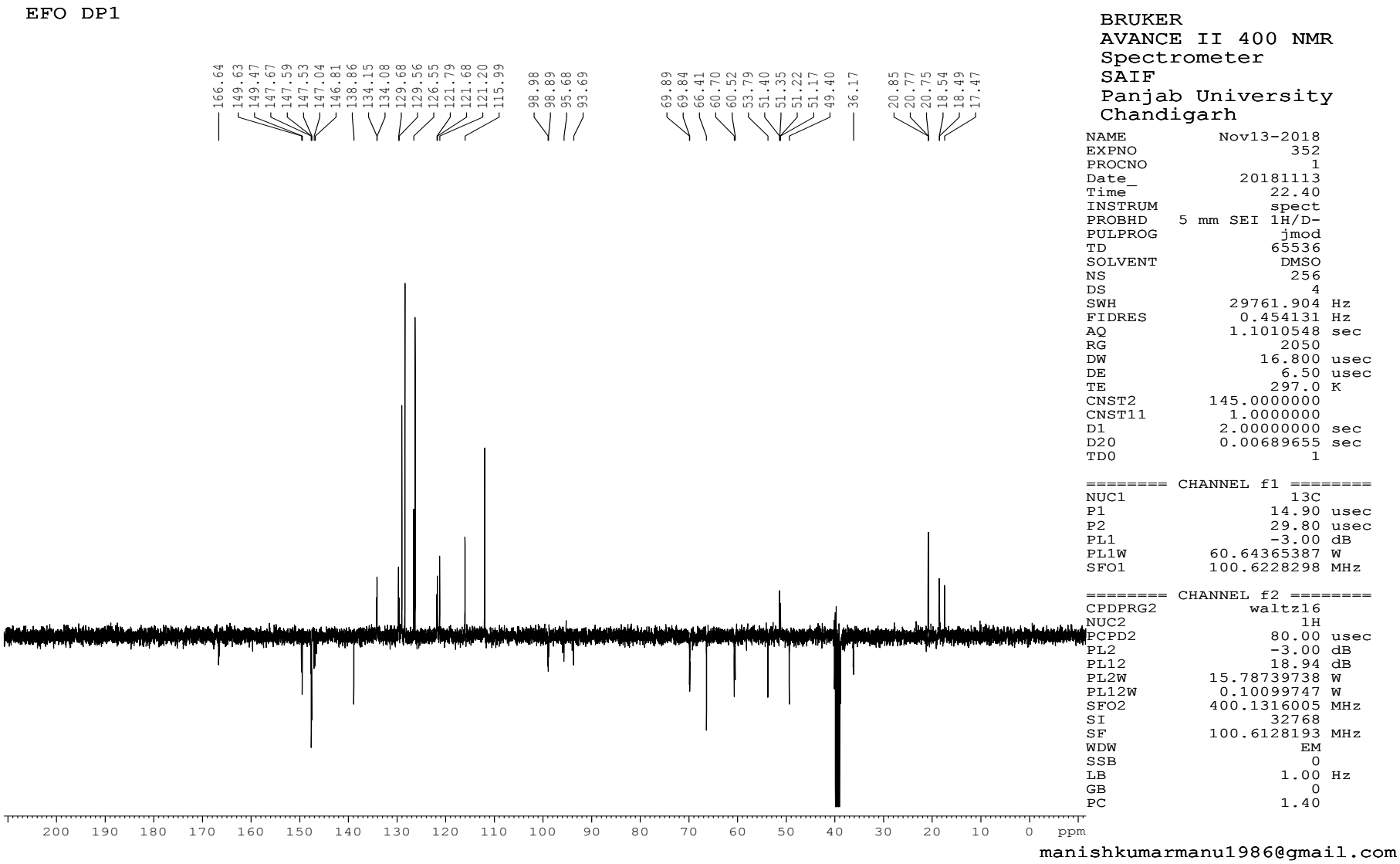

Fig.7. 39- APT spectra of DP1

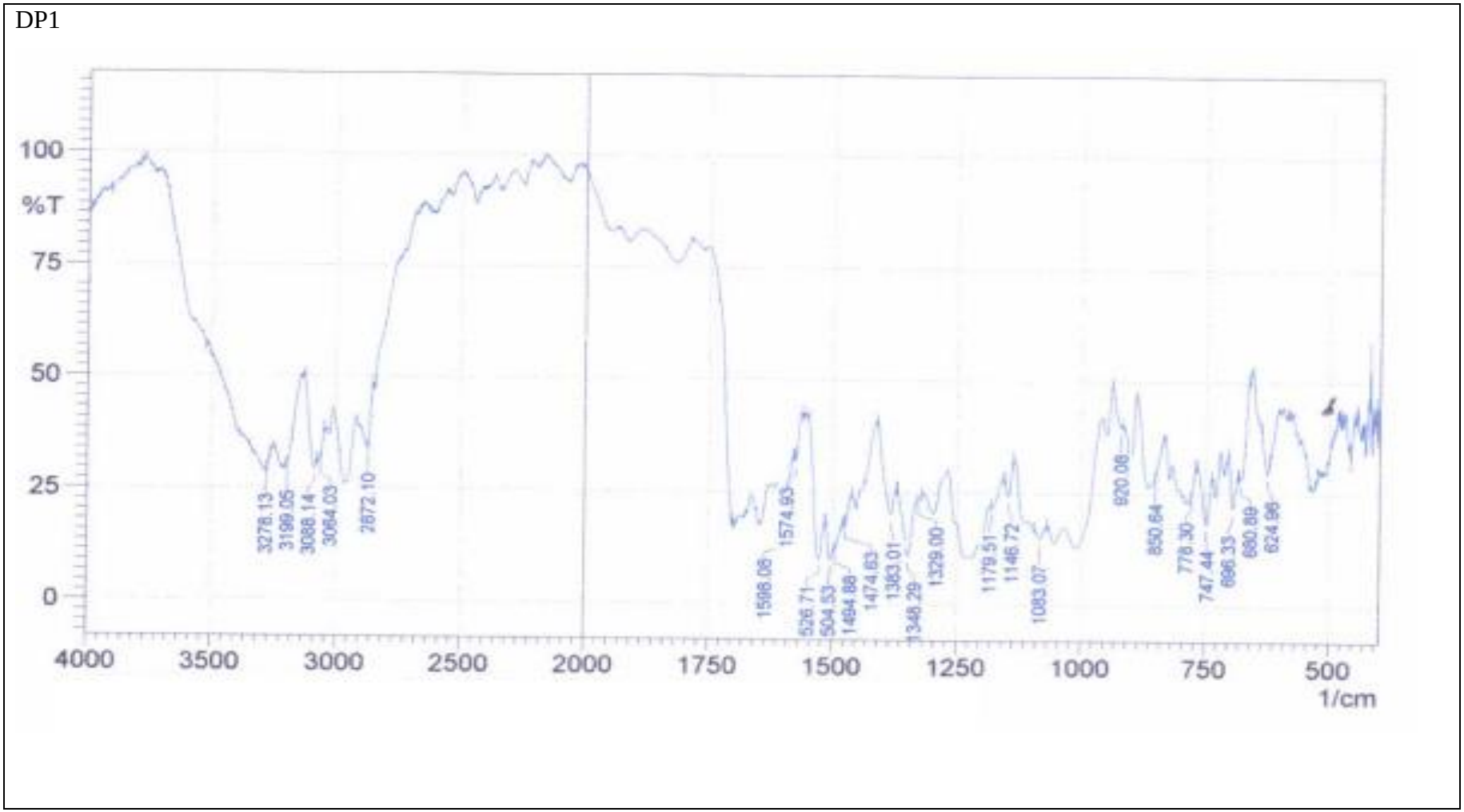

Fig.7. 40 – IR spectra of DP1

(a) DP3

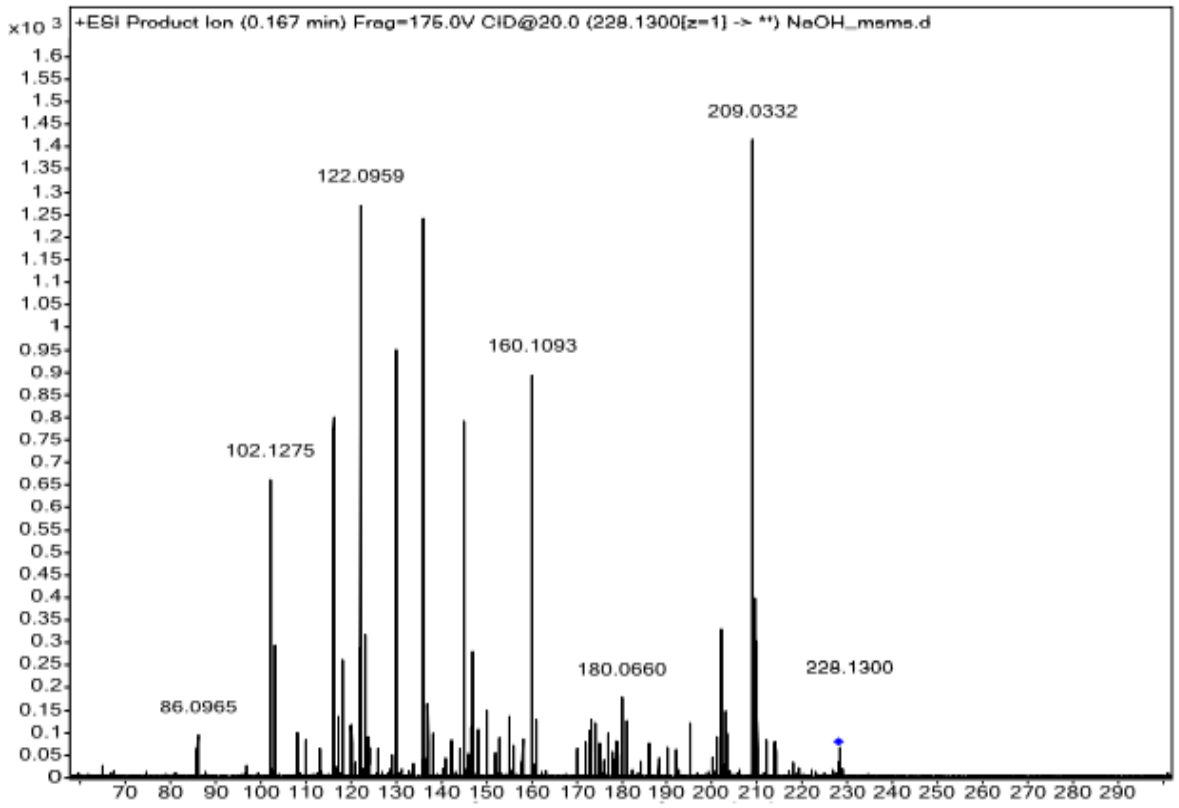
+ESI Product Ion (0.167 min) Frag=175.0V CID@20.0 (228.1300[z=1] -> **) NaOH_msms.d
x10 3
209.0332
122.0959
160.1093
102.1275
180.0660
228.1300
86.0965

(b)

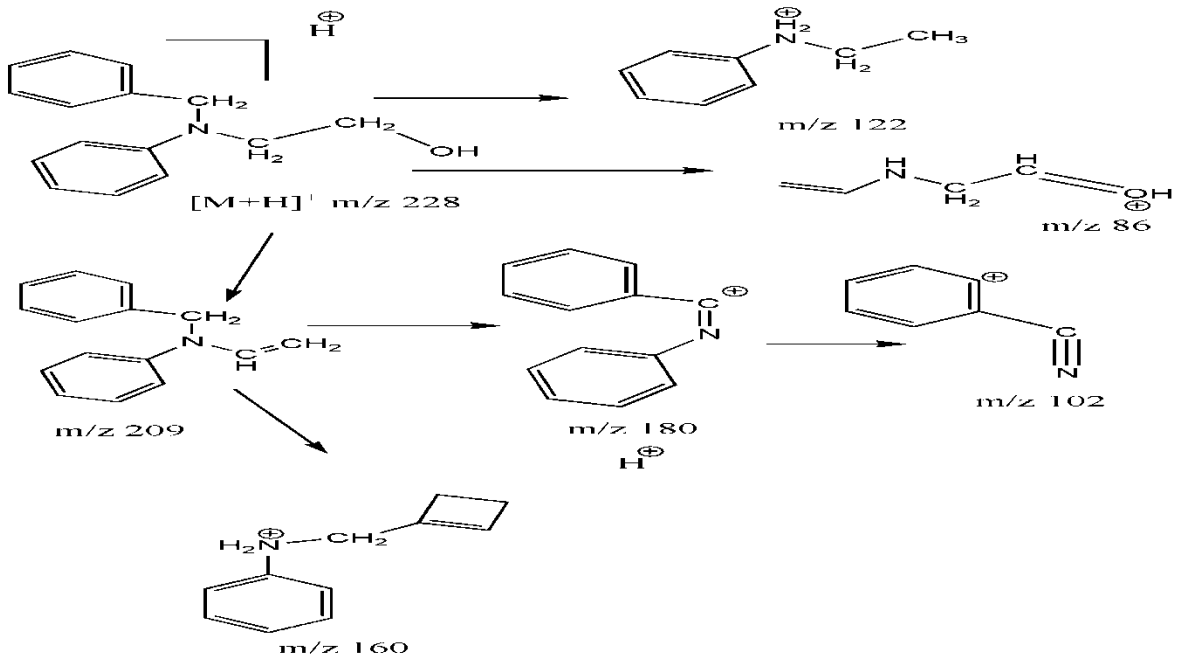
[M+H]+ m/z 228
m/z 122
m/z 86
m/z 209
m/z 180
m/z 102
m/z 160

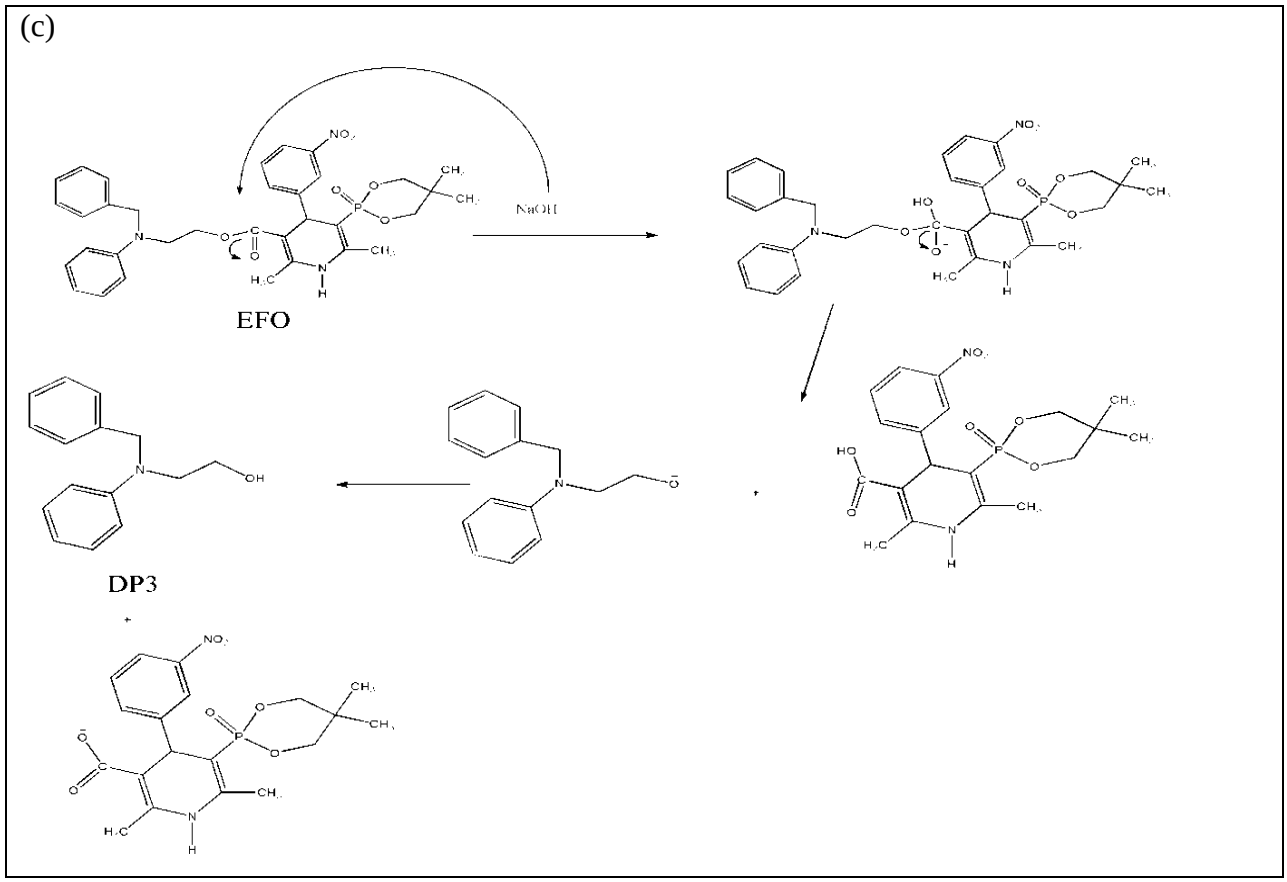

Fig.7. 41- (a) ESI-MS/MS spectra (b) Fragmentation pathway (c) Mechanism of formation of DP3

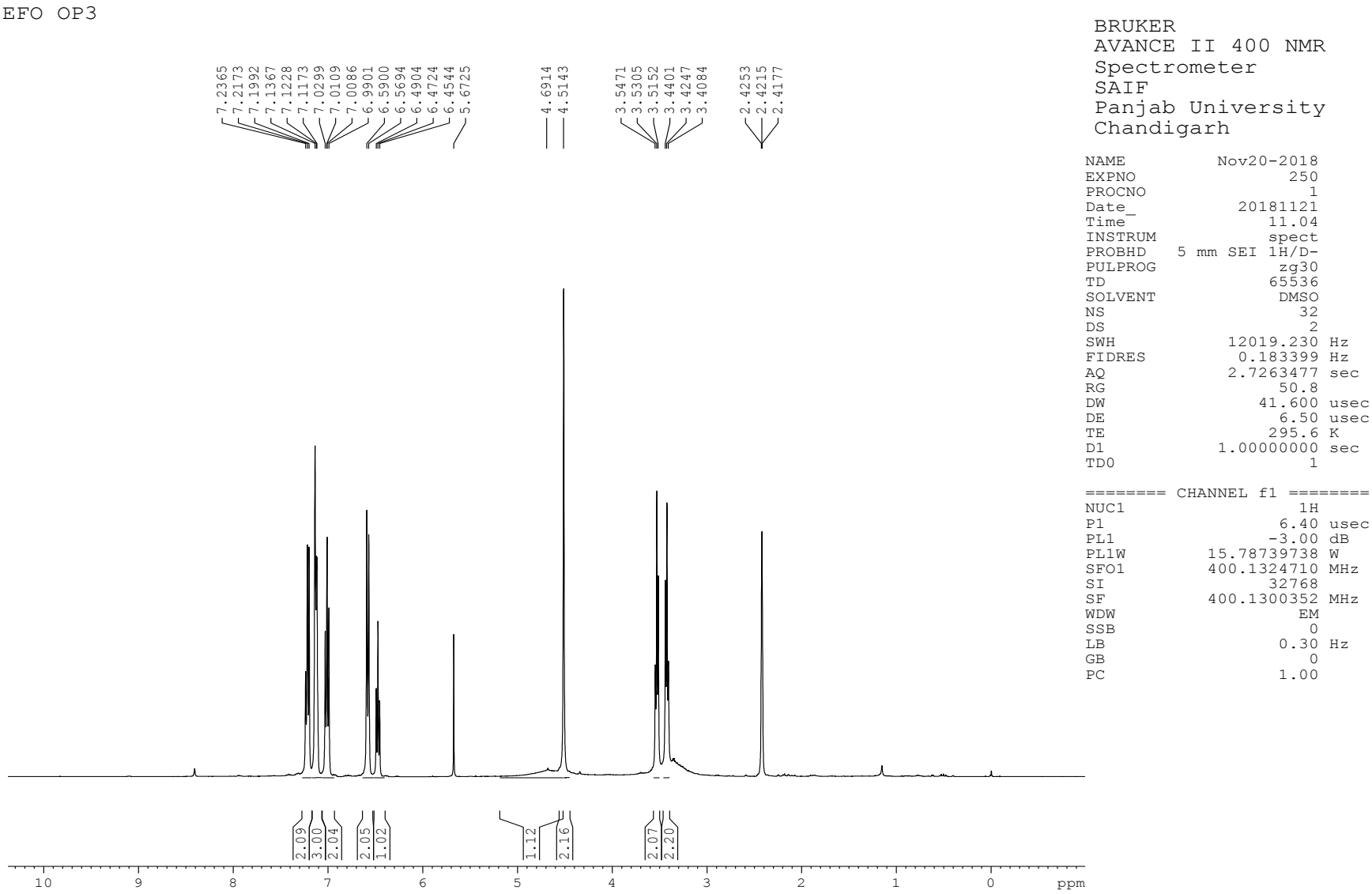

Fig.7. 42- ^{1}H NMR spectra of DP3

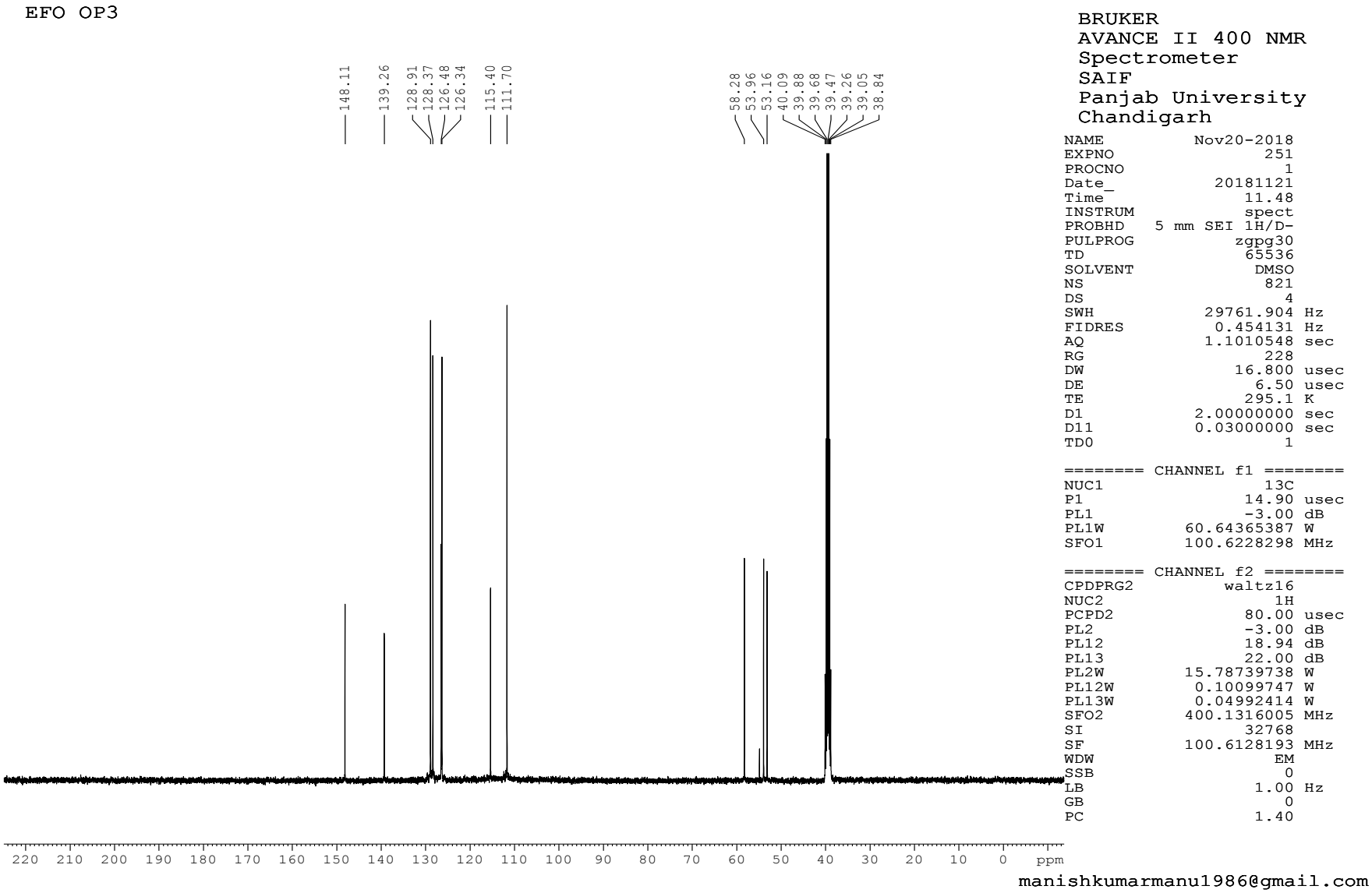

Fig.7. 43 - ^{13}C NMR spectra of DP3

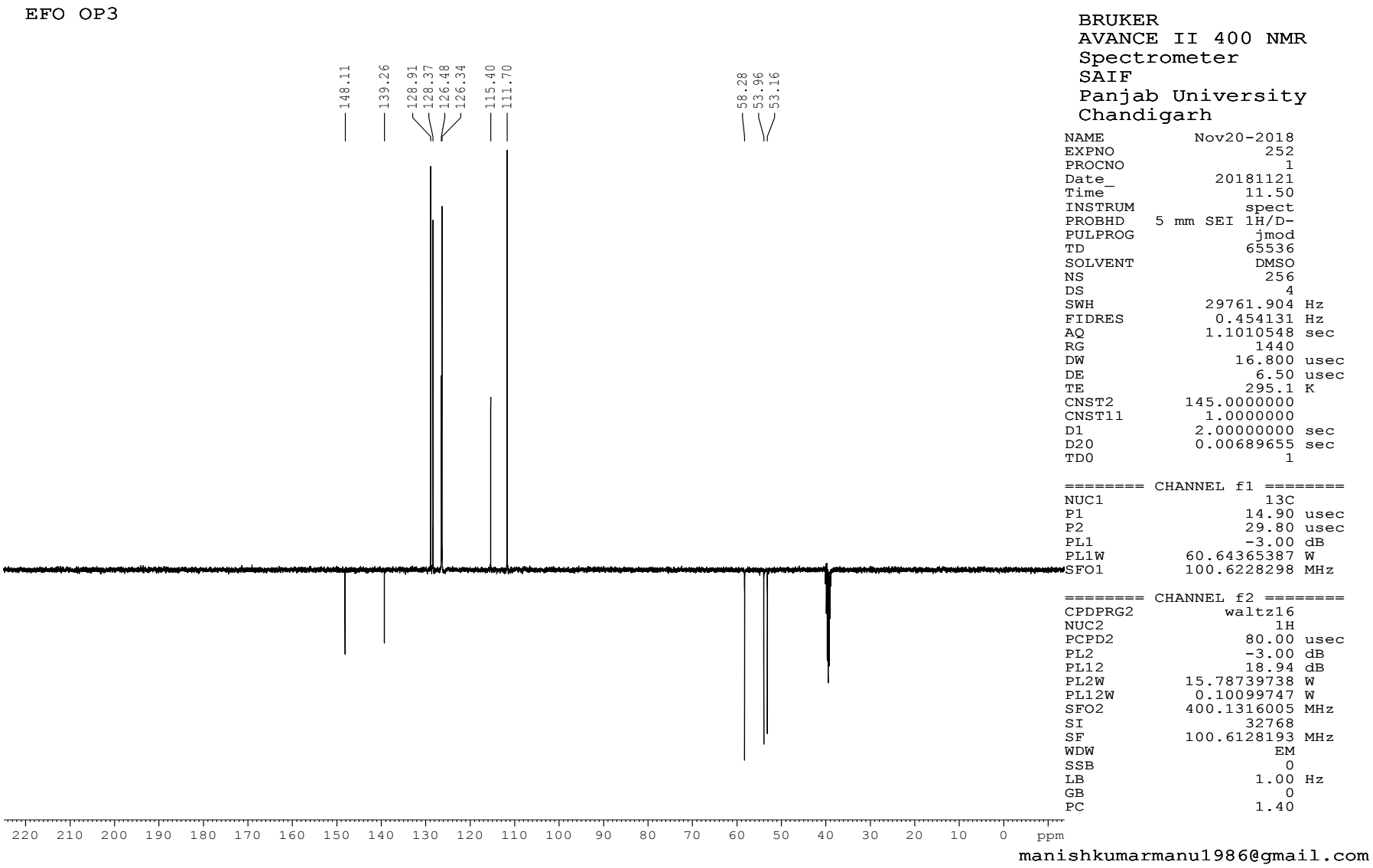

Fig.7. 44 - APT spectra of DP3

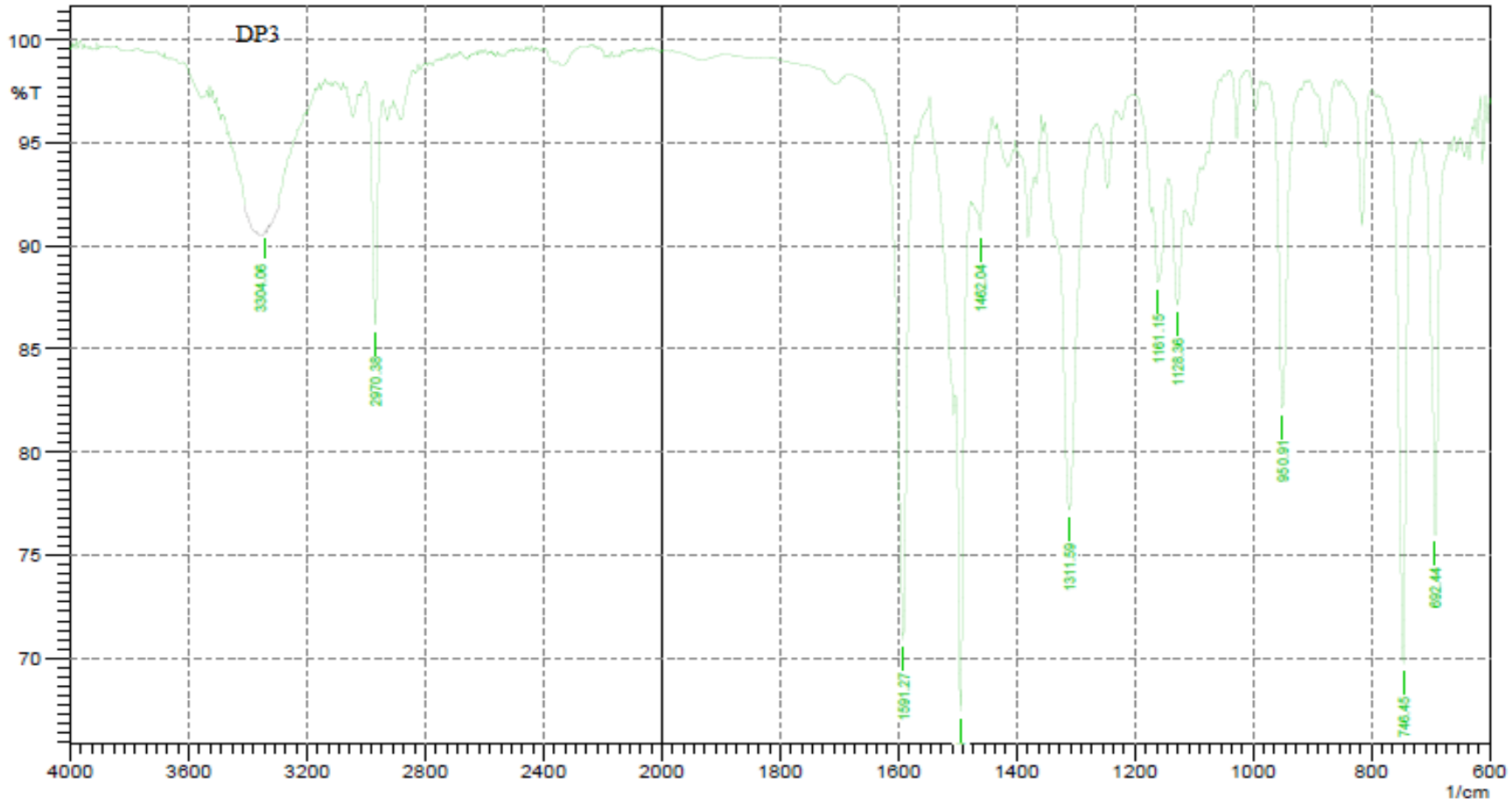

Fig.7. 45 - IR spectra of DP3

(a) DP4

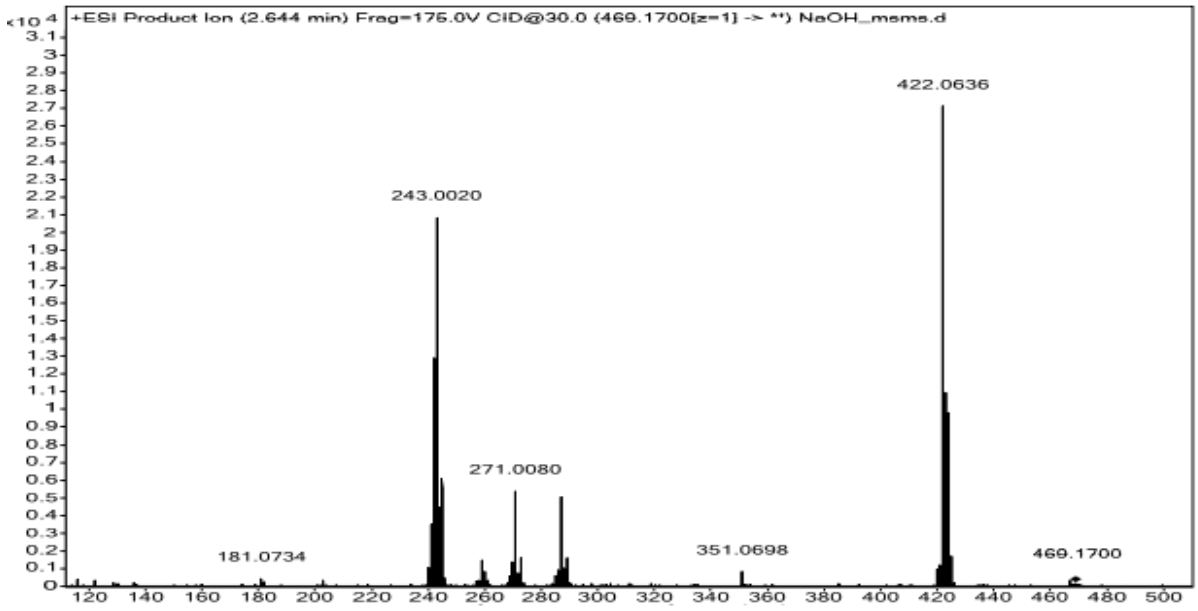
+ESI Product Ion (2.644 min) Frag=175.0V CID@30.0 (469.1700[z=1] -> **) NaOH_msms.d
422.0636
243.0020
271.0080
181.0734
351.0698
469.1700

(b)

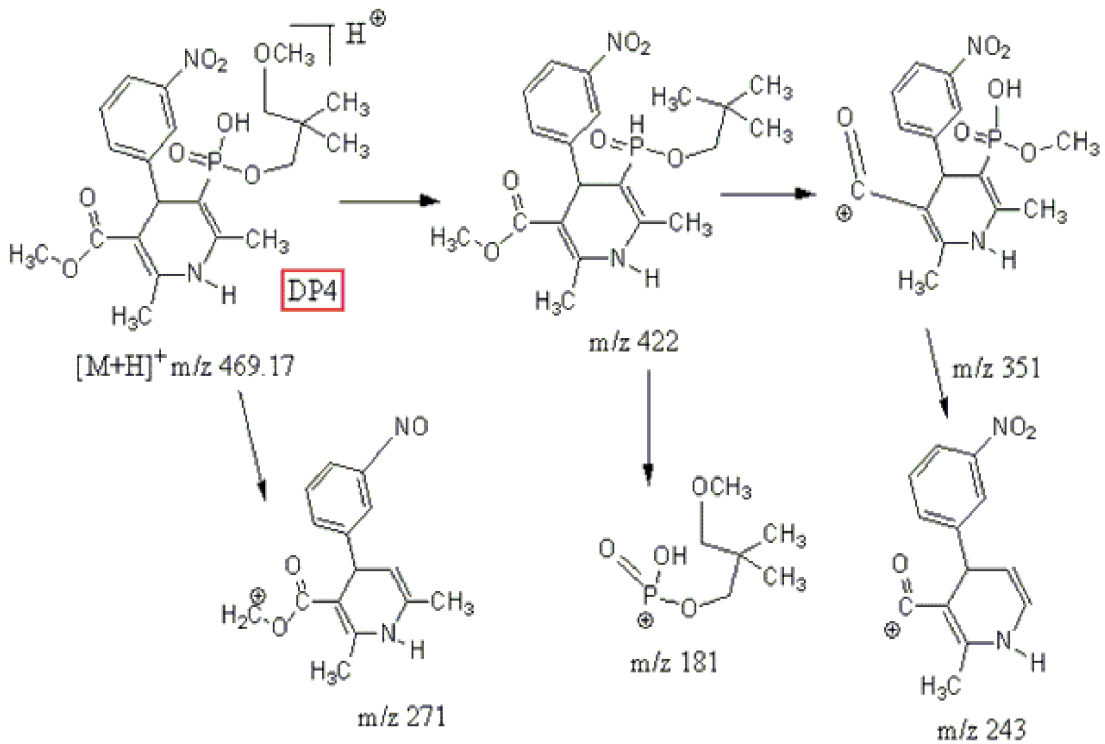
DP4
[M+H]+ m/z 469.17
m/z 422
m/z 351
m/z 271
m/z 181
m/z 243

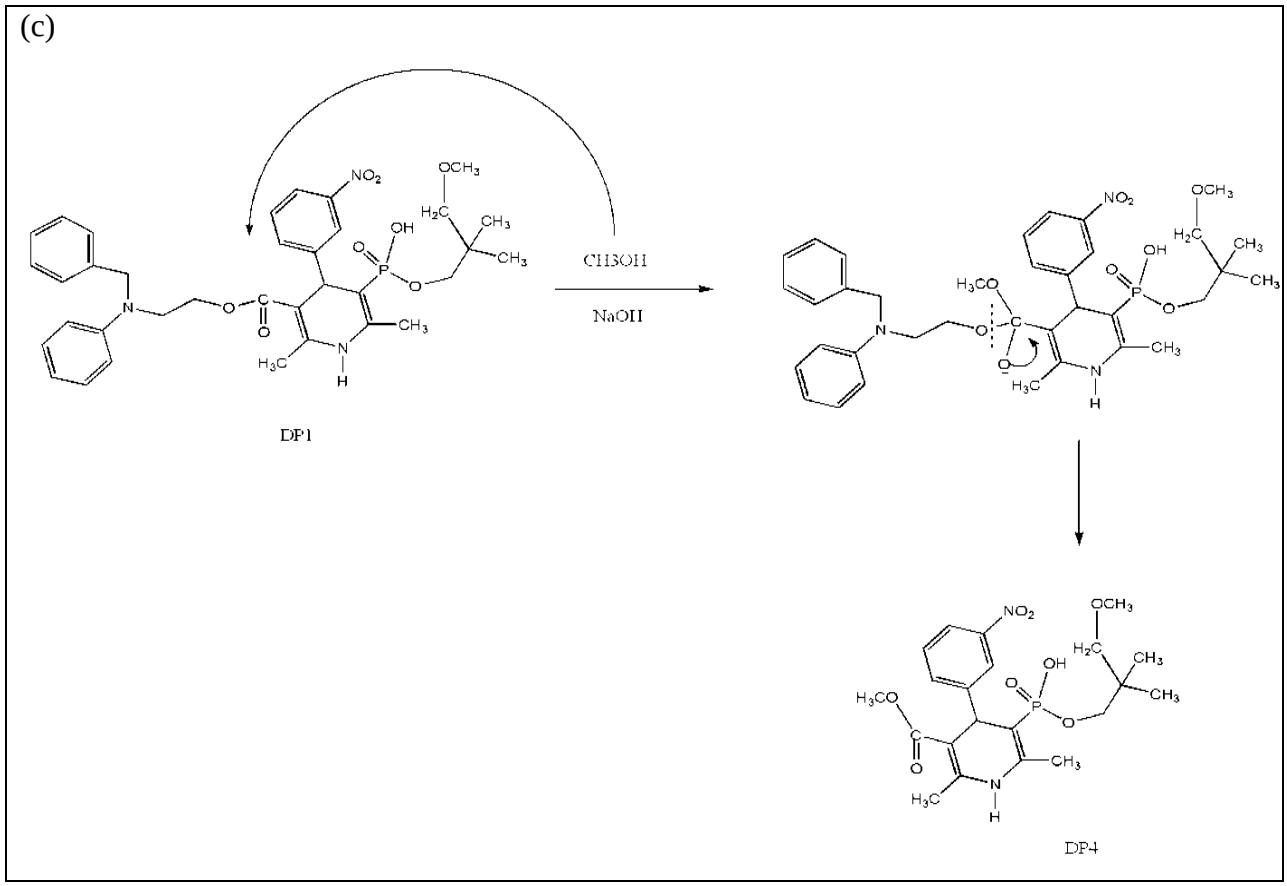

Fig.7. 46 – (a) ESI-MS/MS spectra (b) Fragmentation pathway (c) Mechanism of formation of DP4

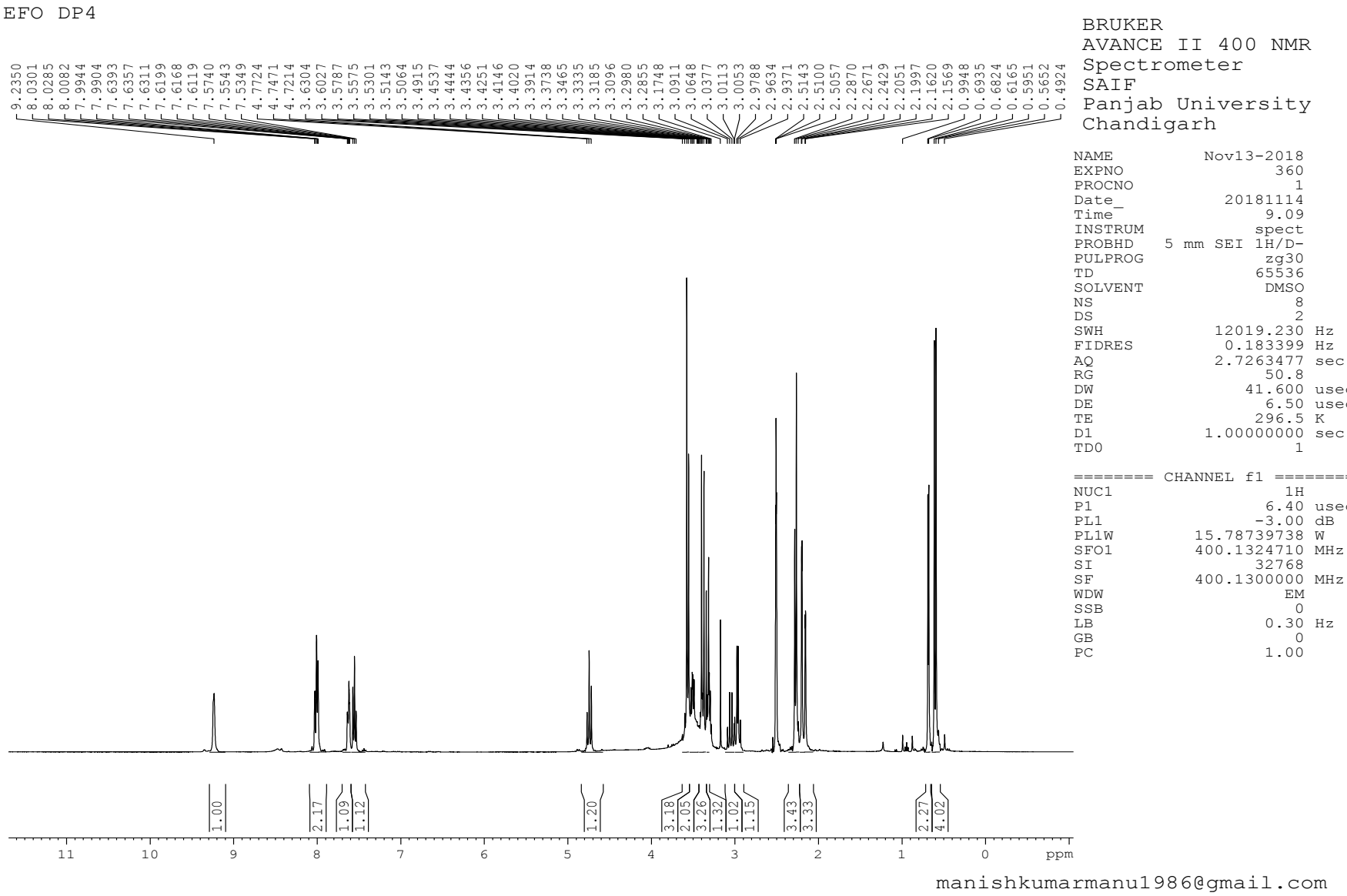

Fig.7. 47 - ^{1}H NMR spectra of DP4

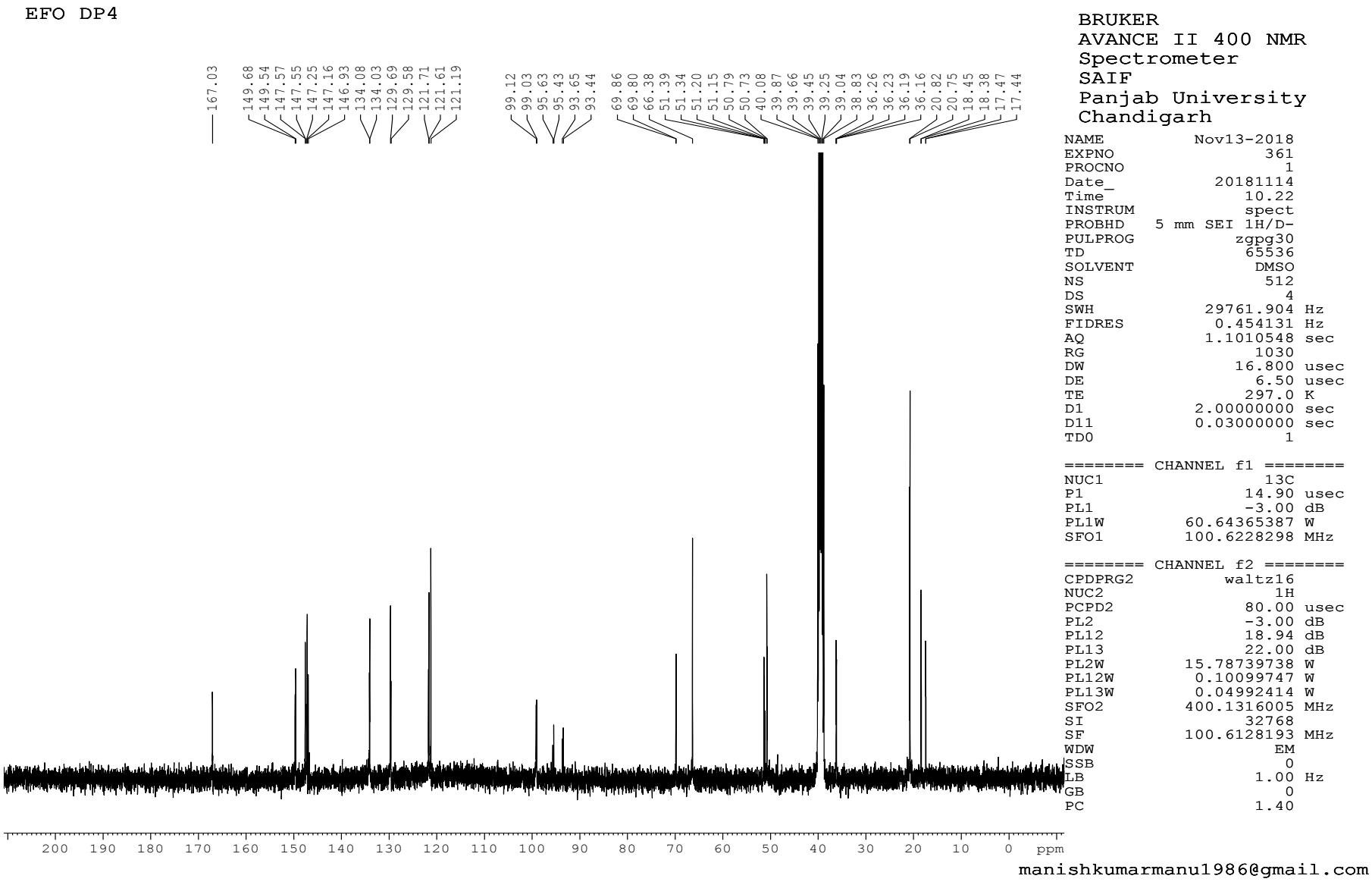

Fig.7. 48- ^{13}C NMR spectra of DP4

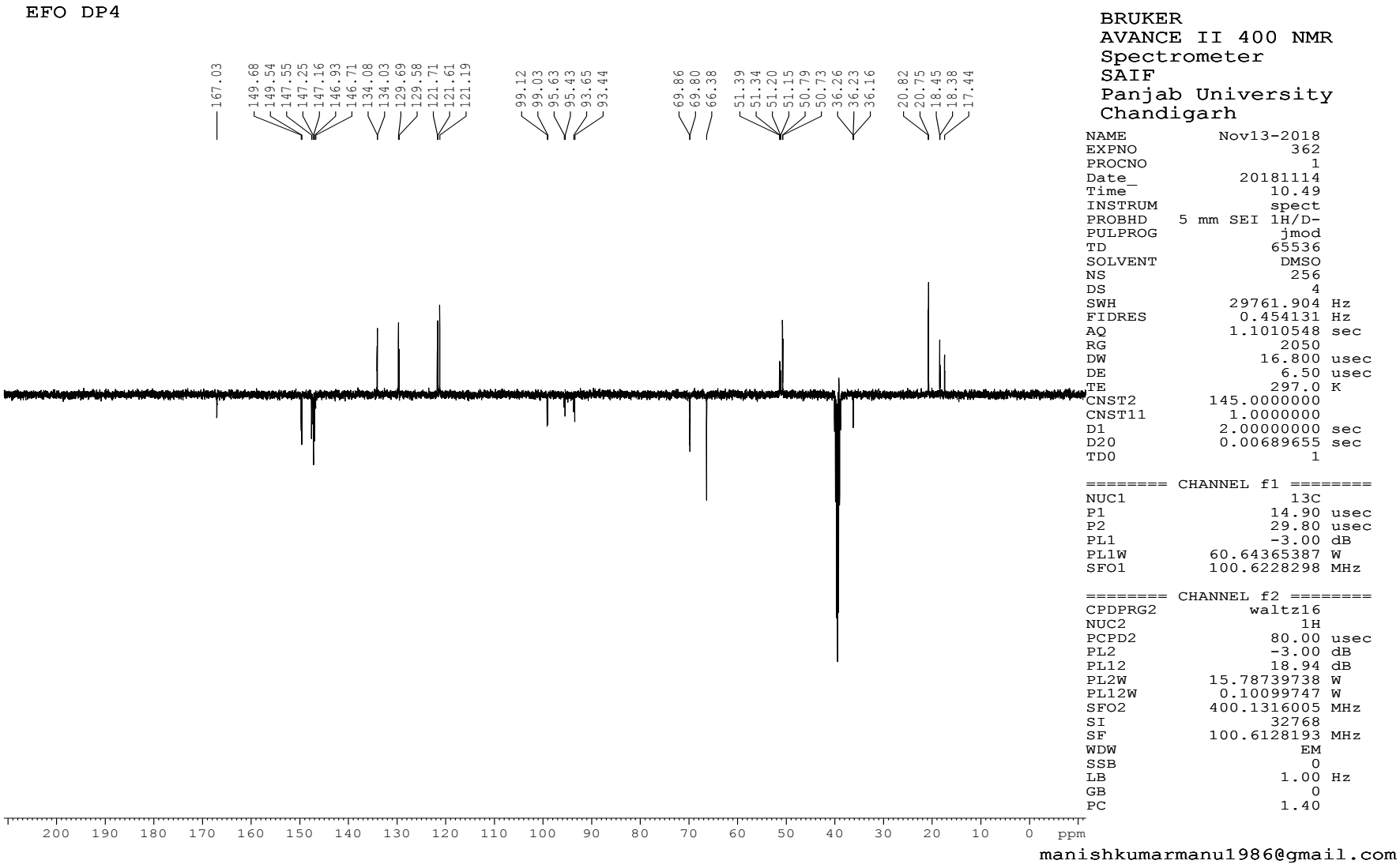

Fig.7. 49- APT spectra of DP4

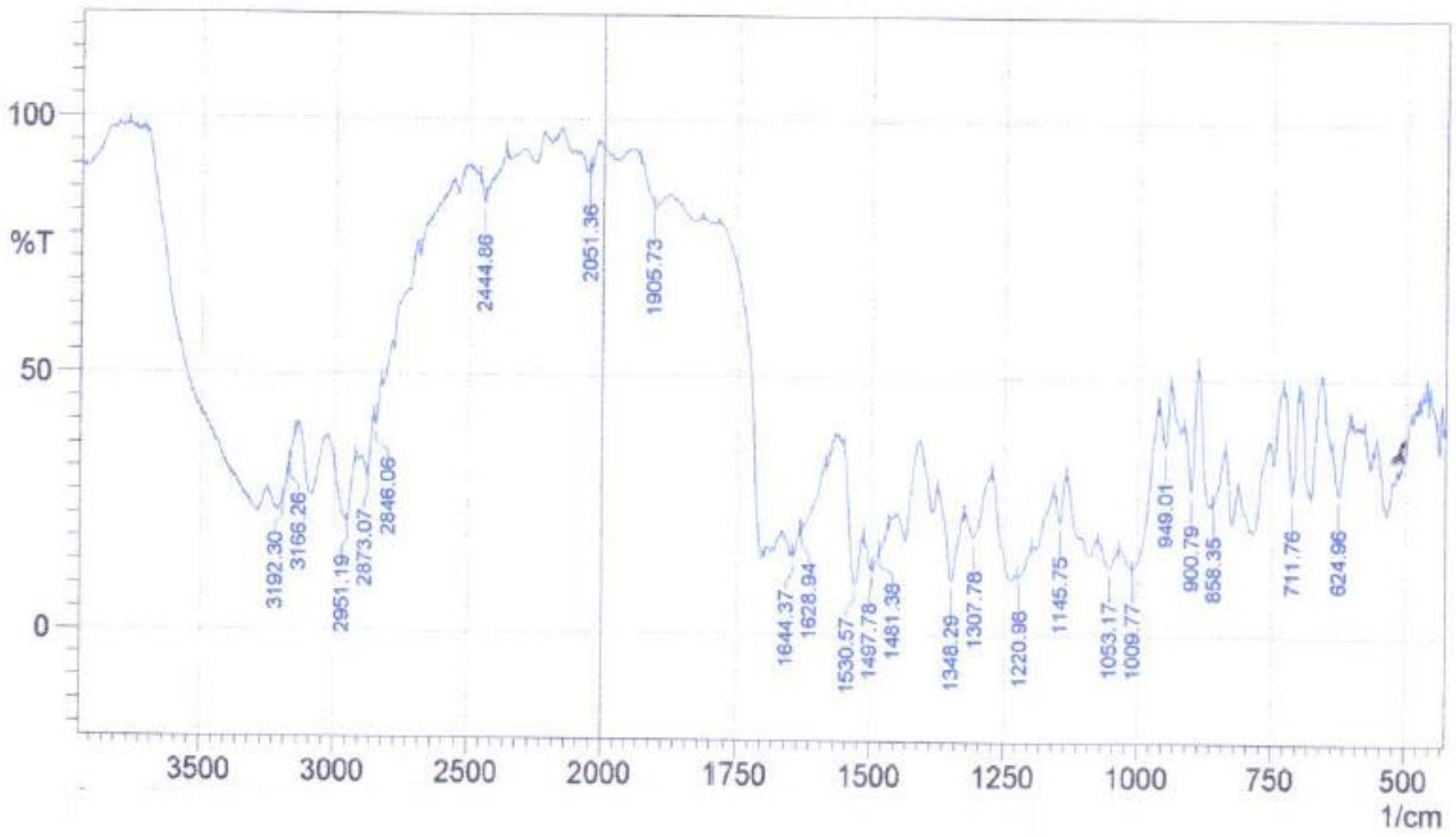

Fig.7. 50- IR spectra of DP4

7.8. SECTION- E

IMPURITY PROFILING AND DEGRADATION STUDY OF EFONIDIPINE HCl ETHANOLATE

7.8.1. EXPERIMENTAL

7.8.1.1. Chemicals and reagents

Chemicals and reagents used in the present section are same as those mentioned in 7.5.1.1.

7.8.1.2. Equipments and Chromatographic conditions

The equipments and chromatographic conditions used in impurity profiling and degradation study are same as those mentioned in section 7.5.1.2.

For LC-Q-TOF-MS analysis, EFO degradation samples were analysed under same chromatographic conditions as mentioned in section 7.4.1.3.The m/z values were determined in both positive and negative ESI mode. On the basis of m/z ratio, structures of DPs were proposed and degradation pathway was postulated.

7.8.1.3. Preparation of stock, sample and buffer solutions

Stock, sample and buffer solutions were prepared in the same way as mentioned in section 7.5.1.5.

7.8.2. RESULTS AND DISCUSSIONS

7.8.2.1. LC-PDA Study

Forced degradation study of EFO showed the formation of degradation products in LC-PDA and are summarized in Table 7.30. Significant degradation were observed in alkaline and photolytic conditions.

Table 7. 30- Summary of forced degradation study of EFO analysed by LC-PDA

Stressor	**Conditions**	**RT of Degradation Products**	**% of Degradation Products in API**	**% of Degradation products in Formulation**
Acidic	1 M HCl at 80ºC for 6 hrs	--	---	---
Alkaline	0.5 M NaOH at RT(40ºC) for 6 hrs	14.33(DP6) 18.83(DP5) 20.29(DP4) 24.09(DP3) 26.66(DP2) 52.91(DP1)	0.63% 0.66% 2.17% 8.8% 4.01% 28.14% (44.18%)	0.60% 0.60% 2.1% 9.1% 4.1% 27.8% (46.4%)
Oxidation	10% hydrogen peroxide at RT(40˚C) for 24 hrs	---	--	---
Thermal	Dry at 80℃ for 11 days	--	--	--
Photolytic				

	Dry for 11 days	--	--	--
	Solution for 11 days	11.67 min(DP10) 30.01min (DP9) 31.9 min(DP7) 55.92 min(DP8)	1.7% 0.48% 0.98% 8.1% (11.6%)	1.0% 0.42% 0.60% 7.8% 9.8%

Total 10 degradation products were formed. DP1, DP3 and DP4 were major DPs and were identified after their isolation. Other DPs were studied by LC-Q-TOF-MS to understand the degradation pathway of EFO.

7.8.2.2. LC-MS study and characterization of DPs

EFO (m/z 632)

ESI-MS/MS spectra of EFO is provided in Fig.7.31a and proposed fragmentation pathway is shown in Fig. 7.31b. Mass spectral interpretation of EFO is mentioned in section 7.7.2.1.1.

DP1(m/z 664)

Structural interpretation of DP1 is mentioned in section 7.7.2.1.2.

DP2 (m/z 650)

An ESI-MS spectrum of DP2 is provided in Fig. 7.51. DP2 is formed with protonated molecular ion *m/z* of 650 with elemental composition of $C_{34}H_{41}N_3O_8P^+$. This mass is formed by ring opening of phosphinane group.

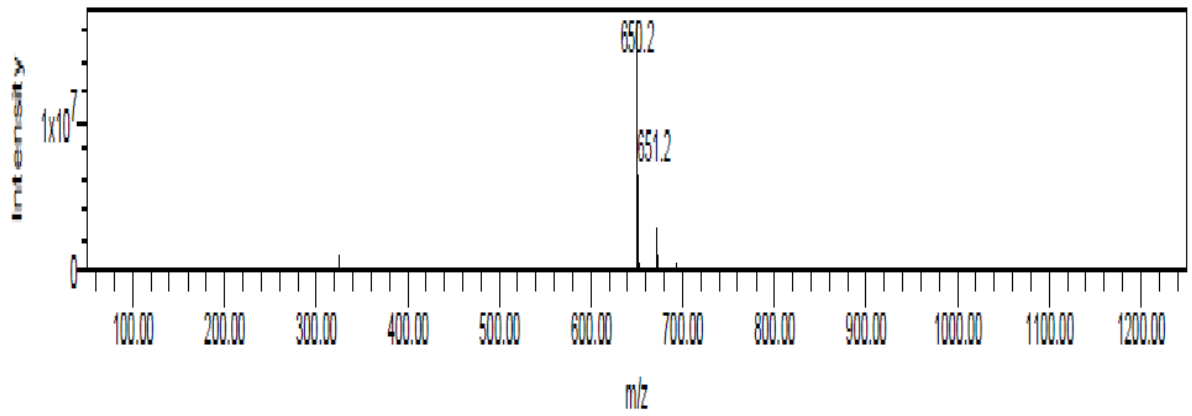

Fig.7. 51-ESI-MS spectra of DP2

DP3 (m/z 228)

DP3 was isolated and identified as mentioned in section 7.7.2.1.3.

DP4 (m/z 469)

Spectral interpretation to establish the structure of DP4 is mentioned in section 7.7.2.1.4.

DP5 (m/z 437)

An ESI-MS/MS spectrum of DP5 is shown in Fig.7.52 a. ESI-MS/MS spectra of DP5 shows protonated molecular ion peak at m/z 437 corresponding to elemental composition $C_{20}H_{26}N_2O_7P^+$. DP5 shows fragment ions of *m/z* 405 (loss of methoxy group from *m/z* 437) and *m/z* 388 (loss of CH_5O_2 from *m/z* 437). m/z 405 undergoes further fragmentation to produce ions of m/z 360 (loss of nitrous acid from *m/z* 405), *m/z* 319 (loss of C_2HO from *m/z* 360), *m/z* 302 (loss of NH_3 from *m/z* 319). Further fragmentation takes place at m/z 388 to produce ions of *m/z* 257(loss of $C_5H_9NO_3$ from *m/z* 388), *m/z* 238 (loss of $C_8H_8NO_2$ from *m/z* 388), *m/z* 203 (loss of H_3O_2 from 238), *m/z* 64(loss of C_2N from *m/z* 203), *m/z* 136(loss of C_2H_5 from *m/z* 164).Fragmentation pathway of DP5 is shown in Fig. 7.52 b.

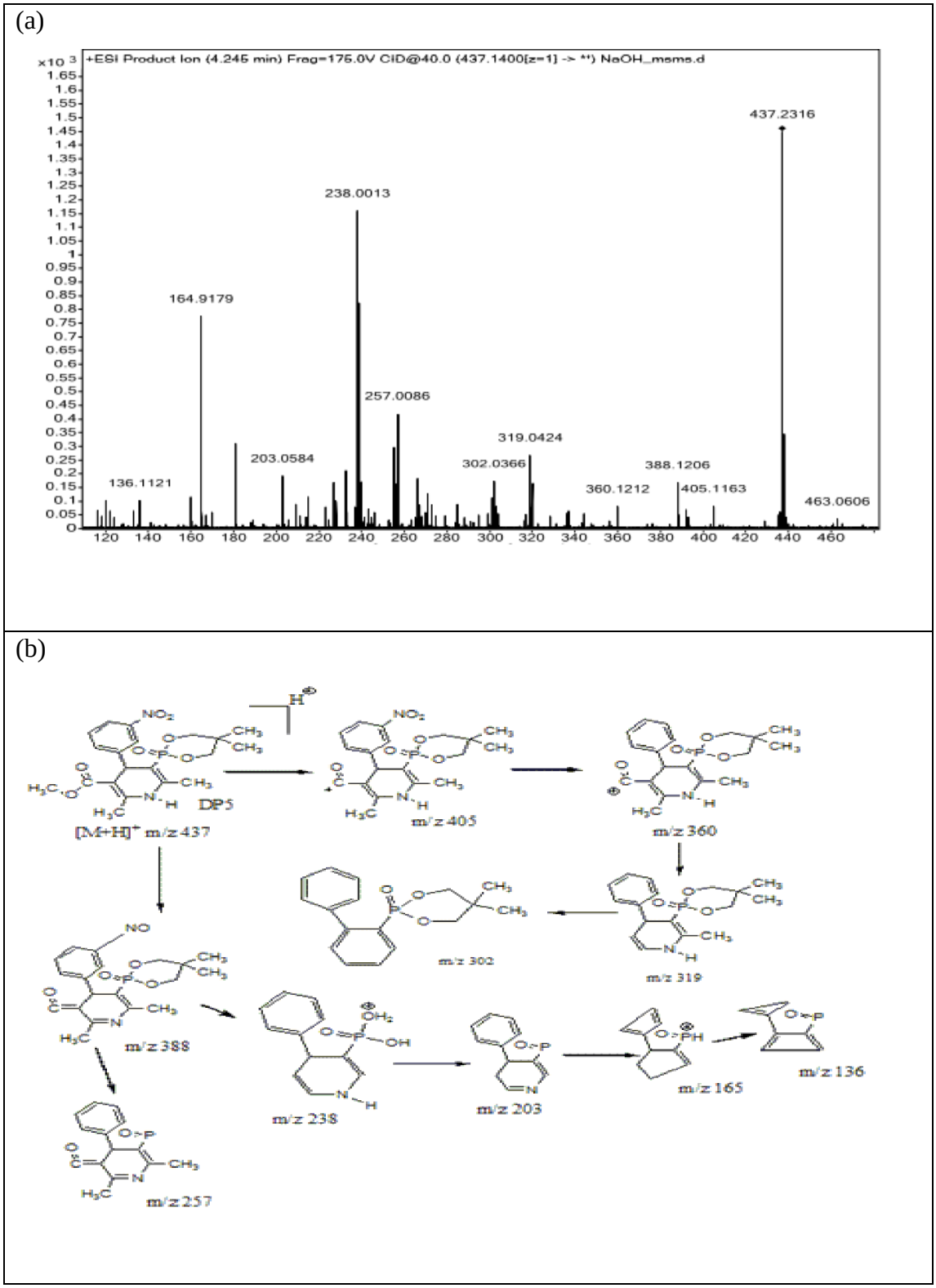

Fig.7. 52- (a) ESI-MS/MS spectra (b) Fragmentation pathway of DP5

DP6 (m/z 455)

ESI-MS of spectra of DP6 is provided in Fig.7.53 a. ESI-MS spectra of DP6 shows protonated molecular ion at *m/z* 455 corresponding to elemental composition $C_{20}H_{28}N_2O_8P^+$. It undergoes fragmentation by removal of methyl group to give *m/z* at 441 (Fig. 7.53b).

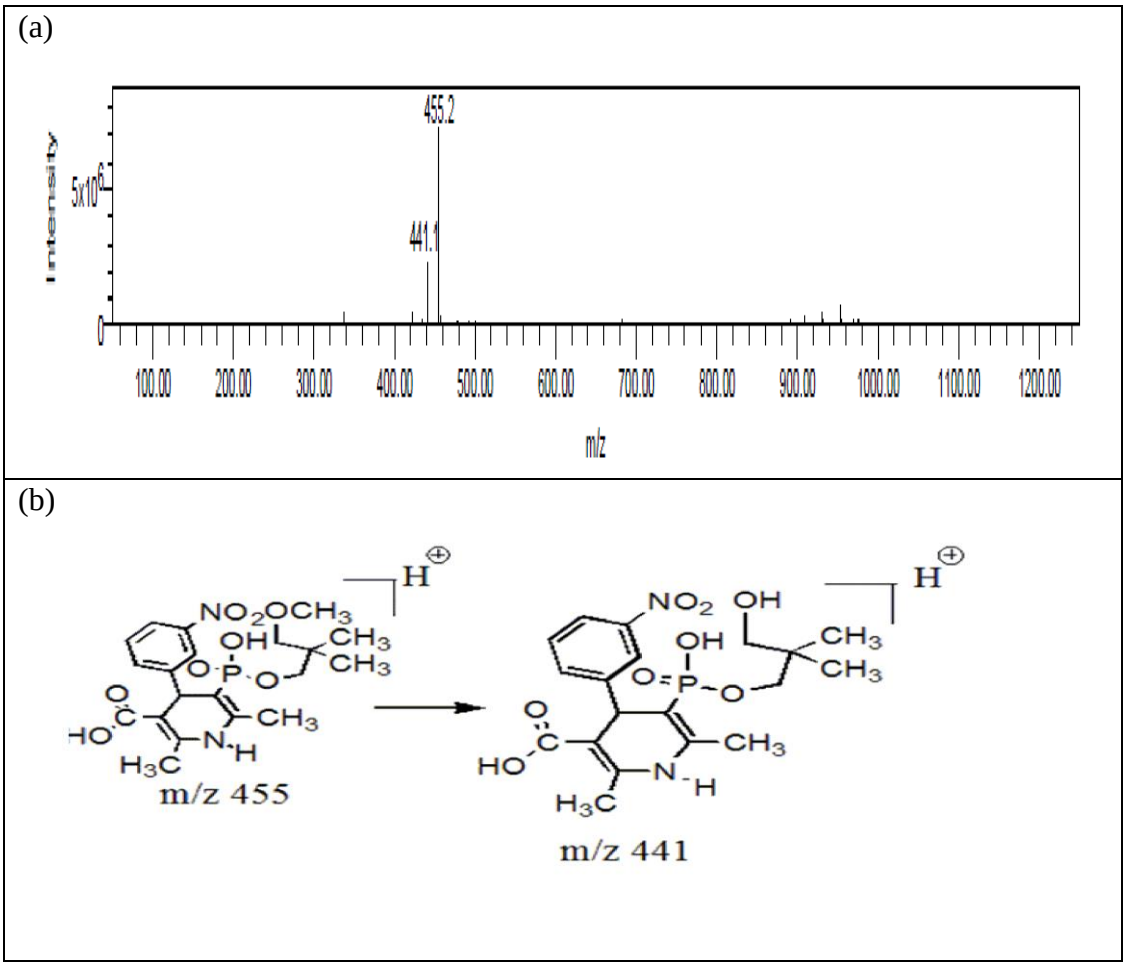

Fig.7. 53- (a) ESI-MS/MS spectra (b) Fragmentation pathway of DP6

DP7 (m/z 540)

ESI-MS/MS of DP7 is provided in Fig.7.54 a. ESI-MS/MS spectra of DP7 shows protonated molecular ion peak at m/z of 540 corresponding to elemental composition $C_{27}H_{31}N_3O_7P^+$. DP7 shows fragment ions of m/z 509(loss of CH_2O from m/z 540) and m/z 447(loss of C_6H_7N from m/z 540. Further fragmentation of *m/z* 509 gives to ions of *m/z* 360 (loss $C_8H_8NO_2$ from *m/z* 540), *m/z* 120(loss of $C_8H_8NO_2$ from *m/z* 509), *m/z* 145 (loss of $C_8H_9NO_4P$ from *m/z* 360). Fragmentation of *m/z* 447 give ions at *m/z*

421 (loss of C_2H_3 from *m/z* 447), *m/z* 283(loss of $C_6H_4NO_3$ from m/z 421), *m/z* 202 (loss of C_5H_4O from m/z 283. DP7 is formed by loss of benzyl group from EFO. Fragmentation pathway of DP7 is provided in Fig. 7.54 b.

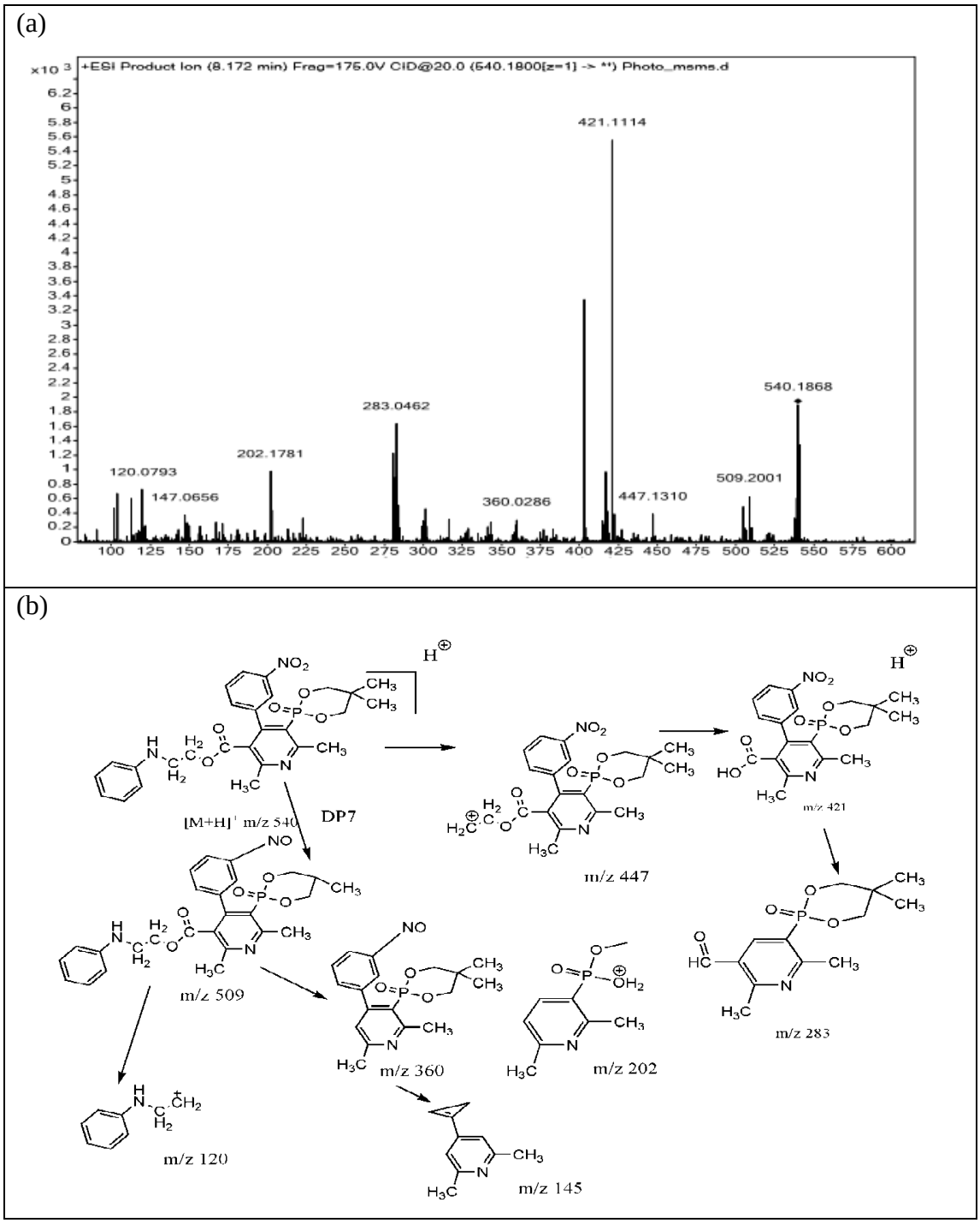

Fig.7. 54 – (a) ESI-MS/MS spectra (b) Fragmentation pathway of DP7

DP8 (m/z 630)

ESI-MS/MS spectra of DP8 is provided in Fig. 7.55 a. DP8 shows protonated molecular ion peak at m/z 630 corresponding to elemental composition $C_{27}H_{33}N_3O_7P^+$. DP8 shows protonated fragment ion at *m/z* 586 (loss of C_2H_4O from *m/z* 630). This fragment undergoes further fragmentation at m/z 511 (loss of $C_3H_7O_2$) and at m/z 373 (loss of $C_{13}H_{11}NO_2$). Fragment ion m/z 373 undergoes further fragmentation at *m/z* 335 (loss of C_3H_2 from *m/z* 373) and *m/z* 271 (loss of meta phosphoric acid from *m/z* 335). DP8 undergoes fragmentation to produce fragment ion at *m/z* 447 (loss $C_{13}H_{13}N$), m/z 403(loss of C_2H_4O from 447, m/z 210 (loss of $C_{19}H_{21}N_2O_7P$ from *m/z* 630), m/z 91 (loss of C_8H_9N from m/z 210.) DP8 is formed from EFO by dehydrogenation at protonated m/z value of 630.23. Fragmentation pathway of DP8 is shown in Fig. 7.55 b.

(a)

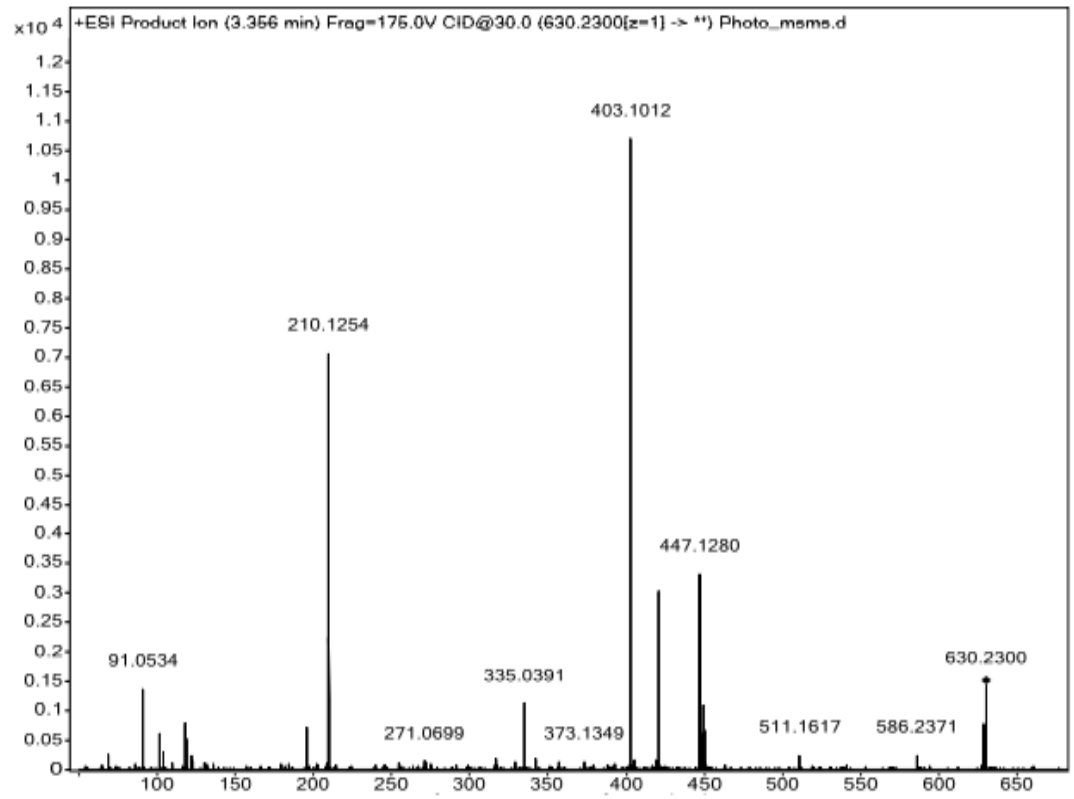

(b)

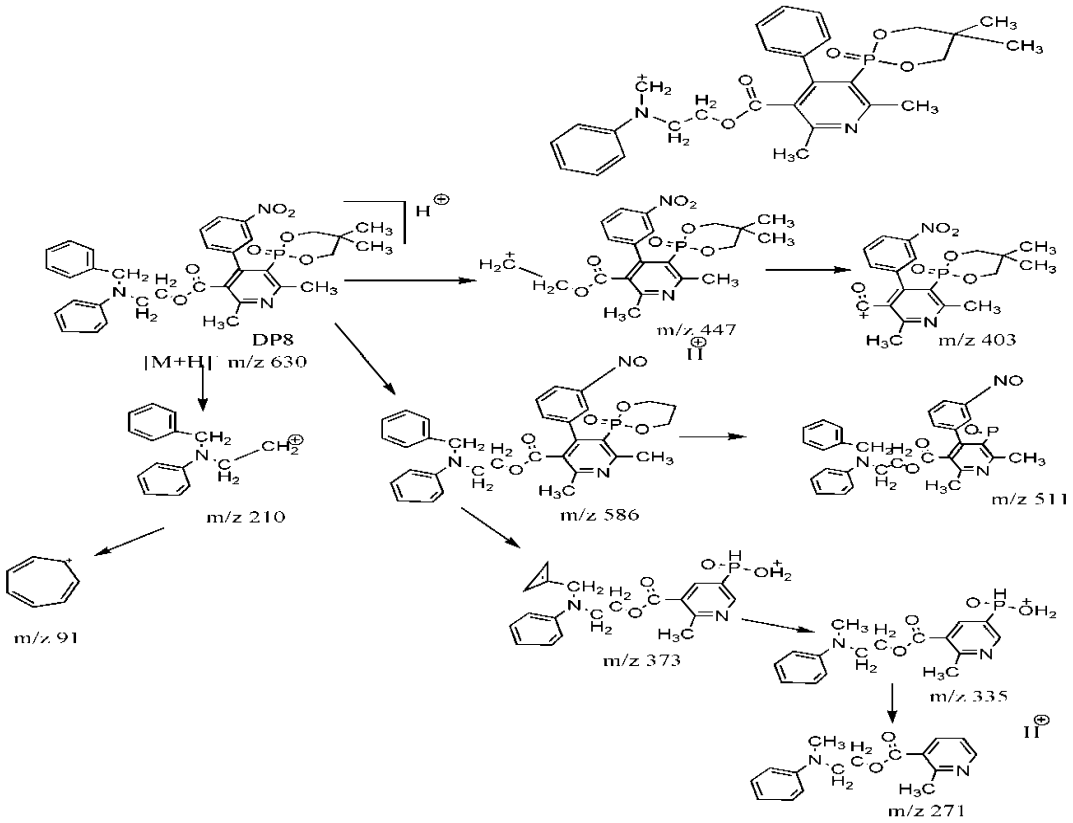

Fig.7. 55 -(a) ESI-MS/MS spectra (b) Fragmentation pathway of DP8

DP9 (m/z 542)

An ESI-MS/MS spectrum of DP9 is provided in Fig.7.56 a. ESI-MS/MS spectrum of DP9 shows protonated molecular ion peak at *m/z* of 542 corresponding to elemental composition $C_{27}H_{33}N_3O_7P^+$. DP9 shows fragment ions of *m/z* 405(loss of $C_8H_{11}NOP$ from *m/z* 542), *m/z* 319(loss of C_2NO_3 from *m/z* 405), *m/z* 104 (loss of $C_{10}H_{16}O_3P$ from *m/z* 542). DP9 is formed by loss of phenyl ethoxy amino group. Fragmentation pathway of DP9 is shown in Fig. 7.56 b.

DP9 (a)

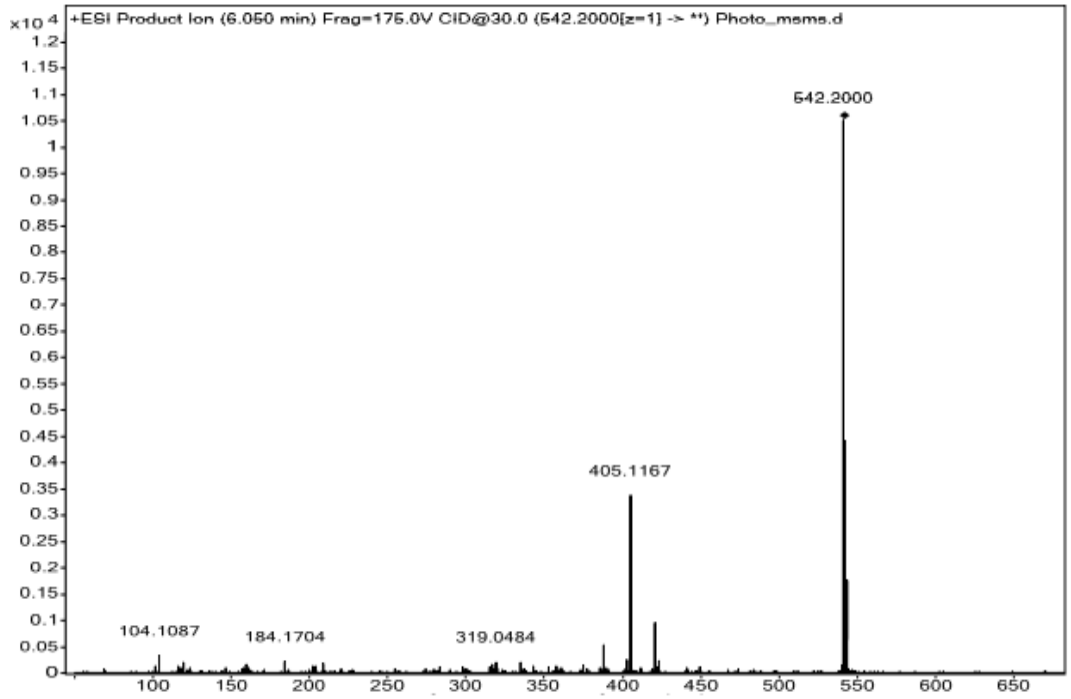

DP9 (b)

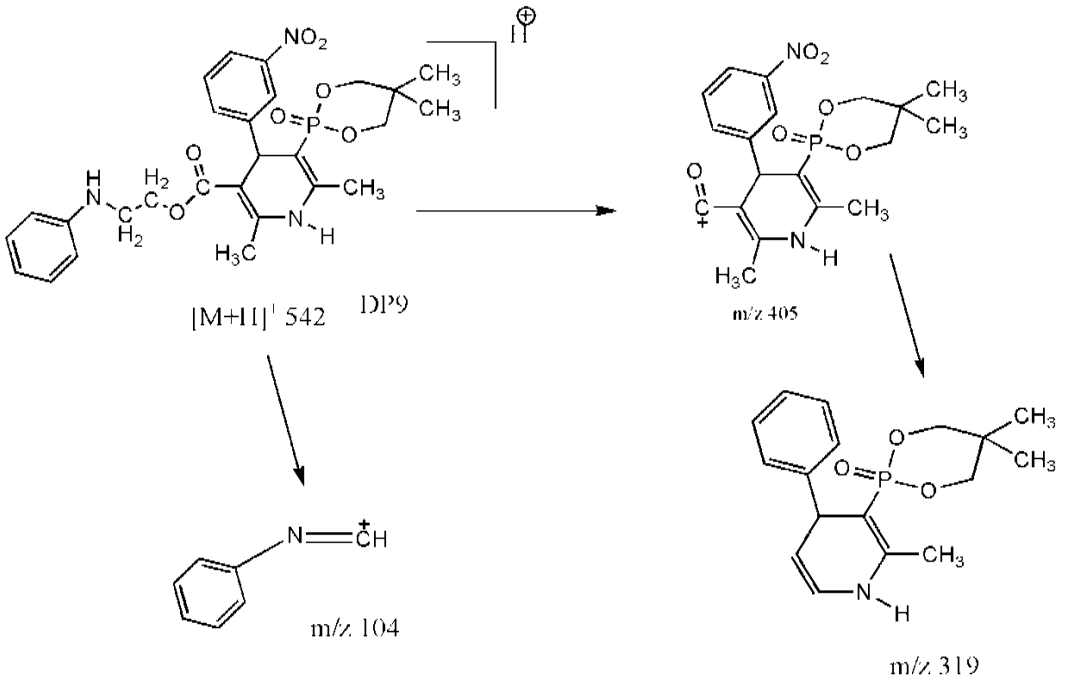

Fig.7. 56- (a) ESI-MS/MS spectra (b) Fragmentation pathway of DP9

DP10 (m/z 510)

An ESI-MS spectrum of DP10 is provided in Fig.7.57. DP10 is formed at m/z of 510 corresponding with elemental composition $C_{28}H_{35}N_2O_5P^+$. DP10 is formed by removal of nitro phenyl group from EFO.

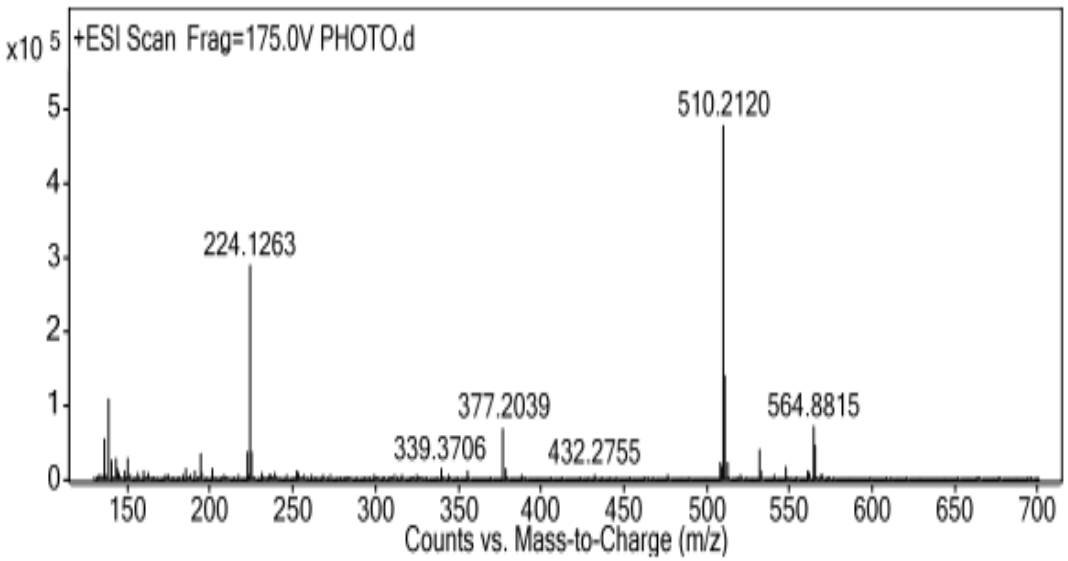

Fig.7. 57 - ESI-MS spectra of DP10

7.8.2.3. Degradation pathway of EFO

7.8.2.3.1. Alkaline condition

EFO contains ester functional group and phosphinane ring. Hydrolysis at phosphinane ring causes ring opening of phosphinane ring and there is formation of DP2.Further esterification with co-solvent methanol, there of formation of pseudo degradation product DP1. Hydrolysis of ester functional group in DP1 causes formation of pseudo degradation product DP4. In all, two direct degradation products DP2 and DP3 are formed by alkaline hydrolysis whereas DP1, DP4, DP5 and DP6 are formed due to these impurities.(Fig. 7.58) When harsh conditions were used for enrichment of degradation product it was found that DP4 was found to be major degradation product and was isolated and characterised. May be under these conditions DP2 is getting converted to DP4 via DP1 formation.

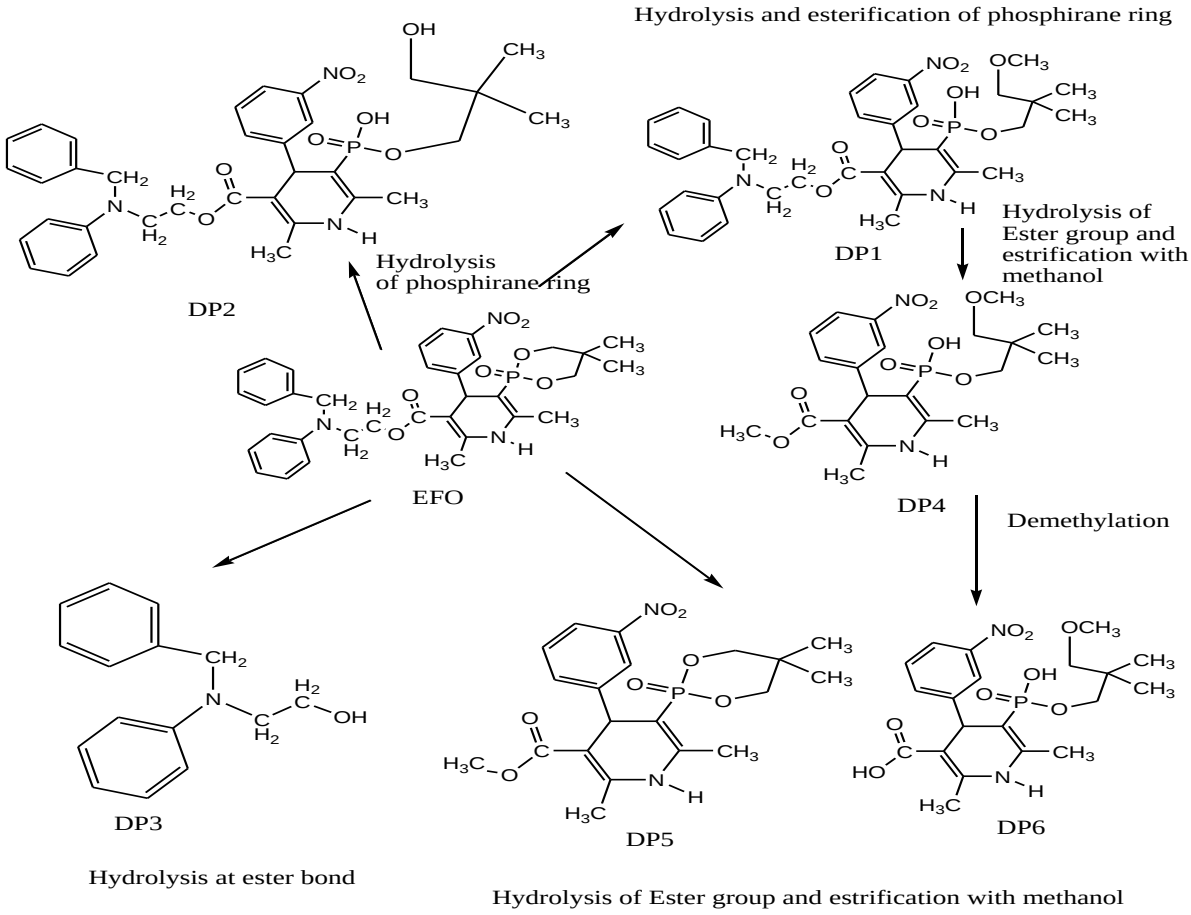

Fig.7. 58 - Degradation pathway of EFO in alkaline condition

7.8.2.3.2. Photolytic condition

Under photolytic condition, EFO on dehydrogenation forms DP 8, DP7 is formed due to removal of benzyl group from DP 8. On direct elimination of nitrophenyl group and benzyl group from EFO, there is formation of DP10 and DP 9. Degradation pathway of photolytic condition is shown in Fig. 7.59.

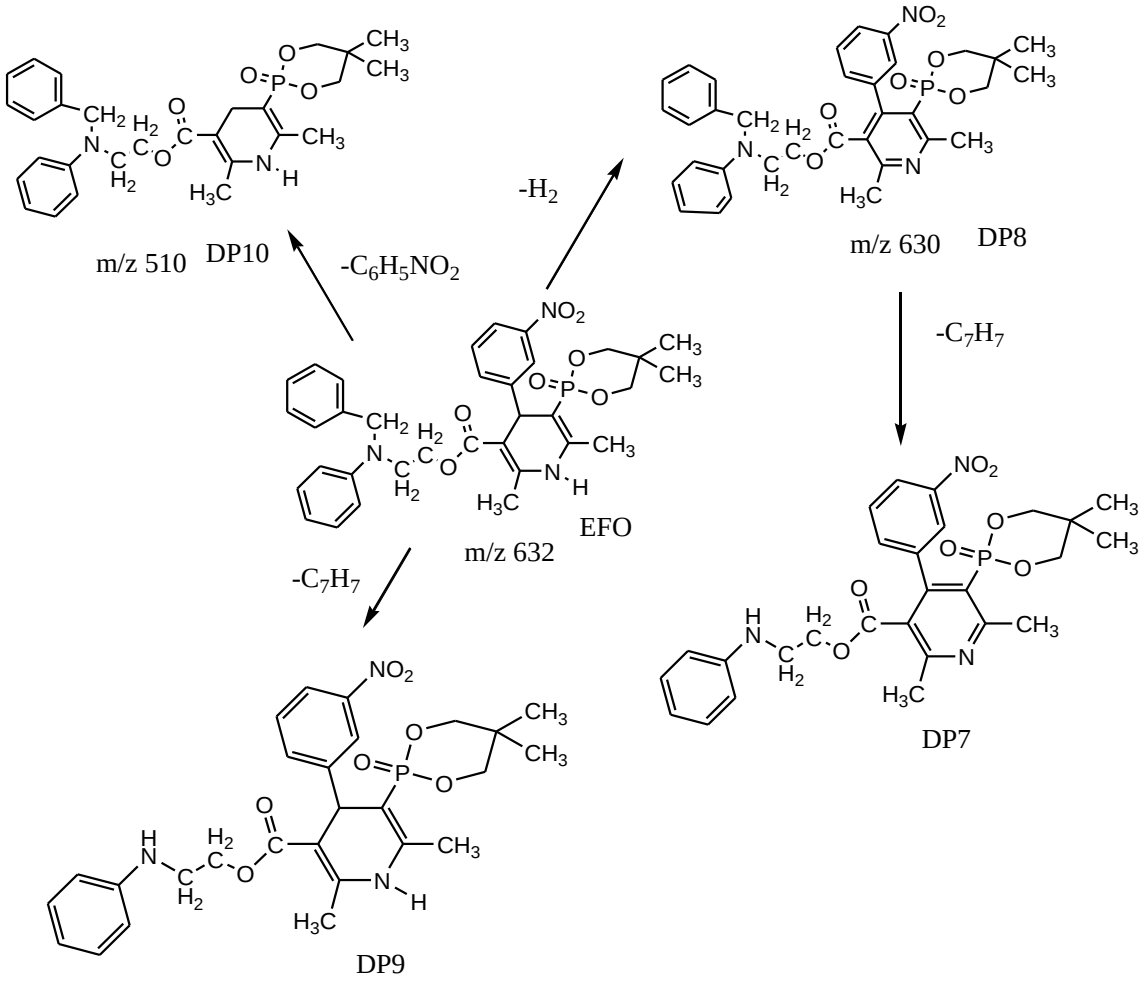

Fig.7. 59 - Degradation pathway in photolytic condition

All degradation products formed after stress degradation of EFO are summarized in Table 7.31.

Table 7. 31 - Chemical structures of EFO and degradation products

Analyte	Structure	Molecular Formula Molecular Weight Fragments(m/z)	Degradation Route	Rt (LC-PDA)
EFO	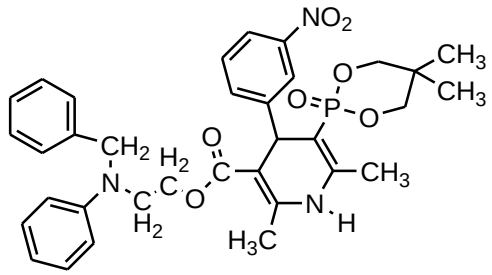 2-(N-benzylanilino)ethyl 5-(5,5-dimethyl-2-oxo-1,3,2$l^{5}-dioxaphosphinan-2-yl)-2,6-dimethyl-4-(3-nitrophenyl)-1,4-dihydropyridine-3-carboxylate	$C_{34}H_{38}N_3O_7P$, 631.65g, Fragments – 562, 495, 449, 405, 337, 210		57.66 min
DP1	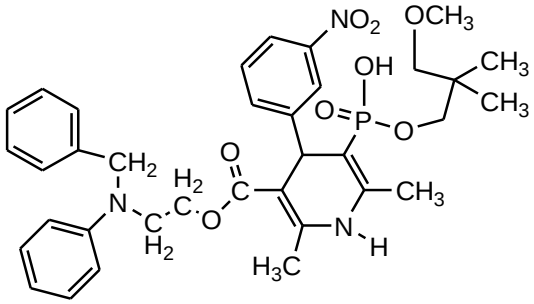 3-2-(N-benzylanilino)ethyl 3-oxo-2,2-dimethylpropyl hydrogen 1,4-dihydro-2,6-dimethyl-4-(3-nitrophenyl)pyridin-3-yl-3-phosphonate	$C_{35}H_{42}N_3O_8P$ 663.69 g, Fragments – 608, 481, 437,351, 269, 210, 181	Alkaline	52.91 min
DP2		$C_{34}H_{40}N_3O_8P$, 649.67g	Alkaline	26.66 min

	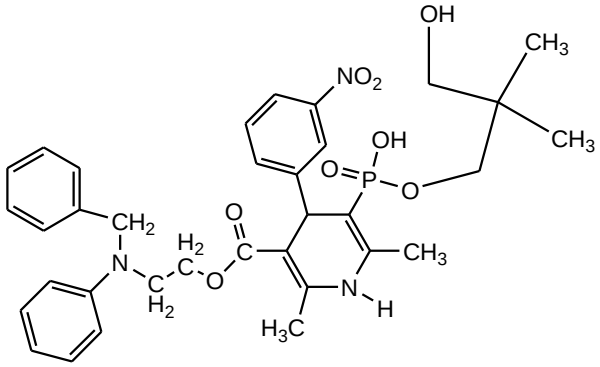 3-hydroxy-2,2-dimethylpropyl hydrogen 1,4-dihydro-2,6-dimethyl-5-methyloxycarbonyl-4-(3-nitro)phenylpyridin-3-yl-3-phosphonate			
DP3	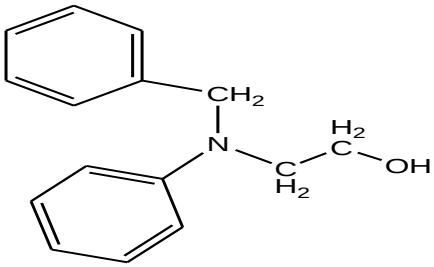 2-(N-benzyl-N-phenylamino)ethanol	$C_{15}H_{17}NO$, 227.30g, Fragments – 209, 180, 160, 122, 102,86	Alkaline	24.09 min
DP4	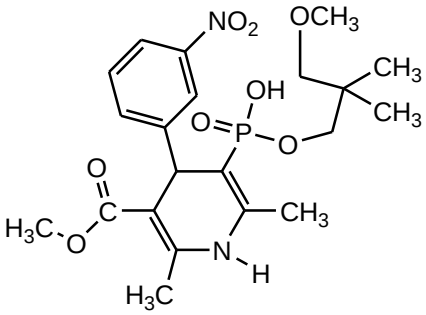 3-methoxy-2,2-dimethylpropyl hydrogen 1,4-dihydro-2,6-dimethyl-5-methyloxycarbonyl-4-(3-nitro)phenylpyridin-3-yl-3-phosphonate	$C_{21}H_{29}N_2O_8P$, 468.43g, Fragments – 422, 351, 271, 243, 181	Alkaline	20.29 min
DP5		$C_{20}H_{25}N_2O_7P$, 436.39g Fragments – 405, 388, 360,	Alkaline	18.83 min

	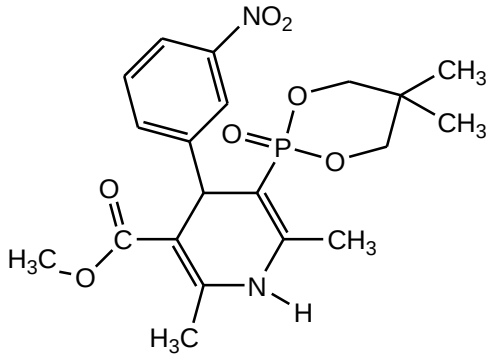 methyl 5-(5,5-dimethyl-2-oxo-1,3,2$l^{5}-dioxaphosphinan-2-yl)-2,6-dimethyl-4-(3-nitrophenyl)-1,4-dihydropyridine-3-carboxylate	310, 302, 257, 238, 203, 164, 136		
DP6	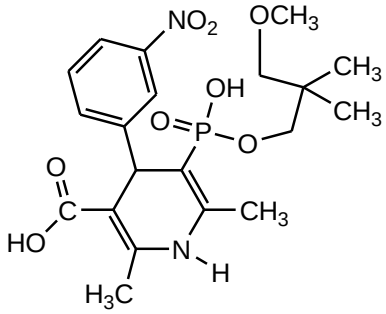 3-methoxy-2,2-dimethylpropyl hydrogen 1,4-dihydro-2,6-dimethyl-5-carboxylate, l-4-(3-nitro)phenylpyridin-3-yl-3-phosphonate	$C_{20}H_{27}N_2O_8P$, 454.41g	Alkaline	14.33 min
DP7	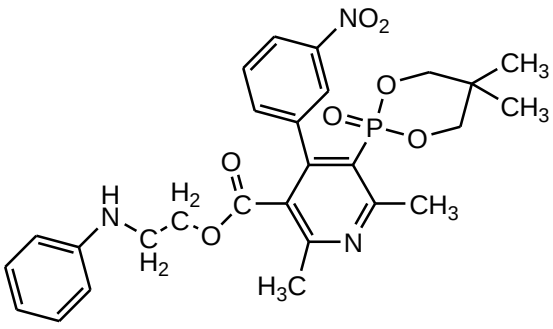 2-(anilino)ethyl 5-(5,5-dimethyl-2-oxo-1,3,2$l^{5}-dioxaphosphinan-2-yl)-2,6-dimethyl-4-(3-nitrophenyl)-pyridine-3-carboxylate	$C_{27}H_{30}N_3O_7P$, 539.51g, Fragments- 509, 447, 421, 360, 283, 202, 145, 120	Photolytic	31.9 min

DP8	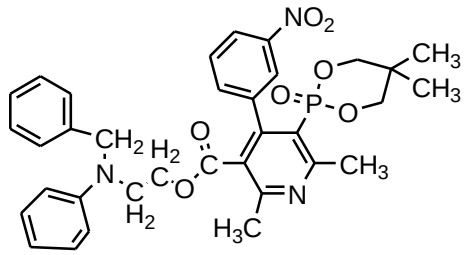 2-(N-benzylanilino)ethyl 5-(5,5-dimethyl-2-oxo-1,3,2$l^{5}-dioxaphosphinan-2-yl)-2,6-dimethyl-4-(3-nitrophenyl)-pyridine-3-carboxylate	$C_{34}H_{36}N_3O_7P$, 629.63g, Fragments – 586, 511, 447, 403, 373, 335, 271, 210, 91	Photolytic	55.92 min
DP9	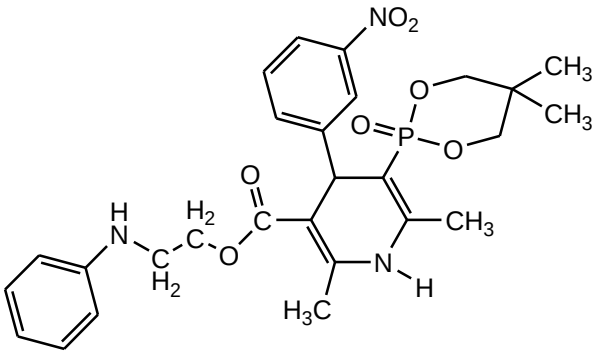 2-(anilino)ethyl 5-(5,5-dimethyl-2-oxo-1,3,2$l^{5}-dioxaphosphinan-2-yl)-2,6-dimethyl-4-(3-nitrophenyl)-1,4-dihydropyridine-3-carboxylate	$C_{27}H_{32}N_3O_7P$, 541.53g , Fragments – 405, 319, 184, 104	Photolytic	30.01 min
DP10	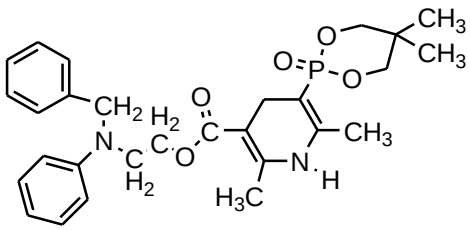 2-(N-benzylanilino)ethyl 5-(5,5-dimethyl-2-oxo-1,3,2$l^{5}-dioxaphosphinan-2-yl)-2,6-dimethyl-1,4-dihydropyridine-3-carboxylate	$C_{28}H_{35}N_2O_5P$, 510.5617	Photolytic	11.67 min

7.9. CONCLUSION

Stability indicating method was developed for determination of EFO by HPLC. Significant degradation was observed in alkaline and photolytic condition. The method developed was validated as per guidelines by ICH. Degradation products in oxidative and photolytic conditions were identified by LC-MS. Total ten degradation products could be identified by LC-MS. Alkaline degradation follows first-order kinetics. Three degradation products in alkaline were isolated and characterized by mass, NMR and IR techniques. The degradation pathway in alkaline and photolytic condition were postulated. Degradation products in alkaline and photolytic condition are hitherto unreported.

7.10. REFERENCES

1. Masuda Y, Tanaka H .Efonidipine Hydrochloride : a dual blocker of L- and T-type calcium channels. Cardiovascular Drugs Reviews. 2002; 12(2) : 123-135.
2. Shimizu M, JKazuhiko O, Sasaki H, Uehara Y, Otsuka Y, Okumura H, Kusaka M, Hasuda M, Yamada T, Mocizuki S. Effects of efonidipine , an L and T-type dual calcium channel blocker on heart rate and blood pressure with mild to severe hypertension : an uncontrolled open-label pilot study. Current Theraupetics Research . 2003; 64(9) : 707-714.
3. Hikaru T, Koki S . Efonidipine hydrochloride – A dual blocker of L& T-type calcium channels. Cardiovacular Drug Reviews.2001; 20: 81-92.
4. Nakano N , Ishimitsu T ,Takahashi T, Inada H , Okamura A , Ohba S , Matsuoka H .Effects of efonidipine, an L- and T-type calcium channel blocker, on the Renin- Angiotensin-aldosterone system in chronic hemodialysis patients. International Heart Jouirnal. 2010 ;5 :1188-192.
5. Hayashi K, Homma K, Wakino S, Tokuyama H, Sugano N, Saruta T, Itoh H. T-type Calcium Channel Blockade as a determinant of Kidney Protection substance. The Keoi Journal of Medicine. 2010; 84-95.
6. Hayashi K, Ozawa Y, Fujiwara K, Wakino S, Kumagai H, Saruta T. Role of actions of calcium Antagonists on Efferent Arterioles – with Special References to Glomerular hypertension. 2003;23: 229-244.

7. Tanaka T, Tsutamoto T, Sakai H, Fujji M, Yamamoto, Horie M. Comparison of the effects of efonidipine and amlodipine on aldosterone in patients with hypertension. Hypertension Research. 2007; 30(8): 691-697.
8. Imagawa K, Okayama S, Takaoka M, Kawaka H, Naya N, Horii M, Uemura S, Saito Y. Inhibitory effect of efonidipine on aldosterone synthesis and secretion in human adrenocarcinoma (H295R) cells. Journal of cardiovascular pharmacology. 2006; 47(1) : 133-138.
9. Koh KK, Lee S, Han S, Ahn JY, Kim J, Chung W, Lee Y, Shin EY. Efonidipine simultaneously improves blood pressure, endothelial function and metabolic parameters in non-diabetic patients with hypertension. Diabetes Care. 2007 ; 30(6) : 1605-1607.
10. http://pubchem.ncbi.nlm.nih.gov/compound/EfonidipineHCl ethanolate/163838(accessed December04,2018)
11. www.drugbank.ca/drugs/DB09235 (accessed December 04,2018).
12. Kumar A, Shoni SK, Dahiya M, Kumar R , Yadav AK, Kumar V, Choudhary H . Development and validation of Liquid chromatography methodology for estimation of Efonidipine HCl Ethanolate. Pharmaceutical Analytical Acta. 2017 ; 8:1-6
13. Liu M, Zhao H, Tong Y, Zhang D, Wang X, Zhang L, Han J, Liu H. Determination of efonidipine in human plasma by LC-MS/MS for pharmacokinetic applications. Journal of Pharmaceutical and Biomedical Analysis. 2015; 103:1-6.
14. Liu M, Deng M, Zhang D, Wang X, Ma J, Zhao H, Zhang L, Tong Y, Liu H. A chiral LC-MS/MS method for the stereospecific determination of efonidipine in human plasma. 2016; 122: 35-41.
15. Pertusati F, Serpi M. Medicinal chemistry of nucleoside phosphonate prodrugs for anti-viral therapy. Antiviral Chemistry and Chemotherapy. 2012; 22: 181-203.
16. Guideline ICH. Pharmaceutical Development Q8, (R2) ; US Department of Health and Human Services. Food and Drug Administration, Center for Drug Evaluation and Research (CDER) : Rockville, MD.2009.
17. ICH. Impurities in new drug substances Q3A(R2), in: International Conference on Harmonisation,IFMPA, Geneva, Switzerland, 2003.

18. ICH. Impurities in new drug products Q3B(R2), in: International Conference on Harmonisation, IFMPA, Geneva, Switzerland, 2003.